SPIN WAVE STUDIES IN ANTIFERROMAGNETS

SPIN WAVE STUDIES IN ANTIFERROMAGNETS

By

VINOD KUMAR TONDON, B.Sc., M.Sc.

A Thesis

Submitted to the Faculty of Graduate Studies

in Partial Fulfilment of the Requirements

for the Degree

Doctor of Philosophy

McMaster University

October 1973

DOCTOR OF PHILOSOPHY (1973) McMASTER UNIVERSITY
(Physics) Hamilton, Ontario

TITLE: Spin Wave Studies in Antiferromagnets

AUTHOR: Vinod Kumar Tondon, B.Sc. (Agra University)
M.Sc. (McMaster University)

SUPERVISOR: Professor M. F. Collins

NUMBER OF PAGES: (x), 203

SCOPE AND CONTENTS:

The thesis investigates three different aspects of spin waves in simple antiferromagnets:

Firstly, the spin wave energies are determined in manganese oxide at low temperatures experimentally using inelastic neutron scattering techniques. This has enabled a determination of the magnetic interactions between the spins.

Secondly, the effects of zero-point motion have been studied theoretically. The particular emphasis is on the way in which the motion affects the spin wave energy, the magnetization and the total energy of the magnetic system. It is found that earlier theoretical treatments, which were restricted to unusually simple cases, can be generalised to encompass a much wider set of conditions.

Finally, a theoretical investigation has been made of the temperature dependence of spin wave energies. Here again, it is found that earlier work restricted to one simple case of an antiferromagnet can be generalised quite extensively. The treatment gives results which predict a different temperature dependence for spin waves of differing wavelengths. Such a dependence is observed experimentally though the theory does not agree quantitively in all cases.

ACKNOWLEDGEMENTS

I would like to express my sincere gratitude to Professor M. F. Collins for his helpful guidance and encouragement throughout the course of this work. It has been an stimulating experience for me to work in the informal atmosphere of his group.

It is a pleasure to acknowledge my gratitude to Dr. W. J. L. Buyers for his guidance in the experimental work done at Chalk River. Mr. R. S. Campbell and Mr. M. M. Potter provided valuable technical assistance. I am thankful to Dr. G. Dolling for his interest and help during part of the experiment.

Section 2.2 follows the general treatment of two sublattice antiferromagnets given by Drs. D. A. Goodings and B. Southern. I wish to thank Dr. E. R. Cowley for use of his 'dipole sum' programme.

I am thankful to Mr. S. Johar for his careful reading of the manuscript and for many useful discussions. Mr. O. Bansal and Dr. A. Bapat helped in making some of the diagrams.

I am indebted to Professor C. Calvo for his encouragement that helped me make the final decision to join Physics.

This research was supported by the Alfred P. Sloan Fellowship Foundation, the Physics Department of McMaster University, the National Research Council of Canada, and by the provisions of the research facilities of the Atomic Energy of Canada Ltd., Chalk River, Ontario.

Finally, I wish to express my sincere thanks to Miss Erie Long for her patience that was much needed for the accurate typing of this thesis.

TABLE OF CONTENTS

TABLE OF CONTENTS - continued

LIST OF FIGURES

LIST OF FIGURES - continued

LIST OF TABLES

CHAPTER I

GENERAL INTRODUCTION

Magnetism has fascinated mankind from the time of the discovery of loadstone. Since then, we have come a long way in putting magnetism to man's benefit as well as in understanding the phenomenon itself. While the early attempts to understand magnetism were confined to the study of macroscopic properties, today, one can discuss the origins of this property on an atomic scale in the language of quantum mechanics.

1.1 Types of Magnetism and Its Origin

To start, however, it is worthwhile to discuss magnetism from a macroscopic point of view. The basic quantity characterizing a system macroscopically is its susceptibility χ. Defining magnetization M as the average magnetic moment per unit volume resulting from a response to an external magnetic field H, χ is the ratio M/H. While paramagnets have a positive value of susceptibility which varies inversely with temperature according to Curie's law, diamagnets have a negative value of susceptibility that is nearly temperature independent. Ferromagnets are paramagnetic

substances which, when cooled below a critical temperature called the Curie temperature, T_c, show spontaneous magnetization, i.e., a magnetization even in the absence of a magnetic field. This amounts to an infinitely large value of susceptibility. Even antiferromagnets are paramagnets as judged by the small positive value of susceptibility; however, they behave differently in that their susceptibility increases with increasing temperature, reaches a certain maximum at a temperature T_N, the Néel temperature, and starts to decrease thereafter approximately according to the Curie-Weiss law (see Fig. I-1). Similarly, the specific heat shows an anomalous dependence on temperature (a logarithmic infinity) around the transition temperature.

In nature, one finds a very wide variety of different types of magnetic materials within the above broad classification. Macroscopically, they differ from one another in having different magnitude and sign of the susceptibility. On an atomic scale, this is due to ordering, disordering or different types of ordering of the magnetic moment of the atoms of a substance.

Since this ordering of the magnetic moment is opposed by the thermal energy, it is only below a certain temperature, e.g., Néel temperature for an antiferromagnet, that an ordered array of the magnetic moments will exist. While in ferromagnets the ordering is simple as all the magnetic moments are ordered in the same direction, ferrimagnets and

Fig. I-1: The temperature dependence of the susceptibility of various types of magnetic substances. It is to be noted that in an antiferromagnet below T_N, $\chi_\perp$ and $\chi_{||}$ behave differently. $\chi_\perp$ and $\chi_{||}$ stand for the applied field as being respectively perpendicular to and parallel to the direction of magnetization.

Paramagnetism

Susceptibility χ

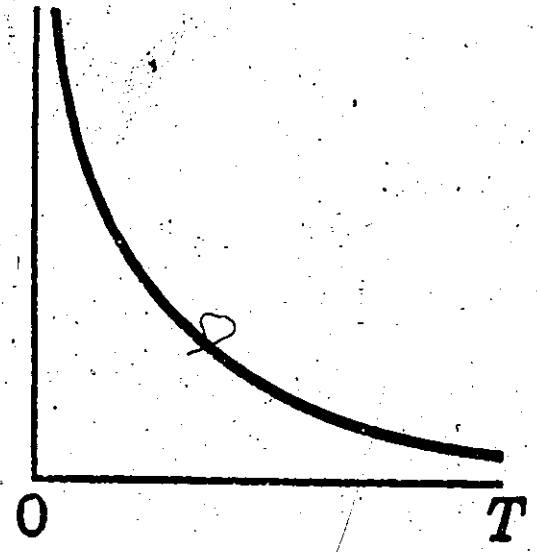

$$\chi = \frac{C}{T}$$

Curie law

Ferromagnetism

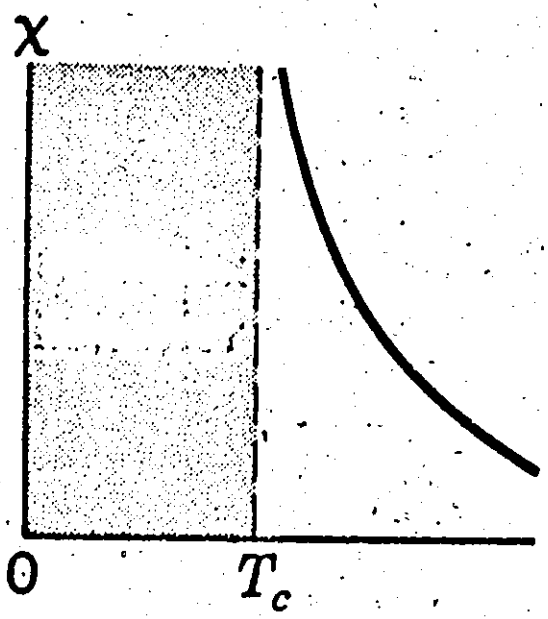

$$\chi = \frac{C}{T - T_c}$$

Curie-Weiss law

$(T > T_c)$

Antiferromagnetism

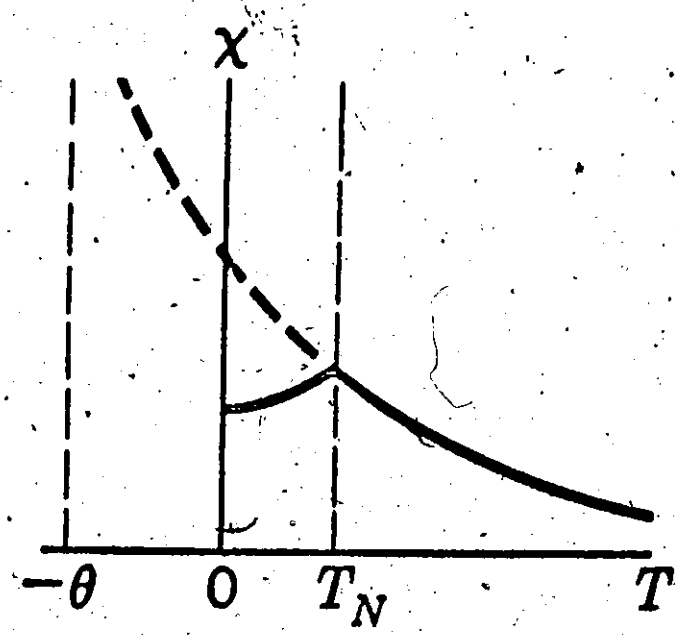

$$\chi = \frac{C}{T + \theta}$$

$(T > T_N)$

antiferromagnets present cases of slightly more complex ordering. Helical, canted and modulated structures have still more complex ordering. In paramagnets long range ordering of the magnetic moments is not present at all. In Fig. I-2, some different types of magnetic ordering are shown.

Quantum mechanically, magnetism has its origin in the angular momentum of the electrons of an atom. The magnetic moment $\underline{\mu}$ of an atom is closely related to its total angular momentum, since

$$\underline{\mu} = - g\mu_B \underline{J} \qquad (I\text{-}1)$$

where g is Lande's g-factor and has the value 2.002 for a free electron, μ_B is the Bohr magneton.

$\underline{J}$, the total angular momentum of an atom, is a vectorial sum of $\underline{L}$ and $\underline{S}$, the total orbital angular momentum and the spin angular momentum of the atom, i.e.,

$$\underline{J} = \underline{L} + \underline{S} \quad . \qquad (I\text{-}2)$$

Apart from these two orbital and spin angular momentum contributions to the magnetic moment of an atom which can be looked upon as an intrinsic angular momentum, change can be induced in the orbital momentum by an applied magnetic field. While this intrinsic angular momentum gives rise to paramagnetism, the induced one gives a diamagnetic

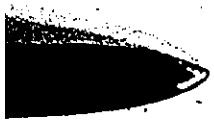

Fig. I-2: Different types of ordering in magnetic substances. a) ferromagnetic, b) antiferromagnetic, c) ferrimagnetic, d) triangular, e) weakly ferromagnetic, f) umbrella and g) multiaxial (arrows perpendicular to the plane of the sketch are shown by corresponding circular currents).

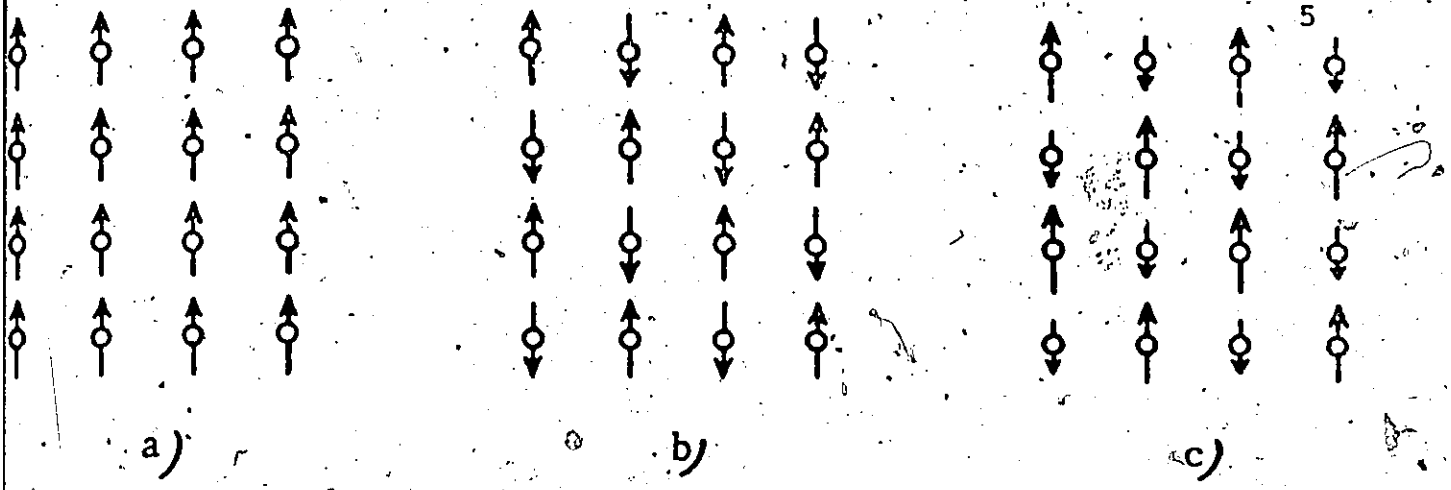

a) b) c)

d) e)

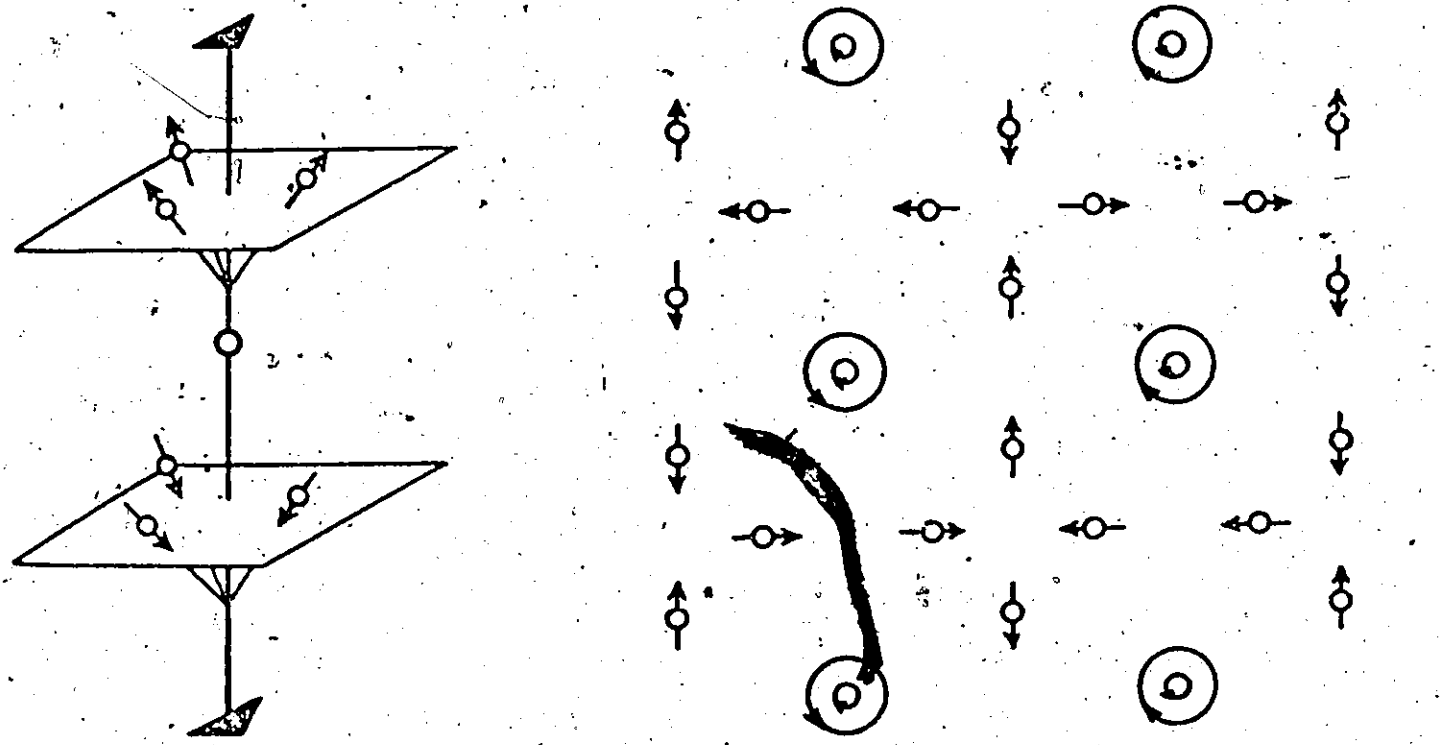

f) g)

contribution to magnetization. Atoms in the ground state may have their orbital momentum zero and similarly filled electron shells have zero spin angular momentum. In MnO, the magnetic atom Mn^{+2} is in a ground state with $L = 0$ and hence all its magnetic moment is due to the spin angular momentum of its incompletely (half) filled d shell.

In this thesis some properties of simple antiferromagnets are studied. The treatment is essentially confined to materials with zero orbital angular momentum. Attention is mainly focussed on the dynamic properties of antiferromagnets. At low temperatures it will be seen that the natural way to describe these properties is in terms of what is known as "spin waves".

1.2 Antiferromagnetism

The concept of antiferromagnetism was first put forward by Néel (1932) in connection with the study of the paramagnetic susceptibility of metals and alloys of the transition elements. He noticed that metals such as Pt, Pd, Mn or alloys such as Pt rich Pt-Co show an almost temperature independent susceptibility which is too large to be explicable in terms of Pauli's free electron paramagnetism. In order to explain the observations Néel guessed that these materials consist of two or more interpenetrating sublattices. These sublattices, though highly ordered magnetically like a ferromagnet, have directions of spontaneous magnetization alternating in such a manner that the resultant magnetization is zero. Today, this hypothesis about the structure of antiferromagnets is well established because of its experimental verification by neutron diffraction on a very large number of materials.

In Table I-1, is given a representative list of known antiferromagnets and their magnetic properties. Although many of the materials such as $RbMnF_3$ have simple structure, there is a growing list of less simple ones. Many of the transition metals such as Chromium and γ iron, their alloys and salts have antiferromagnetic structures. Most of the rare earth metals have rather complex antiferromagnetic ordering. UO_2 and many actinides, and a few unexpected

materials like crystals of molecular oxygen are also known to be antiferromagnetic.

This thesis is restricted to two sublattice antiferromagnets containing only one type of magnetic ion.

TABLE I-1

A LIST OF REPRESENTATIVE ANTIFERROMAGNETS AND THEIR MAGNETIC PROPERTIES

Material	Crystal Structure	Antiferromagnetic Structure	Temperature of the Magnetic Transformations in K	
			T_c	T_N
CoO				291
FeO	Rocksalt	f.c.c.		188
MnO				120
NiO				523
FeF_2				79
CoF_2	Rutile	b.c.		37
MnF_2		tetragonal		67
NiF_2				74
$RbMnF_3$				83
$KMnF_3$	Perovskite	s.c.		88
$KFeF_3$				113

continued...

TABLE I-1 - continued

A LIST OF REPRESENTATIVE ANTIFERROMAGNETS AND THEIR MAGNETIC PROPERTIES

Material	Crystal Structure	Antiferromagnetic Structure	Temperature of the Magnetic Transformations in K	
			T_C	T_N
Dy		Helical	87- 92	179
α-Tb	hcp	Helical	217-223	230
Ho		Helical	19	133
Cr	b.c.c.	Complex		313
α-Mn	complex	Complex		100
$MnAu_2$		Helical		363

1.3 The Exchange Interaction: Direct and Superexchange

Both antiferromagnetism and ferromagnetism are cooperative phenomenon, and hence the assembly of the magnetic moments, giving rise to it must be coupled through some sort of interaction. The most important interactions are the isotropic ones, although, interactions which are anisotropic in nature do have a significant role to play in many magnetic compounds.

Among the isotropic interactions, the exchange interaction is the most important. The exchange energy H_{ex} of a magnetic crystal depends upon the orientation of the spins of its atoms and is written as

$$H_{ex} = - \sum_{i \neq j} J_{ij}(\underline{r}_i - \underline{r}_j) \underline{S}_i \cdot \underline{S}_j \qquad \text{(I-3)}$$

where $\underline{S}_i$ is the spin operator for an atom lying at the point i and $\underline{r}_i$ is the position vector of the point i, and $J_{ij}(\underline{r}_i - \underline{r}_j)$ is the so-called exchange integral or the exchange constant between the atoms i and j. This integral depends upon the distance between atoms i and j, usually falling off rapidly with increasing distance so that in many cases it is sufficient to consider only nearest neighbour exchange interactions, for calculating the exchange energy (I-3).

The concept of exchange energy, which was first put forward by Heisenberg, is a quantum effect arising from

indistinguishibility of identical particles. The Eq. (I-3) is commonly known as Heisenberg's exchange Hamiltonian. Although $\underline{S}_i$ and $\underline{S}_j$ are quantum operators, taking a simple minded approach one can regard them as classical vectors. Then, assuming a coupling between nearest neighbours only, a parallel and antiparallel arrangement of spins can be seen to correspond to energy minimum depending upon whether $J > 0$ (ferromagnetic) or $J < 0$ (antiferromagnetic).

Exchange as envisaged by Heisenberg is the so-called direct exchange due to the overlap of wavefunctions of the electrons of the two neighbouring magnetic atoms. However, it is only for a few magnetic materials that direct exchange is believed to be the dominant mechanism giving rise to the magnetic ordering. For transition metals and alloys the concept of localized moment itself is not valid and one uses an entirely different approach (itinerant model); for the case of rare earth metals, indirect exchange through conduction electrons is known to be the mechanism.

In ionic salts like MnO, an indirect exchange of yet another type, the so-called superexchange, is the source of magnetic ordering. Due to the rapid fall of the exchange integral with distance, one expects the effect of direct exchange to be rather insignificant beyond nearest neighbour separation. Kramer (1934) observed that, however, in order to explain certain adiabatic demagnetization results, there should exist exchange interaction between ions separated by

one or more diamagnetic groups such as O^{-2} or F^{-}. This superexchange interaction was first recognized by Bizette (1946) and Néel (1948). The best known examples of superexchange are provided by monoxides of the iron group ions such as Mn^{+2} and Ni^{+2}. In these cases the interacting ions are ~4 A° apart and the overlap of their actual d shell wavefunctions is negligible. The modern point of view explaining superexchange was put forward by Anderson (1959), in which one attempts to make an explicit separation between two different aspects of the problem: a) finding the wavefunction of a magnetic ion surrounded by various diamagnetic groups exclusive of the exchange effect of the other magnetic ion. One might call this the ligand field theory aspect. Then b) finding out how two magnetic ions defined in the above way interact when they come close together. This approach has the advantage of good convergence since an intervening (diamagnetic) ion is involved only in the solution of (a). The actual mathematics calls for solutions of Hartree-Fock equations. It turns out that the effect of non-magnetic ions amounts to taking an admixture of ligand wavefunction and the magnetic wavefunction (say of p and d wavefunctions for MnO) and the reason that superexchange can be felt over large distances is due to the simple fact that actual magnetic wavefunctions themselves spread over rather long distances because of covalent binding effects with the 'core' electrons of the ligand (Rado and Suhl, 1963).

There exist two broad approaches to the study of excitations of ordered magnetic systems; one is the phenomenological approach, in which the magnetic system is characterized by a magnetization density, which is a continuous function of position, and an energy density which includes all the relevant parts of the magnetic interaction (exchange energy, anisotropic interactions, etc.). Starting with some reasonable form of the equation of motion, small oscillations of the magnetization about its equilibrium value are studied. This approach is not necessarily a classical one though it is often used in a classical context.

The other approach is a microscopic one, and here one deals with localized spins at the lattice sites and starts with a quantum mechanical Hamiltonian to describe the magnetic system. In order to study the excitations we need to solve this Hamiltonian.

In this work, our interest will be limited to insulators (ionic salts) for which the applicability of the latter approach, which has spin localized at a site as its basic assumption, is well accepted. One must mention, however, that microscopic theories, which do not assume localized moments, do exist for spin waves in metals.

1.4 Spin Waves

In a calculation of the low lying excitations of an ordered magnetic system, the natural description is in terms of a collective motion called spin waves or magnons. The concept of spin waves was first introduced by Bloch (1930). In an elastic solid we know that if any of its atom is displaced from the equilibrium position, it oscillates with the normal modes of the crystal, and phonons are the quantization of these normal modes of vibration. Spin waves are the analogous normal modes for a magnetic material, and their quantization leads to magnons.

Let us try to gain some more physical insight as to what a spin wave is like by considering a ferromagnet at the absolute zero of temperature. Assume that an axis of quantization is established, say by a small magnetic field along the z direction. The system being in the ground state, all the spins must be parallel to one another. Let the spin of each atom be S, and its z component be S_z. Let $n = S - S_z$ be a spin deviation quantum operator, which measures the deviation of S_z from its maximum allowed value S. Since S_z can take (2S+1) values S, S-1, ..., -S+1, -S; n has eigenvalues 0, 1, 2, ..., 2S corresponding to a range from a state of no spin deviation to a state with the maximum allowed deviation of 2S on an atom. In the perfectly aligned ground state all the spin deviations vanish. Next, suppose

that the temperature of the system is slightly raised so that the spin of one of the atoms deviates by one unit, i.e., S_z becomes S-1 instead of S. Now each of the N atoms of the system has an equal probability of being the one whose spin is deviated. This suggests that the spin deviation would not remain localized at a particular atom; but because of the exchange interaction with the surrounding atoms it will propagate itself through the lattice, constituting a spin wave. Because of the boundary conditions, only spin waves of certain wave numbers can propagate. Thus, a spin wave corresponds to the propagation of a spin deviation with a definite wave vector. Semiclassically spins are considered as vectors of length $[S(S+1)]^{1/2}$ precessing about the axis of quantization z. In the ground state all the spins have a z-component $M_S = S$ and are precessing in phase. In the first excited state the spin deviation is averaged over all the N spins, that is, the z-component of each spin is $M_S = S - 1/N$, further now there would be a phase difference between the precessing spins. A pictorial representation of spin waves in a linear chain of atoms is given in Fig. I-3.

If the temperature of the system is increased still further, there would occur more than just one spin deviation. In general, these spin deviations or spin waves may get scattered or may even be bound together as a complex. As the temperature rises, complications arise because of the increasing interaction of the spin waves. The lowest order

Fig. I-3: A pictorial representation of spin waves in a linear chain of atoms. The ends of spin vectors precess on the surface of cones, with successive spins advanced in phase by a constant angle.

a) The spins viewed in perspective.

b) Spins viewed from above, showing one wavelength. The wave is drawn through the ends of the spin vectors.

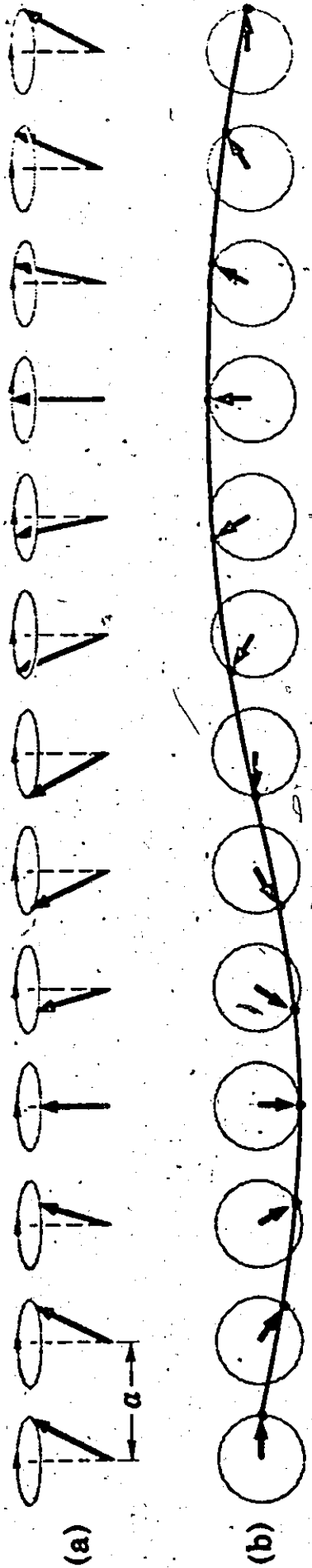
a
(a)
(b)

of approximation in spin wave theory is to neglect these complications and to assume that the spin waves are independent of each other. Then the total energy of a number of spin waves is just the sum of the energy of individual spin waves. This is the so-called 'spin wave approximation'. If the total number of spin waves present in a system is relatively small, and this is so at temperatures well below the transition temperatures, then this approximation is good.

At finite temperatures, because of the spin wave interactions, the approximation starts losing its validity. However, provided one takes into account the effect of spin wave interactions on the energy of the magnons, it is still useful to talk in terms of the spin waves. In Chapter VII, this topic is discussed.

Perhaps, this is the proper place to mention some of the excellent reviews and books available on spin waves. The most recent review is by Hennion (1972), while there are older ones by Keffer (1966) and by Kranendonk and Van Vleck (1958). Among the books, "Magnetic neutron diffraction" by Izyumov (1970), "The theory of magnetism" by Mattis (1965), and "Elements of theoretical magnetism" by Krupicka (1968), should be mentioned. Bloch (1970) reviews spin wave interaction theory and its applications to magnetic salts in two recent articles.

The definite relationship, that exists between the energy $E_{\underline{q}}$ of a spin wave of a system and its wave vector $\underline{q}$

of the propagation, is called a 'dispersion relation'. For example, at small wave vectors $\underline{q}$, the ferromagnetic magnons obey quadratic dispersion law ($E_{\underline{q}} \propto q^2$) and antiferromagnetic ones obey a linear dispersion law ($E_{\underline{q}} \propto q$).

In order to calculate the thermodynamic properties of a magnetic system such as spontaneous magnetization, magnetic contribution to specific heat and the transition temperature one needs to know the magnitude and the sign of the exchange integrals. At present they cannot be calculated from first principles. The most important experimental way to get accurate values for this integral is via measurements of the magnon dispersion curves. In Chapter VI, we shall take up the experimental measurements of the dispersion curves in MnO.

1.5 Measurements with Thermal Neutrons

Thermal neutrons (neutron of energy $\sim$ 0.02 eV), provides us a very important probe for studying the properties of condensed matter because of their many favourable properties. The wavelength of a thermal neutron ($\sim$ 2 Å) is comparable to the mean separation of nuclei in condensed atomic systems, and also its energy is comparable to that of some of the elementary excitations of condensed systems In addition, it has a magnetic moment and is a neutral particle that can penetrate deeply into matter.

The two important interactions of the neutron with matter are the nuclear and the magnetic interaction. The nuclear interaction is due to the nuclear force that acts between the neutron and the nuclei of matter, and the magnetic one is due to the interaction of the magnetic moment of unpaired electrons with that of the neutron. Apart from these two, there are other interactions that are smaller in magnitude, and become important only in especially designed experiments.

The scattering of neutrons from matter can be either coherent or incoherent in nature. In the coherent scattering there is a strong interference between the waves scattered from each atom because of the definite phase relationship that exists between them. In the incoherent scattering there is no interference at all and hence it is isotropic. The

coherent scattering of thermal neutrons, characterized by a given momentum and energy, can either be elastic - the subject of neutron diffraction,or inelastic, with gain or loss of energy - the subject of neutron spectroscopy. The last section of Chapter II deals with the formal scattering theory of neutrons from a spin system.

Neutron diffraction is a technique analogous to X-ray diffraction but can, in addition to determining a crystal structure, also determine magnetic structures. Although in simple cases the spin arrangement present in different magnetic compounds can be inferred from macroscopic measurements such as of susceptibility, the evidence can hardly be called direct since use is made of a chain of arguments to arrive at it. Neutron diffraction provides a direct method of studying the different types of magnetic order. Over the past two and a half decades this technique has established the magnetic structure of a series of metals, alloys and compounds (Bacon, 1962).

When a paramagnetic crystal is cooled through its critical temperature, one notices an increase in the intensity of Bragg (elastic) peaks in cases where the magnetic unit cell is of the same size as the chemical unit cell, or there appear additional peaks - superlattice peaks - if the magnetic unit cell is different from the chemical unit cell. MnO, whose magnetic structure we shall discuss in Chapter V falls into the latter class. By a measurement of the intensities of the

magnetic peaks, it is possible to get the magnitude of the magnetic moment at the different lattice sites. The effects of bonding in magnetically ordered salts can be expected to alter the spatial distribution of the unpaired electrons from that of the free ion case. It is possible to deduce the so-called covalency parameters of an ionic compound (Fender et al., 1968) using this technique.

Neutron spectroscopy is a technique in which the energy distribution of a beam of monoenergetic neutrons, after being scattered from a specimen, is studied. The scattered neutrons show discrete 'neutron groups' in the energy distribution at low temperatures corresponding to creation or annihilation of an energy quantum of an elementary excitation, such as a phonon or a magnon. This is the standard technique for measuring phonon and magnon dispersion curves. In Chapter VI the basic principles of the method and the description of one of the instruments used for this purpose is given.

Although the above method is the one which yields most detailed knowledge about the exchange constants, there exist other methods such as the susceptibility measurements, susceptibility at the Néel temperature being closely related to the exchange interactions, and in principle any quantitative experiments related to the magnetic properties at the low temperature such as low temperature specific heat, magnetization, study of the spin wave resonances would provide

information about the exchange forces operating in a crystal (Rado and Suhl, 1963). These methods have the limitation that they can usually give only a value for a linear combination of exchange constants, while neutron data can be analyzed to yield the sign and magnitude of many different exchange interactions in a magnetic system. Typical energy accuracies obtained with neutrons are about 1%, and if only one exchange interaction is significant the measurements can also determine it to the same accuracy. Measurements with neutrons are the only known method for getting complete magnon dispersion curves, although optical and infrared techniques are more accurate in certain restricted regions, e.g., for the measurements of the $\underline{q} = 0$ mode.

Besides the isotropic interactions discussed earlier, there may be anisotropic interactions present in a magnetic crystal. For materials such as MnO where the magnetic moments arise from electronic spin and there is no net orbital angular momentum, the largest term in the Hamiltonian after the isotropic ones is the dipolar term H_{d-d} given by

$$H_{d-d} = \sum_{j>i} D_{ij}[(\underline{S}_i \cdot \underline{S}_j) - 3(\underline{S}_i \cdot \underline{r}_{ij})(\underline{S}_j \cdot \underline{r}_{ij})/r_{ij}^2] \quad . \quad \text{(I-4)}$$

For true magnetic spin-spin interactions, the constant D_{ij} has the classical value

$$D_{ij} = g^2 \mu_B^2 / r_{ij}^3 \quad \text{with} \quad g = 2 \; . \qquad \text{(I-5)}$$

However, it is known that non-classical values of D_{ij}, and of much larger magnitude at short interatomic distances, can result from indirect spin-orbit coupling (Van Vleck, 1937). Such non-classical values of D_{ij} are often designated as pseudo-dipolar or anisotropic exchange coupling. The most important effects of dipolar couplings are long range. Hence when the value (I-5) is used in (I-4), it is essential that the summation be unrestricted rather than confined to nearest neighbours. Terms that involve summation over small q as well as the long range nature of dipole sums create problems in evaluation. On the other hand, the pseudo-dipolar part of D_{ij} is of comparatively short range, like J_{ij}. For spins greater than 1/2, there may also be present in the Hamiltonian terms corresponding to quadrupolar coupling. While for non cubic materials the contribution of anisotropic interactions (I-4) could be the next most important term of the Hamiltonian, in cubic materials, as a consequence of symmetry requirements, it cannot play a significant role.

The presence of anisotropy results in removing a degeneracy of the magnon branches in an antiferromagnet.

In Chapters III and IV, we study the effect on various properties of antiferromagnets due to the fact that a completely ordered state (Néel state) is not the ground state of an antiferromagnetic system.

CHAPTER II

SPIN WAVE THEORY AT ZERO TEMPERATURE APPLIED TO AN ANTIFERROMAGNET

The ground state of a system of magnetic ions, interacting with positive (ferromagnetic) exchange forces, is a complete parallel alignment of spins of all the magnetic ions. The ground state is less simple when the interaction is negative, as is the case with antiferromagnets. In the next chapter we will discuss the problem of the ground state of an antiferromagnet. In this chapter, however, we are concerned with only spin-wave-like excited states of the antiferromagnetic system. These are the lowest lying states above the ground state, and are the only states which can be appreciably populated when the system is maintained at a temperature close to zero. For ionic crystals, these low lying excited states consist of spin deviations of many different wave vectors.

2.1 The Isotropic Exchange Hamiltonian

Let us consider a magnetic Bravais lattice which can be subdivided into two sublattices ℓ and m, and let $\underline{\ell}$ and $\underline{m}$ be the vectors to an atom on the ℓ and m sublattices from the origin. The spins in one sublattice are all parallel to one another and antiparallel to the spins in the other sublattice. Let $\underline{s}$ be a vector joining atoms on the same sublattice and let $\underline{d}$ be a vector joining atoms on different sublattices; also let J_s and J_d be the corresponding exchange constants (negative in magnitude for antiferromagnets).

To start, we consider the exchange forces as the only interaction coupling magnetic ions. The Heisenberg exchange Hamiltonian can be written as

$$H_{ex} = - \sum_{i,j} J_{ij} \, \underline{S}_i \cdot \underline{S}_j \qquad \text{(II-1)}$$

where S_i and S_j are the spins of atoms at lattice sites i and j respectively.

Before proceeding further, it is important that we describe some of the basic properties of the angular momentum operator S.

Defining S_x, S_y and S_z as the three components of the spin operator S for some particular atom along orthogonal directions x, y and z with z as the equilibrium direction of the spin, one can write

$$S^2 = (S_x)^2 + (S_y)^2 + (S_z)^2 \quad . \qquad \text{(II-2)}$$

The raising and lowering operators S^+ and S^- are defined as

$$S^+ = S_x + iS_y \quad ; \quad S^- = S_x - iS_y \quad . \qquad \text{(II-3)}$$

The representation in which S^2 and S_z are simultaneously diagonal has a basis vector set $\{|sm\rangle\}$ which satisfies ($\hbar \equiv 1$)

$$S^2|sm\rangle = s(s+1)|sm\rangle$$
$$\text{(II-4)}$$
$$S_z|sm\rangle = m|sm\rangle \quad .$$

The eigenvalues of S_z for a given value of s are

$$m = -s, -s+1, \ldots, s-1, s \quad .$$

These provide a $(2s+1)$ dimensional basis for the representation of the angular momentum operator S. The matrix elements of S^2, S_z, S^+ and S^- in this representation are

$$\langle s'm'|S^2|sm\rangle = s(s+1)\delta_{ss'}\delta_{mm'}$$

$$\langle s'm'|S_z|sm\rangle = m\delta_{ss'}\delta_{mm'}$$

$$\langle s'm'|S^+|sm\rangle = [s(s+1) - m(m+1)]^{1/2}\,\delta_{s's}\delta_{m'm+1} \qquad \text{(II-4)}$$

$$\langle s'm'|S^-|sm\rangle = [s(s+1) - m(m-1)]^{1/2}\,\delta_{s's}\delta_{m'm-1}$$

The important commutation relations obeyed by spin operators are

$$[S^+,S^-] = 2S_z;\ [S_x,S_y] = iS_z$$

$$[S^+,S_z] = -S^+;\ [S^-,S_z] = S^- \qquad \text{(II-5)}$$

The exchange Hamiltonian (II-1) can be written in terms of the components of spin operators as

$$H_{ex} = -\sum_{i,j} J_{ij}(S_i^xS_j^x + S_i^yS_j^y + S_i^zS_j^z) \qquad \text{(II-6)}$$

In terms of spin raising and lowering operators S^+ and S^-, this reduces to

$$H_{ex} = -\sum_{ij} J_{ij}\{\tfrac{1}{2}(S_i^+S_j^- + S_i^-S_j^+) + S_i^zS_j^z\} \qquad \text{(II-7)}$$

Splitting the Hamiltonian in terms of sublattices ℓ and m and noting that the ℓ and m sublattices are equivalent and hence interchangeable, one can write the exchange Hamiltonian as

$$H_{ex} = - \sum_{\underline{\ell}\underline{s}} J_s [\tfrac{1}{2} (S^+_{\underline{\ell}} S^-_{\underline{\ell}+\underline{s}} + S^-_{\underline{\ell}} S^+_{\underline{\ell}+\underline{s}}) + S^z_{\underline{\ell}} S^z_{\underline{\ell}+\underline{s}}]$$

$$- \sum_{\underline{m}\underline{s}} J_s [\tfrac{1}{2} (S^+_{\underline{m}} S^-_{\underline{m}+\underline{s}} + S^-_{\underline{m}} S^+_{\underline{m}+\underline{s}}) + S^z_{\underline{m}} S^z_{\underline{m}+\underline{s}}]$$

$$- 2 \sum_{\underline{\ell}\underline{d}} J_d [\tfrac{1}{2} (S^+_{\underline{\ell}} S^-_{\underline{\ell}+\underline{d}} + S^-_{\underline{\ell}} S^+_{\underline{\ell}+\underline{d}}) + S^z_{\underline{\ell}} S^z_{\underline{\ell}+\underline{d}}] \quad \text{(II-8)}$$

The standard method to proceed further is to convert the spin operators to expressions involving boson creation operators $a^\dagger$ and annihilation operators a, and thus make spin wave particles obey bose-statistics. There are two well known approaches for doing so:

i Holstein-Primakoff (H-P) Approach,

ii Dyson-Maleev (D-M) Approach.

H-P Approach

In this approach the spin operators are related to boson operators by the following transformation (Holstein and Primakoff, 1940):

$$S_i^z = S - a_i^\dagger a_i = S - n_i$$

$$S_i^+ = (2S)^{1/2} f_i a_i$$

$$S_i^- = (2S)^{1/2} a_i^\dagger f_i$$

where $f_i = [1 - \frac{a_i^\dagger a_i}{2S}]^{1/2} = [1 - \frac{n_i}{2S}]^{1/2}$ (II-9)

$n_i = a_i^\dagger a_i$ is the occupation number and in this case represents the number of deviations of spin S_i at site i from its maximum magnitude S. $a_i^\dagger$ and a_i can be regarded as the creation and annihilation operators for the spin deviation. The commutation rule followed by a boson is

$$[a_i, a_j^\dagger] = \delta_{ij}$$

$$[a_i, a_j] = [a_i^\dagger, a_j^\dagger] = 0 \quad \text{(II-10)}$$

D-M Approach

The alternative procedure to convert the spin operators to bose operators is to use Dyson-Maleev transformation (Dyson, 1956; Maleev, 1958). One form of such a transformation gives (Dembinski, 1964; Harris, 1966)

$$S_i^z = S - a_i^\dagger a_i$$

$$S_i^+ = (2S)^{1/2}(1 - a_i^\dagger a_i/2S)\, a_i \qquad \text{(II-11)}$$

$$S_i^- = (2S)^{1/2}\, a_i^\dagger \ .$$

This transformation has the obvious advantage that it does not have the awkward square root term which is present in the H-P transformation, though it is achieved at the expense of the transformation being non-unitary, so that the transformed Hamiltonian becomes non-Hermitian.

Since, as we will presently see, both the approaches are identical for the purpose of this chapter, we shall follow only the H-P formalism.

Converting spin operators to boson operators $a_\ell^\dagger$ and a_ℓ for the ℓ sublattice and $b_m^\dagger$ and b_m for the m sublattice, the H-P transformation is given as

$$S_\ell^z = S - a_\ell^\dagger a_\ell \quad ; \quad S_m^z = -S + b_m^\dagger b_m$$

$$S_\ell^+ = (2S)^{1/2}\, f_\ell a_\ell \ ; \quad S_m^+ = (2S)^{1/2}\, b_m^\dagger f_m$$

$$S_\ell^- = (2S)^{1/2}\, a_\ell^\dagger f_\ell \ ; \quad S_m^- = (2S)^{1/2}\, f_m b_m \qquad \text{(II-12)}$$

where

$$f_\ell = [1 - a_\ell^\dagger a_\ell/2S]^{1/2}$$

$$f_m = [1 - b_m^\dagger b_m/2S]^{1/2} \qquad \text{(II-13)}$$

For the case when the number of spin deviations is very small compared to the spin of an atom, one can expand the square root in (II-13) binomially in a power series of $(a^\dagger a/2S)$ so that

$$f_\ell = 1 - a_\ell^\dagger a_\ell/4S + \ldots$$

$$f_m = 1 - b_m^\dagger b_m/4S + \ldots \qquad \text{(II-14)}$$

In the zeroth order approximation, f_ℓ and f_m are replaced by unity. This is the so-called Harmonic or linear approximation for spin waves. It works well when the number of spin deviations is small, a condition which can be met best when the temperature is low, and when the spin of the magnetic atom has a large value. It is obvious that both H-P and D-M transformations are identical in this approximation. Thus in the harmonic approximation, the transformations become

$$S_{\ell}^{z} = S - a_{\ell}^{\dagger}a_{\ell} \quad ; \quad S_{m}^{z} = -S + b_{m}^{\dagger}b_{m}$$

$$S_{\ell}^{+} = (2S)^{1/2}\, a_{\ell} \quad ; \quad S_{m}^{+} = (2S)^{1/2}\, b_{m}^{\dagger} \qquad \text{(II-15)}$$

$$S_{\ell}^{-} = (2S)^{1/2}\, a_{\ell}^{\dagger} \quad ; \quad S_{m}^{-} = (2S)^{1/2}\, b_{m}$$

The Hamiltonian as given by (II-8) can now be expressed in terms of boson operators using (II-15) to yield:

$$\begin{aligned} H_{ex}^{0} = & - \sum_{\underline{\ell}\underline{s}} J_{s}[S^{2} - S(a_{\underline{\ell}}^{\dagger}a_{\underline{\ell}} + a_{\underline{\ell}+\underline{s}}^{\dagger}a_{\underline{\ell}+\underline{s}}) \\ & + S(a_{\underline{\ell}}a_{\underline{\ell}+\underline{s}}^{\dagger} + a_{\underline{\ell}}^{\dagger}a_{\underline{\ell}+\underline{s}})] - \sum_{\underline{m}\underline{s}} J_{s}[S^{2} \\ & - S(b_{\underline{m}}^{\dagger}b_{\underline{m}} + b_{\underline{m}+\underline{s}}^{\dagger}b_{\underline{m}+\underline{s}}) + S(b_{\underline{m}}^{\dagger}b_{\underline{m}+\underline{s}} + b_{\underline{m}}b_{\underline{m}+\underline{s}}^{\dagger})] \\ & - 2\sum_{\underline{\ell}\underline{d}} J_{d}[-S^{2} + S(a_{\underline{\ell}}^{\dagger}a_{\underline{\ell}} + b_{\underline{\ell}+\underline{d}}^{\dagger}b_{\underline{\ell}+\underline{d}}) \\ & + S(a_{\underline{\ell}}b_{\underline{\ell}+\underline{d}} + a_{\underline{\ell}}^{\dagger}b_{\underline{\ell}+\underline{d}}^{\dagger})] \end{aligned} \qquad \text{(II-16)}$$

where we have neglected the bilinear products of the operators of the type $a_{\underline{\ell}+\underline{s}}^{\dagger}\ a_{\underline{\ell}+\underline{s}}\ a_{\underline{\ell}}^{\dagger}a_{\underline{\ell}}$ coming from the terms $S_{\underline{\ell}}^{z}\ S_{\underline{\ell}+\underline{s}}^{z}$ etc., to be consistent with the linear approximation. We are left with a Hamiltonian quadratic in bose operators.

The next step is to Fourier transform the bose operators, the transforms being given as

$$a_{\underline{\ell}} = (2/N)^{1/2} \sum_{\underline{q}} e^{-i\underline{q}\cdot\underline{\ell}} a_{\underline{q}}$$

and

$$b_{\underline{m}} = (2/N)^{1/2} \sum_{\underline{q}} e^{i\underline{q}\cdot\underline{m}} b_{\underline{q}} \qquad \text{(II-17)}$$

where N is the total number of spins and $\underline{q}$, the reduced wave vector, is confined to first Brillouin zone.

The transformed Hamiltonian is

$$H_{ex}^{0} = NS^2[J_d(\underline{0}) - J_s(\underline{0})] - 2S \sum_{\underline{q}} [(J_d(\underline{0}) - J_s(\underline{0}) + J_s(\underline{q}))(a_{\underline{q}}^{\dagger}a_{\underline{q}} + b_{\underline{q}}^{\dagger}b_{\underline{q}})] - 2S \sum_{\underline{q}} [J_d(\underline{q})(a_{\underline{q}}b_{\underline{q}} + a_{\underline{q}}^{\dagger}b_{\underline{q}}^{\dagger})] \qquad \text{(II-18)}$$

where

$$J_d(\underline{q}) = \sum_{\underline{d}} J_d \exp(i\underline{q}\cdot\underline{d}) \quad ;$$

$$J_s(\underline{q}) = \sum_{\underline{s}} J_s \exp(i\underline{q}\cdot\underline{s}) \quad . \qquad \text{(II-19)}$$

One can rewrite H_{ex}^{0} as

$$H_{ex}^{0} = E_0 + \sum_{\underline{q}} A_{\underline{q}}(a_{\underline{q}}^{\dagger}a_{\underline{q}} + b_{\underline{q}}^{\dagger}b_{\underline{q}}) + \sum_{\underline{q}} B_{\underline{q}}(a_{\underline{q}}b_{\underline{q}} + a_{\underline{q}}^{\dagger}b_{\underline{q}}^{\dagger}) \qquad \text{(II-20)}$$

with

$$E_0 = NS^2[J_d(\underline{0}) - J_s(\underline{0})]$$

$$A_q = -2S[J_d(\underline{0}) - J_s(\underline{0}) + J_s(\underline{q})]$$

and

$$B_q = -2S\, J_d(\underline{q}) \quad . \tag{II-21}$$

A general method of dealing with a system of harmonic oscillators in linear approximation is to describe it in terms of some uncoupled oscillators or normal modes, which corresponds to the diagonalization of the quadratic form of H_{ex}^0 as given by Eq. (II-20).

To diagonalize, we look for a new set of bose operators α_q and β_q given by some suitable linear combination of a_q and b_q:

$$\alpha_q = ua_q + vb_q^\dagger$$

$$\beta_q = wa_q^\dagger + xb_q \tag{II-22}$$

such that the Hamiltonian (II-20) can be written in the diagonal form

$$H_{ex}^{0} = E_0 + \sum_q (\lambda_q \alpha_q^{\dagger} \alpha_q + \mu_q \beta_q^{\dagger} \beta_q) \qquad \text{(II-23)}$$

where λ_q and μ_q are the spin wave energies.

The bose operators α_q and β_q must obey the commutation relations

$$[\alpha_q, \alpha_{q'}^{\dagger}] = [\beta_q, \beta_{q'}^{\dagger}] = \delta_{qq'}$$

and

$$[\alpha_q, \beta_{q'}] = [\alpha_q, \beta_{q'}^{\dagger}] = 0 \quad . \qquad \text{(II-24)}$$

From (II-23)

$$[\alpha_q, H_{ex}^{0}] = \lambda_q \alpha_q$$

$$= u(\lambda_q a_q) + v(\lambda_q b_q^{\dagger}) \quad . \qquad \text{(II-25a)}$$

But, from (II-20)

$$[\alpha_q, H_{ex}^{0}] = u(A_q a_q + B_q b_q^{\dagger}) + v(-A_q b_q^{\dagger} - B_q a_q) \quad . \qquad \text{(II-25b)}$$

From (II-25a) and (II-25b), by equating the coefficients of a_q and $b_q^{\dagger}$, one gets

$$A_q u - B_q v = \lambda_q u$$

$$B_q u - v A_q = \lambda_q v \qquad \text{(II-25c)}$$

The eigenvalues λ_q are given by the condition that the determinant of (II-25c) vanish, and one gets

$$\lambda_q = \pm (A_q^2 - B_q^2)^{1/2} \qquad \text{(II-26)}$$

as the two degenerate eigenvalues of the isotropic exchange Hamiltonian.

In order that the linear combination (II-22) be the proper one, it's coefficients u, v, w and x should be such that one has

$$[\alpha_q, \alpha_q^\dagger] = |u|^2 - |v|^2 = 1$$

$$[\beta_q, \beta_q^\dagger] = |x|^2 - |w|^2 = 1 \qquad \text{(II-27)}$$

One of the linear combinations with suitable coefficients can be shown to be the so-called Bogoliubov transformation given as

$$a_q = \alpha_q \cosh\theta_q - \beta_q^\dagger \sinh\theta_q$$

$$b_q = -\alpha_q^\dagger \sinh\theta_q + \beta_q \cosh\theta_q \qquad \text{(II-28)}$$

where the parameter θ_q should be such as to diagonalize the Hamiltonian (II-20).. The Hamiltonian (II-20) is transformed by using Eq. (II-28), θ_q is then calculated from the condition that the coefficient of the non-diagonal term $(\alpha_q\beta_q + \alpha_q^\dagger\beta_q^\dagger)$ should vanish. This condition is satisfied if

$$\tanh 2\theta_q = B_q/A_q = \frac{J_d(\underline{q})}{J_d(\underline{0}) - J_s(\underline{0}) + J_s(\underline{q})} \quad . \qquad \text{(II-29a)}$$

It is easy to show that, then

$$\sinh 2\theta_q = B_q/\lambda_q \quad ; \quad \cosh 2\theta_q = A_q/\lambda_q \qquad \text{(II-29b)}$$

where λ_q is as given by (II-26) and A_q and B_q are as given by (II-21).

2.2 Effects of Dipole-Dipole Interactions on the Spin Waves in Linear Approximation

So far, we have considered a magnetic system described only by the exchange Hamiltonian. Actual physical systems generally do have anisotropic interactions of various origins present which need to be included in the Hamiltonian. Magnetic dipole-dipole type anisotropic interactions are of special interest to us, being the most important source of anisotropy in many antiferromagnets such as MnO and MnF_2. Apart from this lowest order anisotropic interaction, there may be additional sources of anisotropy, e.g., those arising from the spin-orbit couplings (these are short ranged and not so important in cubic materials). We shall limit this discussion to dipole-dipole interactions assuming it to be the only anisotropic interaction present in the magnetic system.

In general, the term in the Hamiltonian due to the dipole-dipole interaction can be written as

$$H_{d-d} = \frac{g^2\mu_B^2}{2} \sum_{i,j} \frac{1}{r_{ij}^5} \left[r_{ij}^2 (\underline{S}_i \cdot \underline{S}_j) - 3 (\underline{S}_i \cdot \underline{r}_{ij})(\underline{S}_j \cdot \underline{r}_{ij}) \right] \qquad \text{(II-30)}$$

where μ_B is the Bohr-magneton, $\underline{S}_i$ is the spin of atom at position i and $\underline{r}_{ij}$ is the position vector $\underline{i}-\underline{j}$. Let $\underline{u}$ be the vector to position i from the origin, then $\underline{u}$ can be vector $\underline{\ell}$ or $\underline{m}$ and similarly $\underline{r}_{ij}$ can be $\underline{s}$ or $\underline{d}$ depending upon the

sublattice the atoms i and j are on. So that (II-30) can be written as

$$= \frac{g^2\mu_B^2}{2} \sum_{\underline{u}} \sum_{\underline{r}} \frac{1}{r_{ij}^5} [(r_{ij}^2 S_{\underline{u}} \cdot S_{\underline{u}+\underline{r}} - 3(S_{\underline{u}} \cdot \underline{r}_{ij})(S_{\underline{u}+\underline{r}} \cdot \underline{r}_{ij})] \quad \text{(II-31)}$$

Similar to operators S^+ and S^- defined earlier (see Eq. (II-3)) one can define

$$r^+ = r_x + ir_y \quad ; \quad r^- = r_x - ir_y$$

with $r_x = x$ etc. (II-32)

which allows us to write H_{d-d} given by (II-31) as

$$= \frac{g^2\mu_B^2}{2} \sum_{\underline{u}} \sum_{\underline{r}} \{\frac{1}{r_{ij}^5} [(r_{ij}^2/2)(S_{\underline{u}}^+ S_{\underline{u}+\underline{r}}^- + S_{\underline{u}}^- S_{\underline{u}+\underline{r}}^+)$$

$$+ (r_{ij}^2 S_{\underline{u}}^z S_{\underline{u}+\underline{r}}^z) - 3(S_{\underline{u}}^z r_z + \tfrac{1}{2} S_{\underline{u}}^+ r^- + \tfrac{1}{2} S_{\underline{u}}^- r^+)$$

$$\times (S_{\underline{u}+\underline{r}}^z r_z + \tfrac{1}{2} S_{\underline{u}+\underline{r}}^+ r^- + \tfrac{1}{2} S_{\underline{u}+\underline{r}}^- r^+)]\} \quad \text{(II-33)}$$

which can be simplified by rearranging terms, noting that $r^-r^+ = r^+r^- = r^2 - r_z^2 = r^2 - z^2$, to be

$$= \frac{g^2\mu_B^2}{2} \sum_{\underline{u}} \sum_{\underline{r}} \{\frac{1}{r^5} [(r^2 - 3z^2) S_{\underline{u}}^z S_{\underline{u}+\underline{r}}^z + \frac{1}{4} (S_{\underline{u}}^+ S_{\underline{u}+\underline{r}}^- + S_{\underline{u}}^- S_{\underline{u}+\underline{r}}^+)$$

$$\times (3z^2 - r^2) - \frac{3}{2} zr^- (S_{\underline{u}}^z S_{\underline{u}+\underline{r}}^+ + S_{\underline{u}}^+ S_{\underline{u}+\underline{r}}^z)$$

$$- \frac{3}{2} zr^+ (S_{\underline{u}}^z S_{\underline{u}+\underline{r}}^- + S_{\underline{u}}^- S_{\underline{u}+\underline{r}}^z) - \frac{3}{4} (S_{\underline{u}}^+ S_{\underline{u}+\underline{r}}^+ (r^-)^2$$

$$+ S_{\underline{u}}^- S_{\underline{u}+\underline{r}}^- (r^+)^2)]\} \quad . \qquad \text{(II-34)}$$

Assuming z to be the equilibrium direction of the spin, the stability condition demands that the terms linear in x or y vanish so that at equilibrium

$$H_{d-d} = \frac{g^2\mu_B^2}{2} \sum_{\underline{u}} \sum_{\underline{r}} \{\frac{1}{r^5} [(r^2 - 3z^2) S_{\underline{u}}^z S_{\underline{u}+\underline{r}}^z$$

$$+ \frac{1}{4} (S_{\underline{u}}^+ S_{\underline{u}+\underline{r}}^- + S_{\underline{u}}^- S_{\underline{u}+\underline{r}}^+) (3z^2 - r^2)$$

$$- \frac{3}{4} (S_{\underline{u}}^+ S_{\underline{u}+\underline{r}}^+ (r^-)^2 + S_{\underline{u}}^- S_{\underline{u}+\underline{r}}^- (r^+)^2)]\} \quad . \qquad \text{(II-35)}$$

Let us define

$$E_r = \frac{g^2\mu_B^2}{4} \frac{3z^2 - r^2}{r^5} \quad , \quad B_r = -\frac{3}{8} g^2\mu_B^2 \frac{(r^-)^2}{r^5}$$

and their Fourier transforms as

$$E_q = \sum_s E_s \exp(i\underline{q}\cdot\underline{s}) \quad , \quad E'_q = \sum_d E_d \exp(i\underline{q}\cdot\underline{d})$$

and

$$B_q = \sum_s B_s \exp(i\underline{q}\cdot\underline{s}) \quad , \quad B'_q = \sum_d B_d \exp(i\underline{q}\cdot\underline{d}) \quad . \tag{II-36}$$

Splitting the summation in terms of ℓ and m sublattices as was done for the exchange Hamiltonian, and combining it with H^0_{ex} as given by (II-8), we get

$$\begin{aligned} H_{TOT} &= H^0_{ex} + H_{d-d} \\ &= -\sum_{\underline{\ell}\underline{s}} [(J_s + 2E_s) S^z_{\underline{\ell}} S^z_{\underline{\ell}+\underline{s}} + \tfrac{1}{2}(J_s - E_s) \\ &\quad \times (S^+_{\underline{\ell}} S^-_{\underline{\ell}+\underline{s}} + S^-_{\underline{\ell}} S^+_{\underline{\ell}+\underline{s}}) - B_s S^+_{\underline{\ell}} S^+_{\underline{\ell}+\underline{s}} \\ &\quad - B^*_s S^-_{\underline{\ell}} S^-_{\underline{\ell}+\underline{s}}] - \sum_{\underline{m}\underline{s}} [(J_s + 2E_s) S^z_{\underline{m}} S^z_{\underline{m}+\underline{s}} \\ &\quad + \tfrac{1}{2}(J_s - E_s)(S^+_{\underline{m}} S^-_{\underline{m}+\underline{s}} + S^-_{\underline{m}} S^+_{\underline{m}+\underline{s}}) - B_s S^+_{\underline{m}} S^+_{\underline{m}+\underline{s}} \\ &\quad - B^*_s S^-_{\underline{m}} S^-_{\underline{m}+\underline{s}}] - 2 \sum_{\underline{\ell}\underline{d}} [(J_d + 2E_d) S^z_{\underline{\ell}} S^z_{\underline{\ell}+\underline{d}} \\ &\quad + \tfrac{1}{2}(J_d - E_d)(S^+_{\underline{\ell}} S^-_{\underline{\ell}+\underline{d}} + S^-_{\underline{\ell}} S^+_{\underline{\ell}+\underline{d}}) - B_d S^+_{\underline{\ell}} S^+_{\underline{\ell}+\underline{d}} \\ &\quad - B^*_d S^-_{\underline{\ell}} S^-_{\underline{\ell}+\underline{d}}] \end{aligned} \tag{II-37}$$

Using Eq. (II-15) for going over to boson operators and then using (II-17) and (II-36) to Fourier transform, we get

$$H_{TOT} = S \sum_q [(a_q^\dagger a_q + b_q^\dagger b_q)(2J_s(\underline{0}) + 4E_{\underline{0}} - 4E'_{\underline{0}}$$

$$+ E_{\underline{q}} + E_{-\underline{q}} - J_s(\underline{q}) - J_s(-\underline{q}) - 2J_d(\underline{0}))]$$

$$+ 2S \sum_q [B_{-q}(a_{-q}a_q + b_{-q}^\dagger b_q^\dagger) + B^*_{-q}(a_{-q}^\dagger a_q^\dagger + b_{-q}b_q)]$$

$$- 2S \sum_q [(J_d(-\underline{q}) - E'_{-\underline{q}})a_q^\dagger b_q^\dagger + (J_d(\underline{q}) - E'_{\underline{q}})a_q b_q]$$

$$+ 4S \sum_q [B'_{-q}a_{-q}b_q^\dagger + B'^*_{-q}a_{-q}^\dagger b_q] \qquad \text{(II-38)}$$

Let us define

$$U_{\underline{q}} = -S[-2J_s(0) - 4E_0 + 4E'_0 - E_{\underline{q}} - E_{-\underline{q}} + J_s(\underline{q})$$

$$+ J_s(-\underline{q}) + 2J_d(0)]$$

$$V_{\underline{q}} = L^*_{\underline{q}} + L^*_{-\underline{q}} = 2S(B^*_{\underline{q}} + B^*_{-\underline{q}}) \qquad \text{(II-39)}$$

$$W_{\underline{q}} = 4SB'^*_{\underline{q}}$$

$$X_{\underline{q}} = -2S(J_d(\underline{q}) - E'_{\underline{q}})$$

so that H_{TOT} can be written as

$$H_{TOT} = \sum_q [U_q(a_q^\dagger a_q + b_q^\dagger b_q) + L_{-q}(a_{-q}a_q + b_{-q}^\dagger b_q^\dagger)$$

$$+ L_{-q}^*(a_{-q}^\dagger a_q^\dagger + b_{-q}b_q) + X_{-q}a_q^\dagger b_q^\dagger + X_q a_q b_q$$

$$+ W_{-q}^* a_{-q} b_q^\dagger + W_{-q} a_{-q}^\dagger b_q] \quad \text{(II-40)}$$

Symmetrizing the Hamiltonian with q restricted to only positive values in the summation, we get

$$H_{TOT} = \sum_q [U_q(a_q^\dagger a_q + b_q^\dagger b_q) + U_{-q}(a_{-q}^\dagger a_{-q} + b_{-q}^\dagger b_{-q})$$

$$+ L_{-q}(a_{-q}a_q + b_{-q}^\dagger b_q^\dagger) + L_q(a_q a_{-q} + b_q^\dagger b_{-q}^\dagger)$$

$$+ L_{-q}^*(a_{-q}^\dagger a_q^\dagger + b_{-q}b_q) + L_q^*(a_q^\dagger a_{-q}^\dagger + b_q b_{-q})$$

$$+ X_{-q}a_q^\dagger b_q^\dagger + X_q a_{-q}^\dagger b_{-q}^\dagger + X_q a_q b_q + X_{-q}a_{-q}b_{-q}$$

$$+ W_{-q}^* a_{-q} b_q^\dagger + W_q^* a_q b_{-q}^\dagger + W_{-q} a_{-q}^\dagger b_q + W_q a_q^\dagger b_{-q}] \quad \text{(II-41)}$$

Let α_q be the suitable linear combination of operators a_q, $a_{-q}^\dagger$, b_{-q}, $b_q^\dagger$ with coefficients as u, v, w and x

$$\alpha_q = ua_q + va_{-q}^\dagger + wb_{-q} + xb_q^\dagger \quad \text{(II-42)}$$

which diagonalizes the Hamiltonian (II-41) with eigenvalue λ_q.

Then one can write

$$[H,\alpha_q] = u[-a_q U_q - a^\dagger_{-q}(L^*_{-q} + L^*_q) - b^\dagger_q X_{-q} - W_q b_{-q}]$$

$$+ v[a^\dagger_{-q} U_{-q} + a_q(L_{-q} + L_q) + b_{-q} X_{-q} + W^*_{-q} b^\dagger_q]$$

$$+ w[-b_{-q} U_{-q} - b^\dagger_q(L_{-q} + L_q) - a^\dagger_{-q} X_q - W^*_q a_q]$$

$$+ x[b^\dagger_q U_q + b_{-q}(L^*_{-q} + L^*_q) + a_q X_q + W_{-q} a^\dagger_{-q}]$$

$$= a_q[-uU_q + vV^*_q - wW^*_q + xX_q]$$

$$+ a^\dagger_{-q}[-uV_q + vU_{-q} - wX_q + xW_{-q}]$$

$$+ b_{-q}[-uW_q + vX_{-q} - wU_{-q} + xV_q]$$

$$+ b^\dagger_q[-uX_{-q} + vW^*_{-q} - wV^*_q + xU_q]$$

$$= a_q u\lambda_q + a^\dagger_{-q} v\lambda_q + b_{-q} w\lambda_q + b^\dagger_q x\lambda_q \qquad \text{(II-43)}$$

where the equality in the last line makes use of

$$[H,\alpha_q] = \lambda_q \alpha_q = \lambda_q(ua_q + va^\dagger_{-q} + wb_{-q} + xb^\dagger_q) \quad . \qquad \text{(II-44)}$$

Hence, the eigenvalue is given by the determinant

$$\begin{vmatrix} -U_q-\lambda_q & V_q^* & -W_q^* & X_q \\ -V_q & U_{-q}-\lambda_q & -X_q & W_{-q} \\ -W_q & X_{-q} & -U_{-q}-\lambda_q & V_q \\ -X_{-q} & W_{-q}^* & -V_q^* & U_q-\lambda_q \end{vmatrix} = 0 \qquad \text{(II-45)}$$

It is possible to put this solution in a more elegant form. Defining A_{qi} as a first rank tensor with a_q, $a_{-q}^{\dagger}$, b_{-q}, $b_q^{\dagger}$ as its four components and M_{qij} as a 4×4 second rank tensor, the Hamiltonian as given by (II-41) can be written as

$$H = \sum_q \sum_{ij} A_{qi}^{\dagger} M_{qij} A_{qj} \qquad \text{(II-46)}$$

which leads to

$$[H, A_{qi}] = \sum_j (-1)^j M_{qij} A_{qj} \qquad \text{(II-47)}$$

and

$$[H, A_{qi}] = -i\hbar \frac{dA_{qi}}{dt} \qquad \text{(II-48)}$$

We look for the solutions of the type

$$\frac{dA_{\underline{q}i}}{dt} = i \frac{\lambda_q}{\hbar} A_{\underline{q}i}$$

so that

$$\sum_j [(-1)^i M_{\underline{q}ij} - \lambda_q \delta_{ij}] A_{\underline{q}j} = 0 \quad . \tag{II-49}$$

Thus the spin wave energies are the solutions of the equation

$$\det \left| (-1)^i M_{\underline{q}ij} - \lambda_q \delta_{ij} \right| = 0 \tag{II-50}$$

and the elements of $M_{\underline{q}ij}$ are given in the matrix format by the equation

$$M_{\underline{q}} = \begin{vmatrix} U_q & -V_q^* & W_q^* & -X_q \\ -V_q & U_{-q} & -X_q & W_{-q} \\ W_q & -X_{-q} & U_{-q} & V_q \\ -X_{-q} & W_{-q}^* & -V_q^* & U_q \end{vmatrix} \tag{II-51}$$

Defining

$$D_s^{IJ}(q) = g^2 \mu_B^2 \sum_s \frac{1}{s^5} [3s_I s_J - s^2 \delta_{IJ}] \exp(i\underline{q} \cdot \underline{s})$$

and

$$D_d^{IJ}(q) = g^2 \mu_B^2 \sum_d \frac{1}{d^5} (3d_I d_J - d^2 \delta_{IJ}) \exp(i\underline{q} \cdot \underline{d}) \tag{II-52}$$

where $\underline{s}$ and $\underline{d}$ vectors have been defined earlier and I and J are any one of the three cartesian coordinates x, y, z with the z axis defined along the direction of sublattice magnetization, one would have

$$D_s^{xx}(q) = g^2\mu_B^2 \sum_s \frac{1}{s^5} [3x_s^2 - s^2]\exp(i\underline{q}\cdot\underline{s})$$

$$D_s^{yy}(q) = g^2\mu_B^2 \sum_s \frac{1}{s^5} [3y_s^2 - s^2]\exp(i\underline{q}\cdot\underline{s})$$

$$D_s^{xy}(q) = g^2\mu_B^2 \sum_s \frac{1}{s^5} [3x_s y_s]\exp(i\underline{q}\cdot\underline{s})$$

$$\therefore \quad \frac{-S}{2}(D_s^{xx}(q) - D_s^{yy}(q) + 2iD_s^{xy}(q))$$

$$= \frac{-3S}{2} g^2\mu_B^2 \sum_s \frac{1}{s^5} (x^2 - y^2 + 2ixy)\exp(i\underline{q}\cdot\underline{s})$$

$$= \frac{-3S}{2} g^2\mu_B^2 \sum_s \frac{1}{s^5} (r_s^+)^2 \exp(i\underline{q}\cdot\underline{s}) \qquad \text{(II-53)}$$

$$= V_q \text{ (from Eq. (II-39), assume } B_q^* = B_{-q}^*)$$

Also one could show in an analogous fashion that

$$W_q = -\frac{S}{2} [D_d^{xx}(q) - D_d^{yy}(q) + 2iD_d^{xy}(q)] \qquad \text{(II-54)}$$

$$D_s^{zz}(q) = g^2\mu_B^2 \sum_s \frac{1}{s^5} (3z_s^2 - s^2)\exp(i\underline{q}\cdot\underline{s})$$

$$= 4E_q$$

and

$$D_d^{zz}(q) = 4E'_q \quad (\text{assume } J_s(q) = J_s(-q)$$

$$D(q) = D(-q))$$

so that one could write Eq. (II-39) as

$$U_{\underline{q}} = - S[2J_d(0) - 2J_s(0) + D_d^{zz}(0) - D_s^{zz}(0) - \tfrac{1}{2} D_s^{zz}(\underline{q})]$$

$$V_{\underline{q}} = - S[\tfrac{1}{2} D_s^{xx}(\underline{q}) - \tfrac{1}{2} D_s^{yy}(\underline{q}) + iD_s^{xy}(\underline{q})]$$

$$W_{\underline{q}} = - S[\tfrac{1}{2} D_d^{xx}(\underline{q}) - \tfrac{1}{2} D_d^{yy}(\underline{q}) + iD_d^{xy}(\underline{q})]$$

$$X_{\underline{q}} = - S[2J_d(\underline{q}) - \tfrac{1}{2} D_d^{zz}(\underline{q})] \quad . \qquad \text{(II-55)}$$

The numerical calculations of the dipole sums can be performed using the Ewald technique. It is based on Eq. (30-31) of 'Dynamical Theory of Crystal Lattices' by Born and Huang (1954). The technique involves doing the sums to near atoms directly, whereas the sums for atoms at more than a certain distance are performed in reciprocal space. This technique is used in Chapter VI to calculate the dipole sums for MnO.

One can see that the full effects of dipole-dipole interactions on the spin wave spectrum of an antiferromagnet

are quite complicated, and they give rise to wave vector dependent contributions to the spin wave energies. However, since the magnitude of these effects is very small compared to exchange interactions except at small wave vectors, often dipole-dipole interactions are treated in an approximate way in which their $\underline{q}$ dependence is ignored. The usual way is to represent all the anisotropy in terms of two parameters D_1 and D_2. They describe the out-of-plane and in-plane anisotropies respectively, and are related to in-plane and out-of-plane anisotropy energies K_1 and K_2 by the equations

$$D_i = \frac{3K_i}{2NS^2} \quad (i = 1, 2) \qquad \text{-(II-56)}$$

where N is the number of spins/c.c. in the system.

This gives rise to energy contributions by dipole-dipole interactions which are wave vector independent. Besides earlier works (e.g., Lines and Jones, 1965), even recently this treatment has been used by Kohgi et al. (1972) and Hutchings et al. (1973) to describe the dipole-dipole interactions in MnO and NiO respectively.

The approximate dipole-dipole interaction Hamiltonian H_{d-d}^{Ap}, which assumes crystal field type single ion anisotropy for an antiferromagnet with ℓ and m sublattices, can be written as

$$H^{Ap}_{d-d} = \sum_{\underline{\ell}} D_1 S^2_{\underline{\ell}x} + \sum_{\underline{m}} D_1 S^2_{\underline{m}x} + \sum_{\underline{\ell}} D_2 S^2_{\underline{\ell}y} + \sum_{\underline{m}} D_2 S^2_{\underline{m}y} \qquad \text{(II-57)}$$

where y and x are directions which are both normal to the direction z of spin alignment and are respectively parallel and perpendicular to the plane to which the spins are confined (say (111) plane for MnO or NiO).

Although the above form of H^{Ap}_{d-d} is the one commonly used when the dipole-dipole interactions are treated in the approximate way, following Keffer et al. (1957); Collins (1964) in his earlier paper on MnO uses a more general form in which in addition to the above terms, the cross terms are also assumed to contribute to the anisotropy.

The total Hamiltonian H^{Ap}_{TOT} will be the sum of H^0_{ex} as given by Eq. (II-8) and H^{Ap}_{d-d} as given by Eq. (II-57). The eigenvalues of H^{Ap}_{TOT}, by following a procedure analogous to one used to obtain eigenvalues of H^0_{ex}, can be shown to be given by two non degenerate solutions

$$\lambda_q = [(A_q - B_q + 2SD_1)(A_q + B_q + 2SD_2)]^{1/2}$$

and (II-58)

$$\mu_q = [(A_q + B_q + 2SD_1)(A_q - B_q + 2SD_2)]^{1/2}$$

with A_q and B_q as defined by Eq. (II-21).

In the case of the in-plane anisotropy term D_2 being

negligible, the energy of the out-of-plane mode can, approximately, be written as

$$\lambda_q = (A_q'^2 - B_q^2)^{1/2} \qquad \text{(II-59)}$$

where

$$A_q' = A_q + 2SD_\perp = A_q + H_A \quad .$$

This approach, with eigenvalues as given by (II-59), is used in Chapter VIII to calculate spin wave energies.

2.3 Scattering Theory as Applied to the Measurements of Spin Waves with Neutrons

The scattering of neutrons by atoms possessing magnetic moments needs the use of the Dirac equation for a proper treatment of the interaction between the neutron and the magnetic electrons (Halpern and Johnson, 1939). The magnetic part of the interaction for a neutron in a magnetic field $\underline{H}$ arising from the unpaired electrons in a crystal can be written in the form (Marshall and Lovesey, 1971)

$$-\gamma\mu_N \hat{\underline{\sigma}}\cdot\underline{H} \qquad \text{(II-60)}$$

where $\hat{\sigma}^\alpha$ are Pauli matrices. It can be shown that for spin-only systems of N spins the neutron scattering cross-section per unit solid angle Ω and per unit energy E' of the scattered neutron is given by

$$\frac{d^2\sigma}{d\Omega dE'} = \left(\frac{\gamma e^2}{m_e c^2}\right)^2 \frac{N}{\hbar}\frac{k'}{k}\,[f(\underline{Q})]^2 \sum_{\alpha\beta}(\delta_{\alpha\beta} - \hat{Q}_\alpha\hat{Q}_\beta)\mathcal{S}^{\alpha\beta}(\underline{Q},\omega) \qquad \text{(II-61)}^*$$

where e and m_e are the charge and the mass of the electron, γ is the gyromagnetic ratio for the neutron and $f(\underline{Q})$ is the neutron form factor. $\underline{k}$, E and $\underline{k}'$, E' are the initial and final wave vector and energy of the neutron respectively, $\underline{Q} = \underline{k}-\underline{k}'$ is the scattering vector, $\hbar\omega = E-E'$ is the neutron

---

* In writing (II-61), the Debye-Waller factor is ignored, amounting to a stationary system of spins.

energy change. $\hat{Q}_\alpha$ is the α direction cosine of $\underline{Q}$, and α,β are coordinates x, y, z. Lande's splitting factor g is assumed to have its spin-only value of g=2. $\mathcal{S}^{\alpha\beta}(\underline{Q},\omega)$ is the Van Hove scattering function defined as

$$\mathcal{S}^{\alpha\beta}(\underline{Q},\omega) = \sum_{if} p_i \sum_{uu'} \exp(i\underline{Q}\cdot(\underline{R}_u - \underline{R}_{u'})) \langle i|S_u^\alpha|f\rangle \times \langle f|S_{u'}^\beta|i\rangle \delta(\hbar\omega + E_f - E_i) \qquad \text{(II-62)}$$

where S_u^α is the α component of the spin operator S on the lattice site denoted by u, $|i\rangle$ and $|f\rangle$ are the initial and final states of the spin system with E_i and E_f as the corresponding energies, and p_i is the probability that the target spin system is in the initial state $|i\rangle$. The energy and the momentum conservation laws demand that

$$\hbar\omega = E - E' = \frac{\hbar^2 k^2}{2m_n} - \frac{\hbar^2 k'^2}{2m_n}$$

and (II-63)

$$\underline{Q} = \underline{k} - \underline{k}' = \underline{q} + \underline{\tau}$$

where m_n is the mass of the neutron, $\underline{q}$ is a wave vector restricted to first Brillouin zone, and $\underline{\tau}$ is a reciprocal lattice vector.

For the sake of simplicity, we shall limit ourselves to just finding out the form that the scattering cross-section assumes for a two sublattice antiferromagnet described by the

exchange Hamiltonian (II-1). This treatment was first given by Nagai and Yoshimori (1961).

For an isotropic exchange Hamiltonian not all the terms given by (II-61) contribute to scattering. Using (II-3) to write, say, S_u^x in terms of S_u^+ and S_u^- and (II-4) to find out the matrix elements that are non-zero, one can show that

$$\mathcal{S}^{xz}(\underline{Q},\omega) = \mathcal{S}^{yz}(\underline{Q},\omega) = \mathcal{S}^{zx}(\underline{Q},\omega) = \mathcal{S}^{zy}(\underline{Q},\omega) = 0 \qquad \text{(II-64)}$$

and

$$\mathcal{S}^{xy}(\underline{Q},\omega) + \mathcal{S}^{yx}(\underline{Q},\omega) = 0 \quad . \qquad \text{(II-65)}$$

Thus, the only non-zero terms are $\mathcal{S}^{zz}(\underline{Q},\omega)$, $\mathcal{S}^{xx}(\underline{Q},\omega)$ and $\mathcal{S}^{yy}(\underline{Q},\omega)$. $\mathcal{S}^{zz}(\underline{Q},\omega)$ leads only to elastic scattering which does not concern us. Moreover, for Hamiltonian (II-1), $\mathcal{S}^{xx}(\underline{Q},\omega)$ and $\mathcal{S}^{yy}(\underline{Q},\omega)$ will have equivalent contributions. With all these simplifications, Eq. (II-61) reduces to

$$\frac{d^2\sigma}{d\Omega dE'} = \left(\frac{\gamma e^2}{m_e c^2}\right)^2 \frac{N}{\hbar}\frac{k'}{k}\,|f(\underline{Q})|^2\,(1 + \hat{Q}_z^2)\,\mathcal{S}^{xx}(\underline{Q},\omega)$$

where

$$\mathcal{S}^{xx}(\underline{Q},\omega) = \sum_{if} p_i \sum_{uu'} \exp(i\underline{Q}\cdot(\underline{R}_u - \underline{R}_{u'}))$$

$$\times \langle i|S_u^x|f\rangle\langle f|S_{u'}^x|i\rangle\,\delta(\hbar\omega + E_f - E_i) \quad . \qquad \text{(II-66)}$$

With some steps of manipulation that involve writing (II-66) in terms of α_q and β_q operators using (II-15), (II-17) and (II-28), etc., it is possible to show that the inelastic scattering cross-section for one magnon creation (a consequence of restricting to linear theory) for a two sublattice antiferromagnet is given by

$$\left(\frac{d^2\sigma}{d\Omega dE'}\right)_{A.F.} = \left(\frac{\gamma e^2}{m_e c^2}\right)^2 \frac{NSk'}{2\hbar k} |f(\underline{Q})|^2 (1 + \hat{Q}_z^2)$$

$$\times \sum_q [\cosh 2\theta_q - \sinh 2\theta_q (\cos \underline{\tau} \cdot \underline{\omega})]$$

$$\times \delta(\lambda_q - \hbar\omega)\, \delta(\underline{Q} - \underline{q} - \underline{\tau}) \qquad \text{(II-67)}$$

where $\underline{\omega}$ is a vector joining the two sublattices, and $(\cosh 2\theta_q - \sinh 2\theta_q \cos(\underline{\tau} \cdot \underline{\omega}))$ is the so-called dynamic structure factor.

Since this formula for the cross-section in which a single magnon is created contains both an energy and momentum conservation condition, neutron inelastic experiments can determine the whole spin wave spectrum. The one magnon cross-sections are of the order of millibarns.

The orientation factor $(1 + \hat{Q}_z^2)$ has a minimum value of unity if the direction of magnetization z is perpendicular to $\underline{Q}$ and has a maximum value of 2 if the direction of magnetization is parallel to the scattering vector $\underline{Q}$. Moreover, because the magnetic form factor $f(\underline{Q})$ falls off

with $\underline{Q}$, experiments should be performed at small values of $\underline{Q}$ for most intensity. These features of magnetic scattering can be used to distinguish it from nuclear scattering.

Let us consider the primitive cubic magnetic cell of a simple antiferromagnet consisting of an atom of spin up at (0,0,0) and of spin down at (1/2,1/2,1/2) in the antiferromagnetic phase. In the paramagnetic phase this would correspond to a body centred cubic cell. For such a case

$$\underline{\omega} = \frac{a}{2}(1,1,1) \quad , \quad \underline{\tau} = \frac{2\pi}{a}(h,k,\ell) \quad .$$

Denoting the static structure factor (structure factor for the elastic scattering) for magnetic and nuclear scattering by F_M and F_N respectively, one has for this cell

$$F_M \propto 1 - \exp\pi i(h + k + \ell)$$

and (II-68)

$$F_N \propto 1 + \exp\pi i(h + k + \ell)$$

so that reflections with $(h + k + \ell) = 2n + 1$, belong to the magnetic zone and with $(h + k + \ell) = 2n$, to the nuclear zone. Then one has

$$\cos(\underline{\tau}_M \cdot \underline{\omega}) = \cos(2n+1)\pi = -1$$

and (II-69)

$$\cos(\underline{\tau}_N \cdot \underline{\omega}) = \cos(2n\pi) = +1$$

where $\underline{\tau}_M$ and $\underline{\tau}_N$ are respectively a magnetic and nuclear reciprocal lattice vector. So that using (II-67) and (II-29),

$$\text{magnetic dynamic S.F.} = \cosh 2\theta_q - \sinh 2\theta_q(-1)$$

$$= (\Lambda_q + B_q)/\lambda_q$$

and (II-70)

$$\text{nuclear dynamic S.F.} = \cosh 2\theta_q - \sinh 2\theta_q(+1)$$

$$= (\Lambda_q - B_q)/\lambda_q \quad .$$

In order to calculate the cross-section for scattering at a particular point in the reciprocal space, care must be taken to include the contribution of each domain in a multidomain crystal.

CHAPTER III

THE ZERO TEMPERATURE PROPERTIES OF HEISENBERG ANTIFERROMAGNETS

The purpose of this chapter is to provide the general background and review earlier work done on zero temperature properties of the Heisenberg antiferromagnet.

The starting point of a spin wave theory of a magnetic system is the ground state of the spin system. It is not possible to understand the magnons, the elementary excitations of the magnetic system, without knowing the ground state, because it is the small deviations from this state that produces them. In ferromagnets the state of complete alignment of spin is taken as the ground state from which the spin waves are generated. There is only one way of achieving the maximum alignment, and it is easy to show that this* $\alpha_1\alpha_2\alpha_3\alpha_4 \ldots\alpha_n$ spin state is an eigenfunction of the exchange Hamiltonian. However, for an antiferromagnet, at the very onset, the theory is faced with the difficulty that the ground state is not known because antiferromagnets, by their very nature, cannot be represented by a simple

---

* α and β are up and down projections of spin 1/2.

nondegenerate ground state. The Néel state, which corresponds to a complete alignment ($S_z = + S$ for all the spins on one sublattice; $S_z = - S$ for all the spins on the other) for an antiferromagnet, e.g., the state $\alpha_1\beta_2\alpha_3\beta_4 \ldots \alpha_{n-1}\beta_n$ for spin 1/2, is not an eigenfunction of the exchange Hamiltonian, since the same total spin of zero is described by $\beta_1\alpha_2\beta_3\alpha_4 \ldots$ and by many others all of which lie very close in energy and must be combined to describe the ground state properly. Thus, one expects that in an antiferromagnet even in its lowest energy state, the ground state, some degree of disorder would be present.

The problem of not being able to know the exact ground state is not unique to an antiferromagnet. As a matter of fact, but for a few exceptions, we do not know the true ground state of any N-body system, and hence are not in a position to obtain the excited states except under some approximation.

The above discussion may lead one to believe that spin wave theory can reasonably be applied to ferromagnetic cases, while it is not so good for antiferromagnetic cases. Spin wave theory is perfectly rigorous for the ground state of a ferromagnet, but in the presence of dipolar interactions, it remains only an approximation, just as it is for an antiferromagnet. Moreover, the difficulties with regard to the excited states seem almost of the same nature in the two

cases. In fact, spin wave theory is applicable to antiferromagnets as much as it is to ferromagnets.

The fact, that the simple Néel state is not the ground state, affects various properties of an antiferromagnet notably the total energy of the system, the spin wave energy and the sublattice magnetization. Also, the zero point spin deviation is yet another factor that reduces the intensities of antiferromagnetic peaks, and hence needs to be known for the accurate determination of covalency parameters (Marshall and Lovesey, 1971).

Historically, Klein and Smith (1951) first pointed out the significance of the zero point energy, and showed that only if it is included does one get the correct energy for the ferromagnetic ground state from the Kramer and Heller's (1934) semiclassical treatment. Anderson (1952) applied the semiclassical method of Kramer and Heller to the approximate determination of the ground state energy of an antiferromagnet in a fashion similar to the work of Klein and Smith (1951) by including the zero point energy. In this semiclassical approach one uses the idea that the commutation rule

$$[S_x, S_y] = iS_z \sim iS \qquad \text{(III-1)}$$

is, if S_z is nearly constant, approximately equivalent to the relation which would hold between S_x and S_y if they were

canonically conjugate variables, and that the expansion

$$S_z = [S(S+1) - S_x^2 - S_y^2]^{1/2} \sim (S - \frac{S_x^2 + S_y^2 - S}{2S}) \quad \text{(III-2)}$$

is also valid in the same approximation.

Using this approach Anderson was able to get good approximations, lying between the limits of his variation method, to the ground states of antiferromagnets. In the case of a linear chain with $S = \frac{1}{2}$, he got results close to the rigorous values earlier obtained by Bethe (1931). The calculations were done for the simple cubic lattice (and for the linear and plane square) and were restricted to nearest neighbour interactions only. The paper gave the first correction terms in the series for ground state energy as well as the first correction terms in the series for the magnetization.

Kubo (1952) was the first to study the properties of antiferromagnets using the approach followed in this thesis - the Holstein-Primakoff (H-P) approach (Eqs. (II-12) and (II-13)). This method is equivalent to the semiclassical method of Anderson, if Eq. (II-12) is approximated by Eq. (II-15), that is in the so-called Harmonic approximation since S_z can then be approximated as in Eq. (III-2). Using the H-P approach Kubo calculated the first two correction terms in the series for the ground state energy and the first correction terms for the magnetization for the simple

cubic lattice (as was done by Anderson) as well as for the body centred cubic lattice, though restricted to nearest neighbour interactions.

Oguchi (1960), using the same model as of Anderson and Kubo, and using the spin wave theory, calculated the next terms in the series for magnetization and also the first correction term in the series for the spin wave energy. The next term in the case of the magnetization series happened to be zero, because of the type of model used.

If one expands f_i as given by Eq. (II-9) binomially in Hilbert space of infinite dimensions, i.e.,

$$f_i = \left[1 - \frac{n_i}{2S}\right]^{1/2} \qquad \text{where } n_i = a_i^\dagger a_i$$

$$= 1 - \frac{n_i}{4S} - \frac{1}{32}\frac{n_i^2}{S^2} \cdots \qquad \text{(III-3)}$$

one observes that it is an expansion of the powers of not only n_i but also $1/S$. Oguchi points out that it is possible to treat the interaction part of the H-P Hamiltonian as a perturbation to the free spin wave Hamiltonian, if one regards the Hamiltonian of the system as an expansion of powers of $1/S$ and shows that one can get essentially the same results as of Dyson (1956) at least to order $1/S$.

Oguchi's paper transforms spin operators to bose operators using the H-P method and there has been little

advance using this approach since. Efforts have been made especially by Armour (1971) to proceed alternatively, using the D-M transformation.

Armour attempted to calculate the thermodynamic properties of antiferromagnets at low temperature using the Dyson-Wortis method. This method was successfully applied by Dyson and Wortis (Dyson, 1956; Wortis, 1965) to the case of ferromagnets. In the boson system corresponding to the ferromagnet, though the full dimensional space itself is infinite dimensional, the physical eigenvectors belong to finite subspaces containing a fixed number of particles, which makes it possible to prove a limited equivalence between the spin and boson system at low temperature. However, in the antiferromagnetic case the subspaces containing the physical eigenvectors are infinite and, in consequence, no such equivalence exists. Thus, the conditions which make a rigorous calculation possible in the case of ferromagnet do not hold for the antiferromagnet.

Various results arrived at by Oguchi using the H-P approach are quoted here, for the purpose of comparison with the expressions in Chapter IV.

The zero-point energy

$$E_0 = - Z|J|SN(S + C + C^2/4S) \qquad \text{(III-4)}$$

where

$$C = \left(\frac{2}{N}\right) \sum_{q} \left[1 - (1 - \gamma_q^2)^{1/2}\right] \qquad \text{(III-5)}$$

and

$$\gamma_q = \sum_{\rho} \frac{e^{i\underline{q}\cdot\underline{\rho}}}{Z} \quad . \qquad \text{(III-6)}$$

$\underline{\rho}$ is vector to the nearest neighbour and Z the number of nearest neighbours.

C and $C^2/4S$ are the first and the second correction terms to the ground state energy.

Spin wave energy with wave vector $\underline{q}$

$$A_q^0 = 2Z|J|S(1 + C/2S)(1 - \gamma_q^2)^{1/2} \qquad \text{(III-7)}$$

C/2S being the correction term.

Sublattice magnetization

$$M/g\mu_B = \frac{N}{2} [S - C'/2 - \text{function (temp)}]$$

$$= \frac{N}{2} [S - C'/2] (\text{at } T = 0K) \qquad \text{(III-8)}$$

C'/2 being the correction term, where

$$C' = \left(\frac{2}{N}\right) \sum_{q} \left[\frac{1}{(1 - \gamma_q^2)^{1/2}} - 1\right] \quad . \qquad \text{(III-9)}$$

We were initially motivated to extend spin wave theory to the face centred cubic antiferromagnets by our interest in applying it to MnO, which cannot be described by the models of Anderson, Kobo or Oguchi since even in the crudest approximation the exchange involves more than just the nearest neighbouring atoms on the different sublattices.

In the next chapter we formulate the theory for exchange interactions of general range. The treatment gives simple expressions for the ground state energy, spin wave energy and the sublattice magnetization. A new term in the sublattice magnetization is derived which was zero in Oguchi's treatment.

Before concluding this chapter it should be mentioned that unlike our and Oguchi's treatment, Harris (1968) has proposed an alternative spin wave expansion in terms of $1/Z$ where Z is the number of nearest neighbours of an atom. This approach is not considered in this thesis.

CHAPTER IV

ANTIFERROMAGNETIC GROUND STATE, IT'S CONTRIBUTION TO SPIN WAVE ENERGY AND THE SUBLATTICE MAGNETIZATION: AN EXTENSION OF THE THEORY TO AN ARBITRARY RANGE OF EXCHANGE INTERACTION

This chapter gives the formal theory of the extension of Oguchi's (1960) work to an arbitrary range of exchange interaction and the numerical calculations of the zero temperature constants for various lattices (Collins and Tondon, 1972).

4.1 Formal Theory

We shall examine the exchange only Heisenberg Hamiltonian in non-linear approximation at zero temperature.

The starting exchange Hamiltonian is as given by Eq. (II-8), which is reproduced here

$$H_{ex} = - \sum_{\underline{\ell}\underline{s}} J_s [\tfrac{1}{2} (S^+_{\underline{\ell}} S^-_{\underline{\ell}+\underline{s}} + S^-_{\underline{\ell}} S^+_{\underline{\ell}+\underline{s}}) + S^z_{\underline{\ell}} S^z_{\underline{\ell}+\underline{s}}]$$

$$+ \sum_{\underline{m}\underline{s}} J_s [\tfrac{1}{2} (S^+_{\underline{m}} S^-_{\underline{m}+\underline{s}} + S^-_{\underline{m}} S^+_{\underline{m}+\underline{s}}) + S^z_{\underline{m}} S^z_{\underline{m}+\underline{s}}]$$

$$- 2 \sum_{\underline{\ell}\underline{d}} J_d [\tfrac{1}{2} (S^+_{\underline{\ell}} S^-_{\underline{\ell}+\underline{d}} + S^-_{\underline{\ell}} S^+_{\underline{\ell}+\underline{d}}) + S^z_{\underline{\ell}} S^z_{\underline{\ell}+\underline{d}}] \qquad \text{(IV-1)}$$

For the sake of convenience, in the equations to follow, the vector sign for lattice vectors $\underline{\ell}$, $\underline{m}$, etc. is dropped.

As discussed in Chapter II there are two approaches of converting spin operators to expressions involving boson creation and annihilation operators, $a_\ell^\dagger$ and a_ℓ for one sublattice and $b_m^\dagger$ and b_m for the other:

a) Holstein-Primakoff Transformation (H-P)

b) Dyson-Maleev Transformation (D-M).

The subsequent analysis has been done using both the approaches.

4.1.1 H-P Approach

Again, we use H-P transformations as given by Eqs. (II-12) and (II-13), but instead of replacing f_ℓ and f_m by unity, one more term of the square-root expansion is taken, so that

$$f_\ell \approx 1 - a_\ell^\dagger a_\ell/4S$$

and (IV-2)

$$f_m \approx 1 - b_m^\dagger b_m/4S$$

Thus

$$S_\ell^z = S - a_\ell^\dagger a_\ell \quad ; \quad S_m^z = -S + b_m^\dagger b_m$$

$$S_\ell^+ = (2S)^{1/2}(1 - a_\ell^\dagger a_\ell / 4S)a_\ell$$

$$S_m^+ = (2S)^{1/2} b_m^\dagger (1 - b_m^\dagger b_m / 4S) \qquad \text{(IV-3)}$$

$$S_\ell^- = (2S)^{1/2} a_\ell^\dagger (1 - a_\ell^\dagger a_\ell / 4S)$$

$$S_m^- = (2S)^{1/2} (1 - b_m^\dagger b_m / 4S) b_m$$

Substituting in (IV-1) and retaining terms only to the order of $1/S^0$ (up to bilinear terms in boson operators)

$$\begin{aligned} H_{TOT}^{H-P} = - \sum_{\ell s} J_s [& S^2 - S(a_\ell^\dagger a_\ell + a_{\ell+s}^\dagger a_{\ell+s} - a_{\ell+s}^\dagger a_\ell - a_\ell^\dagger a_{\ell+s}) \\ & + (a_\ell^\dagger a_{\ell+s}^\dagger a_\ell a_{\ell+s}) - \tfrac{1}{4}(a_{\ell+s}^\dagger a_{\ell+s}^\dagger a_\ell a_{\ell+s} + a_\ell^\dagger a_{\ell+s}^\dagger a_\ell a_\ell \\ & + a_\ell^\dagger a_{\ell+s}^\dagger a_{\ell+s} a_{\ell+s} + a_\ell^\dagger a_\ell^\dagger a_\ell a_{\ell+s})] - \sum_{ms} J_s [S^2 \\ & - S(b_{m+s}^\dagger b_{m+s} + b_m^\dagger b_m - b_m^\dagger b_{m+s} - b_{m+s}^\dagger b_m) \\ & + (b_m^\dagger b_{m+s}^\dagger b_m b_{m+s}) - \tfrac{1}{4}(b_m^\dagger b_{m+s}^\dagger b_{m+s} b_{m+s} \\ & + b_m^\dagger b_m^\dagger b_m b_{m+s} + b_{m+s}^\dagger b_{m+s}^\dagger b_m b_{m+s} + b_m^\dagger b_{m+s}^\dagger b_m b_m)] \end{aligned}$$

continued over...

$$- 2 \sum_{\ell d} J_d [(-S^2) + S(b^\dagger_{\ell+d} b_{\ell+d} + a^\dagger_\ell a_\ell + a_\ell b_{\ell+d}$$

$$+ a^\dagger_\ell b^\dagger_{\ell+d}) - (a^\dagger_\ell b^\dagger_{\ell+d} a_\ell b_{\ell+d}) - \tfrac{1}{4}(b^\dagger_{\ell+d} a_\ell b_{\ell+d} b_{\ell+d}$$

$$+ a^\dagger_\ell a_\ell a_\ell b_{\ell+d} + a^\dagger_\ell b^\dagger_{\ell+d} b^\dagger_{\ell+d} b_{\ell+d} + a^\dagger_\ell a_\ell b^\dagger_{\ell+d} a_\ell)] \quad . \tag{IV-4}$$

The Hamiltonian (IV-4) can be Fourier transformed using Eq. (II-17). The non-linear part of the Hamiltonian is given by

$$H^{H-P}_{non-lin} = (\tfrac{1}{N}) \sum_{q_1 q_2 q_3 q_4} [4J_d(q_4 - q_3) a^\dagger_{q_1} a_{q_2} b^\dagger_{q_3} b_{q_4}$$

$$\times \delta(q_1 + q_4 - q_2 - q_3)$$

$$+ J_d(q_1) a^\dagger_{q_1} b^\dagger_{q_2} b^\dagger_{q_3} b_{q_4} \delta(q_1 + q_4 - q_2 - q_3)$$

$$+ J_d(q_4) a^\dagger_{q_1} a^\dagger_{q_2} a_{q_3} b^\dagger_{q_4} \delta(q_1 + q_2 - q_3 - q_4)$$

$$+ J_d(q_1) a_{q_1} b^\dagger_{q_2} b_{q_3} b_{q_4} \delta(q_3 + q_4 - q_1 - q_2)$$

$$+ J_d(q_4) a^\dagger_{q_1} a_{q_2} a_{q_3} b_{q_4} \delta(q_1 + q_4 - q_2 - q_3)]$$

$$- (\tfrac{2}{N}) \sum_{q_1 q_2 q_3 q_4} [(a^\dagger_{q_1} a^\dagger_{q_2} a_{q_3} a_{q_4} + b^\dagger_{q_1} b^\dagger_{q_2} b_{q_3} b_{q_4})$$

continued over...

$$\times [J_s(q_2 - q_4) - \frac{1}{4}(J_s(q_1) + J_s(q_2)$$

$$+ J_s(q_3) + J_s(q_4))]\delta(q_3 + q_4 - q_1 - q_2)\}$$

(IV-5)

whereas the linear part of the Hamiltonian as given by Eq. (II-20), with E_0, A_q and B_q as defined by Eq. (II-21), is

$$H_{lin}^{H-P} = E_0 + \sum_q A_q(a_q^\dagger a_q + b_q^\dagger b_q)$$

$$+ \sum_q B_q(a_q b_q + a_q^\dagger b_q^\dagger) \quad .$$

(IV-6)

Oguchi has shown that the leading terms in $H_{non-lin}$ are those that can be decoupled to two independent spin waves. The $H_{non-lin}$ can then be written as

$$H_{non-lin}^{H-P} = (\frac{4}{N}) \sum_{q_1 q_2} [J_d(0) a_{q_1}^\dagger a_{q_1} b_{q_2}^\dagger b_{q_2}$$

$$+ J_d(q_2 - q_1) a_{q_1}^\dagger b_{q_1}^\dagger a_{q_2} b_{q_2}]$$

$$+ (\frac{2}{N}) \sum_{q_1 q_2} J_d(q_1) a_{q_1}^\dagger b_{q_1}^\dagger b_{q_2}^\dagger b_{q_2}$$

$$+ (\frac{1}{N}) \sum_{q_1 q_2} (J_d(q_2) a_{q_1}^\dagger a_{q_1} a_{q_2}^\dagger b_{q_2}^\dagger$$

$$+ J_d(q_1) a_{q_1}^\dagger b_{q_1}^\dagger a_{q_2}^\dagger b_{q_2}) + (\frac{2}{N}) \sum_{q_1 q_2} J_d(q_1)$$

continued over...

$$\times a_{q_1} b_{q_1} b^{\dagger}_{q_2} b_{q_2} + \left(\frac{2}{N}\right) \sum_{q_1 q_2} J_d(q_2) a^{\dagger}_{q_1} a_{q_1} a_{q_2} b_{q_2}$$

$$- \left(\frac{2}{N}\right) \sum_{q_1 q_2} [J_s(0) - J_s(q_1) - J_s(q_2)$$

$$+ J_s(q_1 - q_2)] a^{\dagger}_{q_1} a_{q_1} a^{\dagger}_{q_2} a_{q_2} - \left(\frac{2}{N}\right) \sum_{q_1 q_2}$$

$$[J_s(0) - J_s(q_2) - J_s(q_1) + J_s(q_1 - q_2)]$$

$$\times b^{\dagger}_{q_1} b_{q_1} b^{\dagger}_{q_2} b_{q_2} \quad . \qquad \text{(IV-7)}$$

Using the Bogoliubov transformation (Eq. (II-28)) one could diagonalize the bilinear terms as given by (IV-7). [The condition as given by (II-29) ensures that linear terms given by (IV-6) come out to be diagonalized. This transformation puts bilinear terms in the form of Eq. (II-20), whose eigenvalues, we know, are given by an equation of the form (II-26).] After the transformation, the creation operators are commuted so as to be on the left of destruction operators; thus they appear as boson occupation numbers, whose expectation values tend to be small at low temperature. Only terms linear in α and β operators are retained.

Let us pick up a bilinear term, (in operators a and b) from Eq. (IV-7) and get its transformed form. We pick up, say the first term

$$\left(\frac{4}{N}\right) \sum_{q_1 q_2} J_d(0) a^\dagger_{q_1} a_{q_1} b^\dagger_{q_2} b_{q_2}$$

$$= \left(\frac{4}{N}\right) \sum_{q_1 q_2} J_d(0) [(\alpha^\dagger_{q_1} \cosh\theta_{q_1} - \beta_{q_1} \sinh\theta_{q_1})$$

$$\times (\alpha_{q_1} \cosh\theta_{q_1} - \beta^\dagger_{q_1} \sinh\theta_{q_1})(-\alpha_{q_2} \sinh\theta_{q_2} + \beta^\dagger_{q_2} \cosh\theta_{q_2})$$

$$\times (-\alpha^\dagger_{q_2} \sinh\theta_{q_2} + \beta_{q_2} \cosh\theta_{q_2})]$$

$$= \left(\frac{4}{N}\right) \sum_{q_1 q_2} J_d(0) \{[\alpha^\dagger_{q_1} \alpha_{q_1} \cosh^2\theta_{q_1} - (\alpha^\dagger_{q_1} \beta^\dagger_{q_1} + \alpha_{q_1} \beta_{q_1})$$

$$\times \sinh\theta_{q_1} \cosh\theta_{q_1} + \underline{\beta_{q_1} \beta^\dagger_{q_1}} \sinh^2\theta_{q_1}][\underline{\alpha_{q_2} \alpha^\dagger_{q_2}} \sinh^2\theta_{q_2}$$

$$- (\alpha^\dagger_{q_2} \beta^\dagger_{q_2} + \alpha_{q_2} \beta_{q_2}) \sinh\theta_{q_2} \cosh\theta_{q_2} + \beta^\dagger_{q_2} \beta_{q_2} \cosh^2\theta_{q_2}]\} .$$

Using the commutation relationship on the underlined terms

$$= \left(\frac{4}{N}\right) \sum_{q_1 q_2} J_d(0) \{[\alpha^\dagger_{q_1} \alpha_{q_1} \cosh^2\theta_{q_1} - \ldots$$

$$+ \underline{\beta^\dagger_{q_1} \beta_{q_1} \sinh^2\theta_{q_1} + \sinh^2\theta_{q_1}}][\underline{\alpha^\dagger_{q_2} \alpha_{q_2} \sinh^2\theta_{q_2} + \sinh^2\theta_{q_2}}$$

$$+ \ldots]\}$$

$$= \left(\frac{4}{N}\right) \sum_{q_1 q_2} J_d(0) \{\sinh^2\theta_{q_1} \sinh^2\theta_{q_2} + \sinh^2\theta_{q_1}$$

continued over...

$$\times [\alpha^{\dagger}_{q_2}\alpha_{q_2}\sinh^2\theta_{q_2} + \beta^{\dagger}_{q_2}\beta_{q_2}\cosh^2\theta_{q_2} - (\alpha_{q_2}\beta_{q_2}+\alpha^{\dagger}_{q_2}\beta^{\dagger}_{q_2})$$

$$\times \sinh\theta_{q_2}\cosh\theta_{q_2}] + \sinh^2\theta_{q_2}[\alpha^{\dagger}_{q_1}\alpha_{q_1}\cosh^2\theta_{q_1}$$

$$+ \beta^{\dagger}_{q_1}\beta_{q_1}\sinh^2\theta_{q_1} - (\alpha_{q_1}\beta_{q_1}+\alpha^{\dagger}_{q_1}\beta^{\dagger}_{q_1})\sinh\theta_{q_1}\cosh\theta_{q_1}]\}$$

+ terms involving higher order products in α and β operators . (IV-8)

Picking up higher order products such as $\alpha^{\dagger}_{q_1}\alpha_{q_1}\beta^{\dagger}_{q_1}\beta_{q_2}$, will need yet another Bogoliubov transformation to diagonalize the Hamiltonian.

Thus, collecting all the constant terms (ground state energy) and spin wave terms of the total Hamiltonian as given by the sum of Eqs. (IV-6) and (IV-7); one gets

Zero-Point Energy

$$H_0 = NS^2(J_d(\underline{0})-J_s(\underline{0})) + \sum_q \{A_q(\cosh 2\theta_q - 1)\} - \sum_q \{B_q \sinh 2\theta_q\}$$

$$+ \left(\frac{4}{N}\right) \sum_{q_1 q_2} \{[J_d(\underline{0})-J_s(\underline{0})-J_s(q_2-q_1)+J_s(q_1)+J_s(q_2)]$$

$$\times \sinh^2\theta_{q_1}\sinh^2\theta_{q_2}\} + \left(\frac{4}{N}\right) \sum_{q_1 q_2} \{J_d(q_2-q_1)$$

$$\times \sinh 2\theta_{q_1}\sinh 2\theta_{q_2}\} - \left(\frac{4}{N}\right) \sum_{q_1 q_2} \{J_d(q_1)\sinh 2\theta_{q_1}$$

$$\times \sinh^2\theta_{q_2}\} \qquad \text{(IV-9)}$$

and Spin wave Terms (S.W.T.)

$$= -2S \sum_q \{(\alpha_q^\dagger \alpha_q + \beta_q^\dagger \beta_q)[\cosh 2\theta_q (J_d(\underline{0}) - J_s(\underline{0}) + J_s(\underline{q}))$$

$$- \sinh 2\theta_q J_d(\underline{q})]\} + \left(\frac{2}{N}\right) \sum_{q_1 q_2} \{[J_d(\underline{q}_2 - \underline{q}_1)\sinh 2\theta_{q_1}$$

$$- 2J_d(\underline{q}_2)\sinh^2\theta_{q_1}][(\alpha_{q_2}^\dagger \alpha_{q_2} + \beta_{q_2}^\dagger \beta_{q_2})\sinh 2\theta_{q_2}$$

$$- (\alpha_{q_2}^\dagger \beta_{q_2}^\dagger + \alpha_{q_2}\beta_{q_2})\cosh 2\theta_{q_2}]\} + \left(\frac{4}{N}\right)\{[\sum_q J_d(\underline{0})\sinh^2\theta_q]$$

$$\times [\sum_q (\alpha_q^\dagger \alpha_q + \beta_q^\dagger \beta_q)\cosh 2\theta_q - (\alpha_q^\dagger \beta_q^\dagger + \alpha_q \beta_q)\sinh 2\theta_q]\}$$

$$- \left(\frac{2}{N}\right)\{[\sum_q J_d(\underline{q})\sinh 2\theta_q][\sum_q (\alpha_q^\dagger \alpha_q + \beta_q^\dagger \beta_q)\cosh 2\theta_q$$

$$- (\alpha_q^\dagger \beta_q^\dagger + \alpha_q \beta_q)\sinh 2\theta_q]\} + \left(\frac{4}{N}\right) \sum_{q_1 q_2} \{[J_s(\underline{q}_1) + J_s(\underline{q}_2)$$

$$- J_s(\underline{0}) - J_s(\underline{q}_2 - \underline{q}_1)][\sinh^2\theta_{q_1}][(\alpha_{q_2}^\dagger \alpha_{q_2} + \beta_{q_2}^\dagger \beta_{q_2})\cosh 2\theta_{q_2}$$

$$- (\alpha_{q_2}\beta_{q_2} + \alpha_{q_2}^\dagger \beta_{q_2}^\dagger)\sinh 2\theta_{q_2}]\} \quad . \qquad \text{(IV-10)}$$

It is possible to simplify these rather long-looking expressions substantially and put them in an elegant form, that can also be physically interpreted.

Using the definitions of exchange constants (Eq. (II-19))

$$J_s(\underline{q}) = \sum_s J_s e^{i\underline{q}\cdot\underline{s}} = \sum_s J_s \cos(\underline{q}\cdot\underline{s})$$

$$J_d(\underline{q}) = \sum_d J_d e^{i\underline{q}\cdot\underline{d}} = \sum_d J_d \cos(\underline{q}\cdot\underline{d})$$

$$J_d(\underline{q}_2-\underline{q}_1) = \sum_d J_d \cos((\underline{q}_2-\underline{q}_1)\cdot\underline{d}) = \sum_d J_d \cos(\underline{q}_1\cdot\underline{d})\cos(\underline{q}_2\cdot\underline{d})$$

$$J_s(\underline{q}_2-\underline{q}_1) = \sum_s J_s \cos((\underline{q}_2-\underline{q}_1)\cdot\underline{s}) = \sum_s J_s \cos(\underline{q}_1\cdot\underline{s})\cos(\underline{q}_2\cdot\underline{s}) \qquad \text{(IV-11)}$$

and noting that exchange constants are real and summation of the sine terms over the Brillouin zone yields zero, one can write H_0, given by (IV-9), as

$$\begin{aligned} H_0 = {} & NS^2\left[\sum_d J_d - \sum_s J_s\right] - 2S \sum_d J_d \sum_q X_q + 2S \sum_s J_s \sum_q X_q \\ & - 2S \sum_s J_s \sum_q \cos\underline{q}\cdot\underline{s}(X_q) + 2S \sum_d J_d \sum_q Y_q \\ & + \left(\frac{1}{N}\right) \sum_d J_d\left[\sum_q X_q\right]^2 - \left(\frac{1}{N}\right) \sum_s J_s\left[\sum_q X_q\right]^2 \\ & - \left(\frac{1}{N}\right) \sum_s J_s\left[\sum_q X_q \cos\underline{q}\cdot\underline{s}\right]^2 + \left(\frac{2}{N}\right) \sum_s J_s\left[\sum_q \cos\underline{q}\cdot\underline{s}\, X_q\right] \\ & \times \left[\sum_q X_q\right] + \left(\frac{1}{N}\right) \sum_d J_d\left[\sum_q Y_q\right]^2 - \left(\frac{2}{N}\right) \sum_d J_d\left[\sum_q X_q\right]\left[\sum_q Y_q\right] \\ = {} & NS^2 \sum_d J_d - 2S \sum_d J_d \sum_q (X_q - Y_q) + \left(\frac{1}{N}\right) \sum_d J_d\left[\sum_q (X_q - Y_q)\right]^2 \\ & - NS^2 \sum_s J_s + 2S \sum_s J_s \sum_q (X_q - (\cos\underline{q}\cdot\underline{s})X_q) \\ & - \left(\frac{1}{N}\right) \sum_s J_s\left[\sum_q (X_q - (\cos\underline{q}\cdot\underline{s})X_q)\right]^2 \end{aligned}$$

where $X_q = (\cosh 2\theta_q - 1)$ and $Y_q = \cos(\underline{q}\cdot\underline{d})\sinh 2\theta_q$. (IV-12)

This can be put in an elegant form as

$$H_0 = NS^2 \sum_d J_d[1 + C_d/S + C_d^2/4S^2]$$

$$- NS^2 \sum_s J_s[1 + C_s/S + C_s^2/4S^2] \qquad \text{(IV-13)}$$

where

$$C_d = \left(\frac{2}{N}\right) \sum_q [1 - \cosh 2\theta_q + \sinh 2\theta_q \cos(\underline{q}\cdot\underline{d})] < 0$$

and (IV-14)

$$C_s = -\left(\frac{2}{N}\right) \sum_q \{(1 - \cos\underline{q}\cdot\underline{s})(\cosh 2\theta_q - 1)\} < 0 \ .$$

An exactly similar approach would simplify the spin wave terms given by Eq. (IV-10) to

$$\text{S.W.T.} = \sum_q E_q(\alpha_q^\dagger\alpha_q + \beta_q^\dagger\beta_q) + \sum_q E_q'(\alpha_q^\dagger\beta_q^\dagger + \alpha_q\beta_q) \qquad \text{(IV-15)}$$

with

$$H_{H-P} = H_0 + \sum_q E_q(\alpha_q^\dagger\alpha_q + \beta_q^\dagger\beta_q) + \sum_q E_q'(\alpha_q^\dagger\beta_q^\dagger + \alpha_q\beta_q) \qquad \text{(IV-16)}$$

where

$$E_q = -2S \sum_d J_d[\cosh 2\theta_q - \sinh 2\theta_q \cos(\underline{q}\cdot\underline{d})] \times [1 + C_d/2S]\} + 2S \sum_s \{J_s[\cosh 2\theta_q (1 - \cos(\underline{q}\cdot\underline{s})] \times [1 + C_s/2S]\} \qquad \text{(IV-17a)}$$

and

$$E'_q = \sum_d \{J_d C_d[\cosh 2\theta_q \cos(\underline{q}\cdot\underline{d}) - \sinh 2\theta_q]\} + \sum_s \{J_s C_s[\sinh 2\theta_q (1 - \cos(\underline{q}\cdot\underline{s}))]\} \qquad \text{(IV-17b)}$$

Equation (IV-13) gives the ground state energy. This is equal to the molecular field term (E_0 as given by (II-21)) together with correction terms C/S and $C^2/4S^2$ which form a series in S^{-1}. The constant C are numbers less than unity. Kubo (1952) and Oguchi (1960) have given expressions for these terms (see Eq. (III-5)), though for the case with $J_s = 0$ and J_d restricted to nearest neighbour interactions only. Expression (IV-13) shows that the extension to general range of interaction goes very simply with different correction terms existing for each set of neighbours.

An analogous situation exists for E_q, the spin wave energy (Eq. (IV-17a)) where each J appears to be corrected by a term (1 + C/2S). This is important to experimentalists since many recent works have determined exchange constants to

within errors of less than the correction term. Equation (IV-16) actually gives a spin wave energy of $(E_q^2 - E_q'^2)^{1/2}$, but since E_q'/E_q is of the order of S^{-1}, the correction to the spin wave energy from the term E_q' is of lower order than the one considered above, and, if the logical scheme of retaining terms to the same order S^{-1} is followed (Oguchi, 1960), the term in E_q' should be dropped.

It is noteworthy that for the case of just nearest neighbour interactions between atoms on different sublattices $E_q' = 0$, since for $J_s = 0$ one has

$$\sum_d J_d \tanh 2\theta_q = \sum_d J_d \cos(\underline{q}\cdot\underline{d}) \quad \text{(from Eq. (II-29))}$$

so that

$$\begin{aligned} E_q' &= \sum_d C_d J_d \cosh 2\theta_q (\cos\underline{q}\cdot\underline{d} - \tanh 2\theta_q) \\ &= C^{n.n} \cosh 2\theta_q \left(\sum_d J_d \cos(\underline{q}\cdot\underline{d}) - \sum_d J_d \tanh 2\theta_q\right) \\ &= 0 \end{aligned} \qquad \text{(IV-18)}$$

$C^{n.n}$ being the constant value of C_d for all the nearest neighbours of d type.

The Sublattice Magnetization at Zero Temperature

This treatment can also be applied usefully to calculate the sublattice magnetization

$$M_{s-\ell} = \sum_{\ell} \langle S_{\ell}^{z} \rangle = \sum_{\ell} [S - \langle a_{\ell}^{\dagger} a_{\ell} \rangle]$$

$$= NS/2 - \sum_{q} \langle a_{q}^{\dagger} a_{q} \rangle$$

$$= NS/2 - \sum_{q} \sinh^{2}\theta_{q} - \sum_{q} \langle \alpha_{q}^{\dagger} \alpha_{q} \cosh^{2}\theta_{q}$$

$$+ \beta_{q}^{\dagger} \beta_{q} \sinh^{2}\theta_{q} \rangle + \sum_{q} \langle (\alpha_{q}\beta_{q} + \alpha_{q}^{\dagger}\beta_{q}^{\dagger}) \sinh\theta_{q} \cosh\theta_{q} \rangle . \quad \text{(IV-19)}$$

Next let us define yet another transformation analogous to Eq. (II-28) of Bogoliubov transformation by

$$\alpha_{q} = f_{q} \cosh\phi_{q} - g_{q}^{\dagger} \sinh\phi_{q}$$

$$\beta_{q} = - f_{q}^{\dagger} \sinh\phi_{q} + g_{q} \cosh\phi_{q}$$

with

$$\tanh 2\phi_{q} = E_{q}'/E_{q} . \quad \text{(IV-20)}$$

Using this transformation, the expectation values in Eq. (IV-19) can be evaluated at zero temperature to yield

$$\langle \alpha_q^\dagger \alpha_q \rangle = \sinh^2\phi_q = \langle \beta_q^\dagger \beta_q \rangle$$

and

$$\langle \alpha_q \beta_q + \alpha_q^\dagger \beta_q^\dagger \rangle = -\sinh 2\phi_q \qquad \text{(IV-21)}$$

so that (IV-19) can be written as

$$M_{s-\ell} = \frac{NS}{2} - \sum_q [\sinh^2\theta_q + \sinh^2\phi_q \cosh 2\theta_q + \frac{1}{2}\sinh 2\phi_q \sinh 2\theta_q]$$

$$= \frac{NS}{2} - \sum_q [(\frac{\cosh 2\theta_q - 1}{2}) + \frac{1}{2}(\cosh 2\theta_q \cosh 2\phi_q - \cosh 2\theta_q + \sinh 2\phi_q \sinh 2\theta_q)] \qquad \text{(IV-22)}$$

Since $E'_q << E_q$, $\phi << 1$, one can use small angle expansion, $2\phi = E'_q/E_q$ taking $\tanh 2\phi \approx 2\phi$

$$M_{s-\ell} = \frac{NS}{2} - \sum_q [(\frac{\cosh 2\theta_q - 1}{2}) + (\frac{E'_q}{2E_q})\sinh 2\theta_q + (\frac{E'_q}{2E_q})^2 \cosh 2\theta_q + 0(\phi^3) \ldots] \qquad \text{(IV-23)}$$

The leading term E'_q/E_q is of $0(1/S)$ and retaining terms up to $0(1/S)$.

$$M_{s-\ell} = \frac{NS}{2}(1 - C'/2S - \Sigma'/4S^2) \qquad \text{(IV-24)}$$

where

$$C' = \left(\frac{2}{N}\right) \sum_q (\cosh 2\theta_q - 1)$$

and

$$\Sigma' = \left(\frac{2}{N}\right) \sum_q (2S) \sinh 2\theta_q (E_q'/E_q) \qquad \text{(IV-25)}$$

The last term in the expression for the magnetization is new. In Oguchi's treatment $\Sigma' = 0$, since it is limited to the cases of simple lattices where $E_q' = 0$.

4.1.2 D-M Approach

Equations of the Dyson-Maleev transformation as given by (II-11) can be written for two sublattices ℓ and m as

$$S_\ell^z = S - a_\ell^\dagger a_\ell \quad ; \quad S_m^z = -S + b_m^\dagger b_m$$

$$S_\ell^+ = (2S)^{1/2}(1 - a_\ell^\dagger a_\ell/2S) a_\ell \quad ; \quad S_m^+ = (2S)^{1/2} b_m^\dagger$$

$$S_\ell^- = (2S)^{1/2} a_\ell^\dagger \quad ; \quad S_m^- = (2S)^{1/2}(1 - b_m^\dagger b_m/2S) b_m \qquad \text{(IV-26)}$$

Since the procedure to carry out subsequent analysis with the D-M approach is completely analogous to the H-P approach, it is sufficient to write down the final form of the Hamiltonian obtained, which is

$$H_{D-M} = H_0 + \sum_q E_q(\alpha_q^\dagger\alpha_q+\beta_q^\dagger\beta_q) + \sum_q E'_q(\alpha_q^\dagger\beta_q^\dagger+\alpha_q\beta_q)$$

$$- C' \sum_q J_d(q)\alpha_q\beta_q \quad . \qquad \text{(IV-27)}$$

This is the same as the H_{H-P} given by Eq. (IV-16) except that there is an extra term. This term is non-Hermitian in character and will not contribute to expressions for the ground state energy, the spin wave energy, or the sublattice magnetization (Eqs. (IV-13), (IV-17a) and (IV-24)) to the order of terms we have retained.

Thus, one gets identical results with both D-M and H-P approaches to the order of series used in this treatment. The work of Harris (1966) anticipated this result in that it showed that the D-M and H-P transformations, and in fact a still wider class of transformations, yield identical results to the order of (1/S) for just nearest neighbour interactions.

4.2 Comparison with Oguchi's Expressions

It is easy to show how the expressions for zero point energy, spin wave energy, and sublattice magnetization reduce to those given by Oguchi (1960) for the case of just one exchange constant.

First, we shall show that C' and C as defined by Eqs. (IV-25) and (IV-14) reduce to those given by Oguchi (Eqs. (III-9) and (III-5)) for the case of $J_s = 0$ and J_d restricted to nearest neighbours.

For $J_s = 0$ and $J_d = J_d^{n.n.}$ only, $\tanh 2\theta_q$ as given by (II-29) reduces to

$$\tanh 2\theta_q = \frac{J_d^{n.n.} \sum_{\rho} e^{i\underline{q}\cdot\underline{\rho}}}{J_d^{n.n.} z} = \gamma_q \quad \text{(Oguchi)}$$

$\underline{\rho}$ being the vector joining nearest neighbours on different spin sublattice and z is the number of them (see Eq. (III-6)).

In general

$$C' = \left(\frac{2}{N}\right) \sum_q (\cosh 2\theta_q - 1) \quad \text{(from Eq. (IV-25))}$$

$$= \left(\frac{2}{N}\right) \sum_q \left[\left(\frac{1}{1 - \tanh^2 2\theta_q}\right)^{1/2} - 1\right]$$

$$= \left(\frac{2}{N}\right) \sum_q \left(\frac{1}{(1 - \gamma_q^2)^{1/2}} - 1\right)$$

$$= C' \quad \text{(Oguchi)}$$

In general from Eq. (IV-14)

$$C_d = \left(\frac{2}{N}\right) \sum_q [1 - \cosh 2\theta_q + \sinh 2\theta_q \cos(\underline{q}\cdot\underline{d})]$$

$$= \left(\frac{2}{N}\right) \sum_q [1 - \cosh 2\theta_q + \sinh 2\theta_q \left(\sum_\rho \cos \underline{q}\cdot\underline{\rho}/z\right)]$$

$$= \left(\frac{2}{N}\right) \sum_q [1 - (1 - \gamma_q^2)^{1/2}] = C \quad \text{(Oguchi)}$$

The value of the zero point energy, as given by Eq. (IV-13) for $J_s = 0$ is

$$H_0 = NS^2 \sum_d J_d (1 + C_d/S + C_d^2/4S^2)$$

$$= - NS|J|z\,(S + C + C^2/4S) = E_0 \quad \text{(Oguchi)}$$

(see Eq. (III-4))

provided $\underline{d}$ is restricted to nearest neighbours only. Similarly, the value of the spin wave energy as given in general by Eq. (IV-17) for $E_q' = 0$ and $J_s = 0$ would be

$$E_q(J_s = 0) = - 2S \sum_d J_d [\cosh 2\theta_q - \sinh 2\theta_q (\cos \underline{q}\cdot\underline{d})]$$

$$\times [1 + C_d/2S]$$

$$= - 2S \sum_d J_d (1 - \gamma_q^2)^{1/2} (1 + C_d/2S)$$

$$= A_q^0 \quad \text{(Oguchi)} \quad \text{(see Eq. (III-7))}$$

The expression for the sublattice magnetization (IV-24) differs from the corresponding Oguchi's expression (III-8) only in having an additional Σ' term which is, as discussed earlier, zero in Oguchi's treatment.

4.3 The Numerical Calculations of Zero Temperature Constants For Various Types of Antiferromagnetic Lattice

In this last section of the chapter, the calculations of lattice sums C, G' and Σ' for a number of different lattices using Eqs. (IV-14) and (IV-25) are done and the results discussed.

The evaluation of lattice sums basically involves summation over q, with q covering the whole of the first Brillouin zone. The summations are performed by 'brute force' methods using N×N×N meshes with axes in the direction of the reciprocal lattice vectors. It is important that the mesh is displaced from the origin and that the displacement is by different amounts in the three directions so that no points lie along directions of high symmetry. A symmetrical value of q is avoided in order to scan the function at unique points and not equivalent ones. A change in the amount of displacement in any or all the three directions did not alter the value of summation over q to any significant extent. The summations can be extrapolated to an infinitely fine mesh by plotting the calculated values for a number of different sizes, N, against 1/N and extrapolating it to $N = \infty$. As an example, we take the case of evaluating C_{1d} for the simple cubic case. In Fig. IV-1 the calculated sum over q of C_{1d} against 1/N is plotted. The points are very reasonably assumed to lie on a straight line. The summation can be seen

Fig. IV-1: The plot of calculated sum of C_{1d} for the simple cubic case versus 1/N, N being the mesh size. The values of N used are 60, 80, 100, 120 and 160.

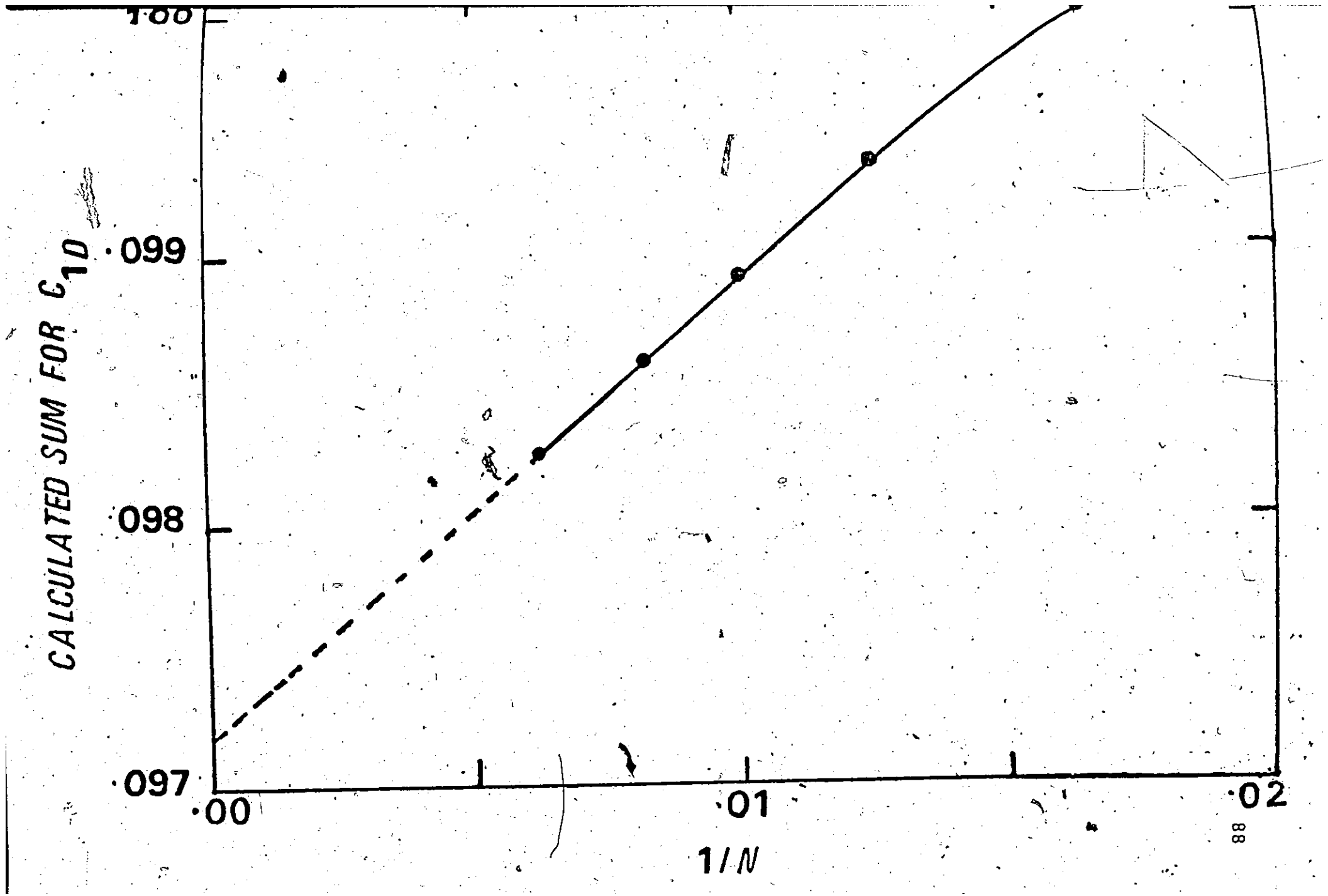
1·00
·099
·098
·097
CALCULATED SUM FOR C_{10}
·00
·01
·02
1/N

to be converging with the increasing value of N. The extrapolation of the line to $N = \infty$ reads $C_{ld} = 0.09719$.

A more accurate method of performing the extrapolation is to assume that the results form a simple power series in N^{-1}. A least square fit to such a power series gives a polynomial of degree 2 for the apparent value of C_{ld} as

$$C_{ld} = 0.09715840 + 0.17601045 \times N^{-1} - 0.21127461 \times N^{-2}$$

The fitted polynomial of degree 3 is

$$C_{ld} = 0.09715794 + 0.1761485 \times N^{-1} - 0.22425440 \times N^{-2} + 0.38141164 \times N^{-3}$$

and for degree 4, the fitted polynomial is

$$C_{ld} = 0.09715802 + 0.17611552 \times N^{-1} - 0.21939304 \times N^{-2} + 0.076286093 \times N^{-3} + 6.891354 \times N^{-4}$$

The constant term of the polynomial, which corresponds to

$N = \infty$ mesh size, is the value of C_{1d} for a real lattice with a very large number of atoms. One can see that varying the degree of fitted polynomial does not change the value of C_{1d} by more than a few parts in a million.

In cases like that of C_d (see Eq. (IV-14)) which can be looked upon as the sum of two series with terms $(1 - \cosh 2\theta_q)$ and $(\sinh 2\theta_q \cos \underline{q} \cdot \underline{d})$, each sum was separately found to be convergent and also added up to the calculated value of C_{1d}. As discussed later, our value of C' for a b.c.c. lattice is in excellent agreement with that of Davis (1962). This provides yet another check on the accuracy of our methods. The calculations were normally made with the number of different values of q ranging from 10,000 to 200,000 and the sums obtained should be sufficiently accurate for practical purposes. In calculating the constants C_d and C_s it is not necessary to make the calculations for every value of $\underline{d}$ or $\underline{s}$ since the summation over $\underline{q}$ renders the constant the same for every symmetry-related set of neighbours.

Calculations have been made for the simple cubic, body-centred cubic and face-centred cubic lattices (types I and II) and the results are given in Table IV-1. Type I and type II f.c.c., though having the same chemical symmetry, differ in magnetic symmetry. While type I has out of twelve nearest neighbours, eight of different spin and four of same spin as that at the origin, type II has an equal number (six) of each. All the second nearest neighbours of type I have

TABLE IV-1

VALUES OF LATTICE SUMS AS DEFINED IN THE TEXT FOR VARIOUS ANTIFERROMAGNETIC LATTICES. NUMBERS IN BRACKETS ARE ESTIMATED ERRORS OF THE LAST DIGIT QUOTED

Lattice	Exchange Model	C_{1d}	C_{1s}	C_2	C'	Σ'
b.c.c.	$J_2 \to 0$	0.073038(1)	-	-0.0433549(3)	0.11863(2)	0
s.c.	$J_2 \to 0$	0.0971579(4)	-	-0.0780223(3)	0.156707(10)	0
f.c.c. type II	$J_{1d}=J_{1s}=J_2$	-0.059638(3)	-0.164937(5)	-0.044212(3)	0.215896(3)	0.28(4)
f.c.c. type II	MnO	0.024760(1)	-0.072464(1)	0.045770(1)	0.133949(1)	0.014946(5)
f.c.c. type II	NiO	-0.16479(12)	-0.15663(15)	0.096867(4)	0.15422(10)	0.000308(12)
f.c.c. type I	$J_{1d}=J_{1s}$ $J_2 \to 0$	-0.106845(1)	-0.457718(2)	-0.352331(1)	0.677(1)	-
f.c.c. type I	$J_{1d}=1.2J_{1s}$ $J_2 \to 0$	0.043809(2)	-0.145222(5)	-0.163432(6)	0.288888(6)	0.09937(12)

the same spin as at the origin, and for type II they have different spin from that at the origin.

The values of C_{1d} and C' as given by Anderson (1952) and Kubo (1952) are 0.097 and 0.156 for simple cubic; 0.073 and 0.150 for b.c.c. The value C' = .150 for b.c.c. had an error and was recalculated by Davis (1962) to be 0.118636. A comparison with the first two rows of Table IV-1 shows that our calculated values agree well with the earlier calculations, though the earlier values are quoted to less significant figures except in one case. For the face-centred cubic lattices the twelve nearest neighbouring atoms to a given atom are split up into a group labelled 1d of atoms on the sub-lattice with the opposite spin and a group labelled 1s of atoms on the sublattice with the same spin as of the given atom. Separate sums have been computed for these two groups. In the type II face-centred antiferromagnets, Lines and Jones (1965) have shown that the lattice will normally distort so as to split the equality of exchange constants between the 1d and 1s atoms. MnO, which is discussed in more detail in Chapter V, is an actual case with such a splitting. These sums have been calculated for MnO with $J_{1d}/J_{1s} = 1.27$, $J_{1d} = 1.03\ J_2$ (Collins, Tondon and Buyers, 1973). A look at Table IV-1 shows that the splitting has considerable effect on the values of the constants.

We have also made explicit calculations for NiO with the exchange energies observed by Hutchings and Samuelson

(1971). NiO is also type II f.c.c. like MnO with $J_{1d} = 0.674$, $J_{1s} = 0.694$ and $J_2 = -9.497$ in meV. The correction term to the sublattice magnetization has extra importance in this oxide since it must be known before neutron diffraction data (Alperin, 1962; Fender et al., 1968) can be used to determine covalency parameters. Our value of C' of 0.1542 for NiO supports the earlier implicit assumption that it will be similar to the value for the simple cubic antiferromagnet (0.1567) since the lattice can be approximated by four such independent interpenetrating sublattices.

The lattice of type I face-centred cubic antiferromagnets is, as with type II, likely to distort on passing to the antiferromagnetic state and calculations have been made for both the undistorted lattice ($J_{1d} = J_{1s}$) and a distorted lattice ($J_{1d} = 1.2\ J_{1s}$). The large difference in the value of constants again suggests the importance of distortions in determining the properties. The instability of the undistorted type I antiferromagnet is brought out by the large values of the constants calculated. The series for Σ' did not converge well over the mesh sizes used, values in excess of 10 were obtained, indicating a probable breakdown in our type of treatment because of a lack of convergence.

Experimental work on covalency parameters in other materials (Fender et al., 1968; Tofield and Fender, 1970), particularly the face-centred cubic antiferromagnets, can use

the numbers given in Table IV-1 to remove uncertainties in zero-point magnetization corrections.

For all the antiferromagnets which are likely to occur in real materials (i.e., all except the undistorted lattices) the corrections calculated to elementary spin wave theory are small, but not so small as to be undetectable experimentally.

CHAPTER V

MANGANESE OXIDE: A REVIEW

This chapter discusses the magnetic structure of Manganese Oxide and reviews the earlier work done on the measurement of the magnon dispersion curves and other relevant aspects of it's properties.

The study of various aspects of MnO over the last two decades has been rather extensive, because of the interesting case it presents from both a theoretical and an experimental point of view. MnO possesses rocksalt (NaCl) crystal structure above T_N. It has a large atomic spin of 5/2 and has no orbital contribution to its magnetic state. It is possible to get the big crystals of MnO necessary for neutron work. While all these considerations tend to simplify the study, it has other features such as anisotropy due to dipole-dipole interaction, temperature dependent distortion below T_N, and the multidomain nature of its crystals, which complicate the analysis. Very often, however, it is just these complicating features which enrich the investigation and lead to new physical insight.

Historically MnO was the first material that was shown by neutron diffraction to be antiferromagnetic at low temperatures (Shull and Smart, 1949). Although, from the study of the variation of the susceptibility with temperature,

MnO was believed to be antiferromagnetic as far back as 1938 (Bizette et al., 1938), Shull and Smart's work provided the first direct experimental verification of the Néel's hypothesis of an ordered antiferromagnetic arrangement of atomic spins.

Figure V-1 shows the neutron diffraction patterns of powdered MnO at 80K and 293K obtained by Shull et al. (1951). The room temperature pattern shows coherent nuclear reflection peaks at the regular face-centred cubic reflection positions. The diffraction pattern is of reversed NaCl type, i.e., odd reflections are stronger than even ones, because the coherent nuclear scattering amplitude for Mn and O are of opposite sign. The low temperature pattern also shows the same nuclear peaks, but in addition shows superstructure peaks at positions not allowed on the basis of a chemical unit cell with $a_{chem} = 4.426$ Å . A comparison of the two pattern shows that the most noteworthy difference is a presence of strong low angle reflection at ∿6°. It is possible to account for this low angle reflection and for the other additional peaks in terms of a magnetic unit cell that has a side twice of the chemical unit cell, namely $a = 8.852$ Å . On this basis the low angle reflection is the (111) reflection of the magnetic cell. Shull et al. (1951) studied the intensity of this peak with increasing temperature and showed that it goes to zero in the neighbourhood of the Néel temperature of 120K as inferred

Fig. V-1: The neutron diffraction pattern of MnO at 80K and 293K (below and above the Néel temperature of 120K, respectively). The low temperature pattern shows extra antiferromagnetic reflections which can be indexed in terms of a magnetic unit cell with dimensions twice that of the chemical unit cell.

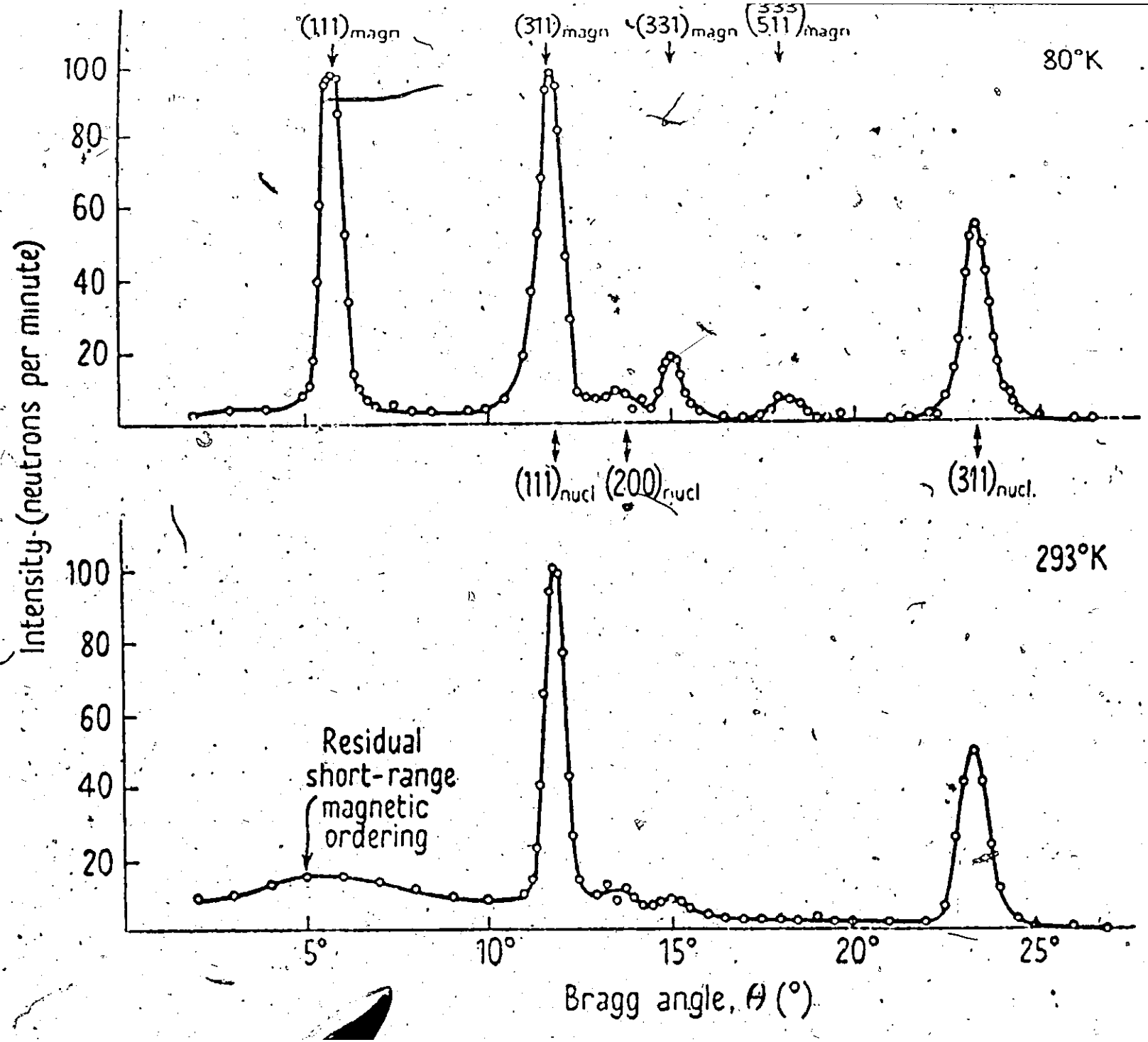
(111)magn
(311)magn
(331)magn
(333/511)magn
80°K
100
80
60
40
20
(111)nucl
(200)nucl
(311)nucl.
293°K
Residual short-range magnetic ordering
Intensity (neutrons per minute)
5°
10°
15°
20°
25°
Bragg angle, θ (°)

from susceptibility and specific heat measurements. A fuller description of the magnetic structure of MnO was given by Roth (1958). Roth, with his better resolved data at 4.2K, showed that the two earlier models proposed by Shull (1951) and by Li (1955) were only partially correct. Roth concluded (also confirmed by Corliss, Elliott and Hastings (1956)) that good agreement can be found with the observed intensities of the diffraction pattern if the structure is assumed to consist of alternating ferromagnetic sheets of (111) plane, with spins constrained to lie within the (111) plane. The powder data does not discriminate between directions within the (111) plane, so that various spin directions such as $[11\bar{2}]$ or $[\bar{1}10]$ etc. are possible. Roth assumed a single magnetic axis in the unit cell in his analysis.

Tombs and Rooksby (1950) were first to notice by X-ray studies that MnO undergoes a crystallographic distortion in passing from the paramagnetic to the antiferromagnetic state. In the paramagnetic state the symmetry is cubic, in the antiferromagnetic state MnO becomes rhombohedral with $\alpha = 90°26'$. The distortion from cubic symmetry at 4.2K was sufficiently large for Roth to identify the magnetic reflection as (111) rather than $(11\bar{1})$ and thus confirm that the structure is based on ferromagnetic sheets of spins in (111) planes antiferromagnetically stacked along the rhombohedral axis [111]. In general, this is known

as Type-II f.c.c. antiferromagnetic structure. In Fig. V-2, it is shown for MnO. Ignoring the distortion for a moment, each Mn^{+2} atom has twelve nearest neighbours (n.n.), six second nearest neighbours and twenty-four third nearest neighbours. Table V-1 lists their positions and the spin orientations. By looking at the Table, we can see that out of twelve n.n., six are parallel and six are antiparallel to a reference magnetic ion. The six parallel spins are located on the same ferromagnetic sheets as the reference spin, and the six antiferromagnetic n.n. spins are arranged centrosymmetrically in sets of three in the plane below and above the reference spin. Actually it is this relative orientation of nearest neighbours spins in Type-II f.c.c. pattern which results in a rhombohedral distortion of MnO below T_N. Since, if we consider a possible anisotropic deformation of the cubic structure, such a system will gain exchange energy from a contraction along the body diagonal [111]. For MnO, the balance between elastic and exchange forces occurs when the distorted cube angles are $\frac{\pi}{2} \pm \Delta$ with $\Delta = 1.1 \times 10^{-2}$ radians at the absolute zero of temperature (Rodbell, Osika and Lawrence, 1965). This distortion splits nearest neighbours of a Mn^{+2} atom into two groups, six of them with spins antiparallel come closer and the other six with spin parallel get more distant (Lines and Jones, 1965; Rodbell and Owen, 1964). The nearest neighbour exchange

Fig. V-2: The magnetic structure of MnO as determined by neutron diffraction. The structure is a Type-II face-centered cubic antiferromagnet with (111) sheets of magnetic atoms in which the spins are parallel, but with antiparallel spin directions in adjacent sheets.

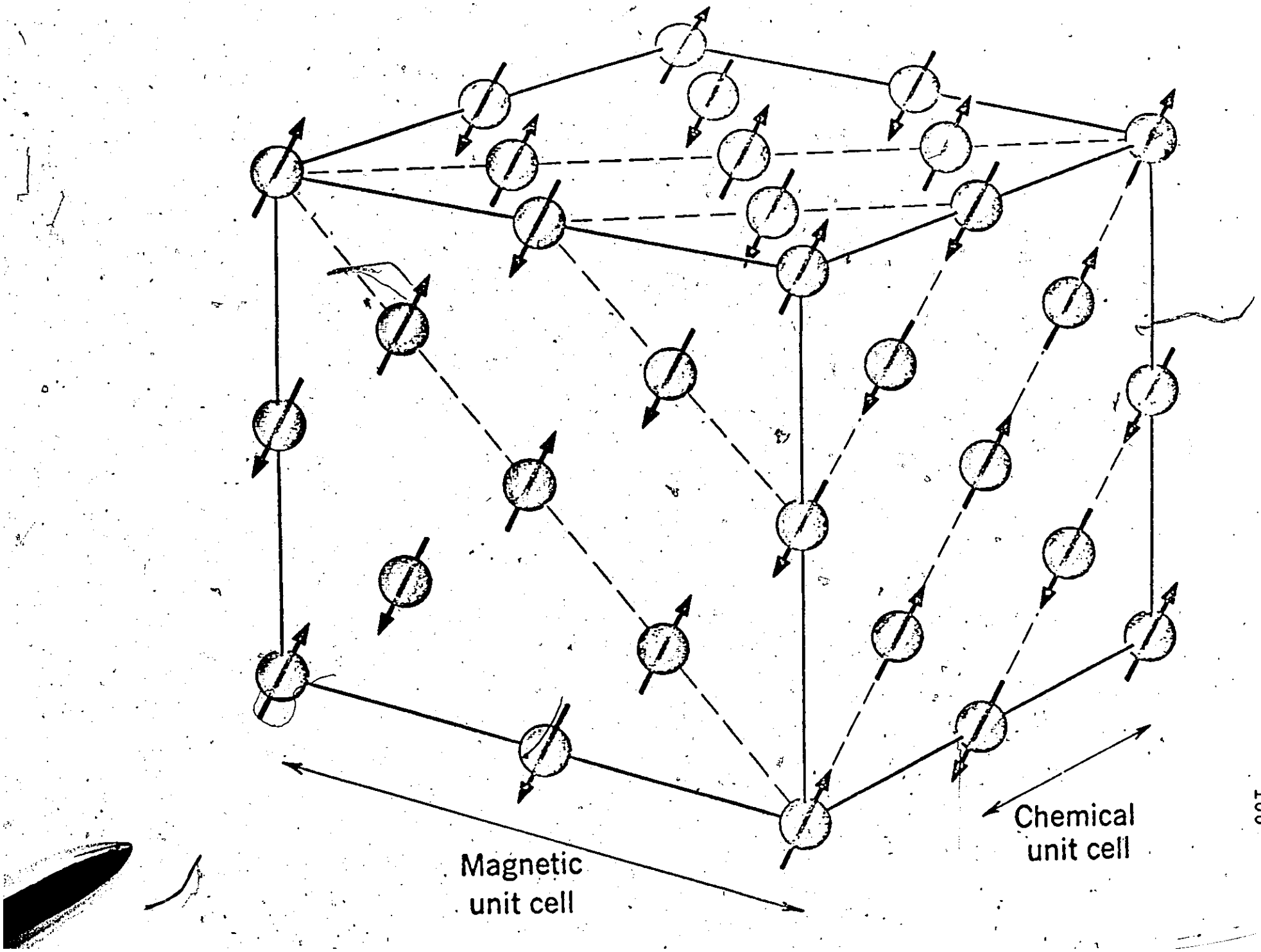
Magnetic
unit cell
Chemical
unit cell

TABLE V-1

THE POSITIONS AND SPIN ORIENTATIONS OF NEIGHBOURS IN MnO

Neighbours	Spins	Type	Number	Position
1	anti ||	d	6	{h, h, 0} $h = \pm \frac{1}{2}$
1	||	s	6	{h,-h, 0}
2	anti ||	d	6	{k, 0, 0} $k = \pm 1$
3	anti ||	d	12	{h,-h,±k}
3	||	s	12	{h, h,±k}

constant J_1 splits up as J_{1d} and J_{1s}, with the value of J_{1d} greater than J_{1s} (Lines and Jones call these J_1^+ and J_1^-). J_2 the second nearest neighbour exchange remains unsplit, while J_3 the third nearest neighbour constant will also split up into J_{3d} and J_{3s}.

We can see from the above discussion that the distortion that MnO undergoes below T_N is directly related to the rhombohedral magnetic symmetry that MnO has, being a Type-II f.c.c. structure. Strictly speaking, the magnetic symmetry of MnO is even lower (orthorhombic) because of the fact that spins themselves point in one certain direction within the (111) plane. This will, in principal, give rise to the magnetostriction effect. This secondary effect is quite small and has not been observed experimentally in MnO.

Although so far we have discussed the magnetic structure of MnO implicitly assuming a single domain, the single crystals normally used for the experimental work are multidomain in nature.

A single crystal of MnO has four principal domains, called T domains, since the spins can be confined to any of the four planes (111), (11$\bar{1}$), (1$\bar{1}$1) and ($\bar{1}$11) corresponding to four symmetry-equivalent directions [111], [11$\bar{1}$], [1$\bar{1}$1] and [$\bar{1}$11]. Thus the contraction, which MnO undergoes, could be along any of the four <111> directions in a multidomain crystal. Moreover with each T domain, there will be at least three 'S' domains corresponding to the possible directions of

the spins within the {111} plane. There will also be domains corresponding to a reversal of spin direction in each of the above, thus at least 24 different domains are possible in a MnO crystal. At present, it is not possible to distinguish the scattering from different S domains within a given T domain. The four T domains in a multidomain crystal give rise to different spin wave energies at any particular scattering vector $\underline{Q}$. These multidomain effects add to the difficulty in the interpretation of data, e.g., it happens that the zone centre of one domain may coincide with the zone boundary of another.

In MnO, the nearest neighbour (say at $(\frac{1}{2}\ \frac{1}{2}\ 0)$) and the next n.n. (say at (1 1 0)) manganese atom interacts with the manganese atom at the origin (0 0 0) through intervening oxygen atoms at $(\frac{1}{2}\ 0\ 0)$ via 90° and 180° superexchange respectively. Early susceptibility measurements (Smart, 1963) had indicated that the first and second neighbour exchange energies are of the same order of magnitude. Casselman and Keffer (1960) have presented theoretic arguments to support their near equality. Lines and Jones estimated the values as $J_1 = 0.431$ meV and $J_2 = 0.474$ meV by susceptibility data. For small values of Δ, r^+ and r^-, the distance between parallel and antiparallel nearest neighbours, is related to r_0 the nearest neighbour distance $a/\sqrt{2}$ without distortion by

$$r^{\pm} = r_0(1 \pm \frac{\Delta}{2}) \qquad \text{(V-1)}$$

and

$$J_{1d} = J_1(1 + \frac{\varepsilon\Delta}{2}) \quad ; \quad J_{1s} = J_1(1 - \frac{\varepsilon\Delta}{2})$$

where

$$\varepsilon = \frac{d\ell n(|J_1|)}{d\ell n(r)} \qquad \text{(V-2)}$$

$\varepsilon < 0$ for lattices that contract along [111] below T_N. Lines and Jonès estimated J_{1d} and J_{1s} to differ in energy by the order of 20%. The variation of the angle Δ with temperature below T_N (Morosin, 1970) is shown in Fig. V-3. The distortion vanishes at T_N and has a maximum value of 1.1×10^{-2} radians at T = 0K.

Morosin obtained a value of $\varepsilon = -23$ on the basis of elastic constant data and his measurements of the value of Δ. Harris (1972) obtained a value of -19 from EPR measurements of manganese pairs in MgO and CaO. Morosin also obtained a precise measurement of the lattice constants of MnO using X-ray diffraction techniques. The values are $a = 4.4457 \pm .0002$ Å at 23 ± 1°C and $a = 4.4316 \pm .0003$ Å and $\alpha = 90.624 \pm .008°$ at 4.2K.

Kaplan (1954) had pointed, before the experimental verification by Roth, that since Mn^{+2} ions are in the S states,

Fig. V-3: The variation of angle Δ of the pseudocubic unit cell, $\frac{\pi}{2} + \Delta$, with temperature for MnO below T_N.

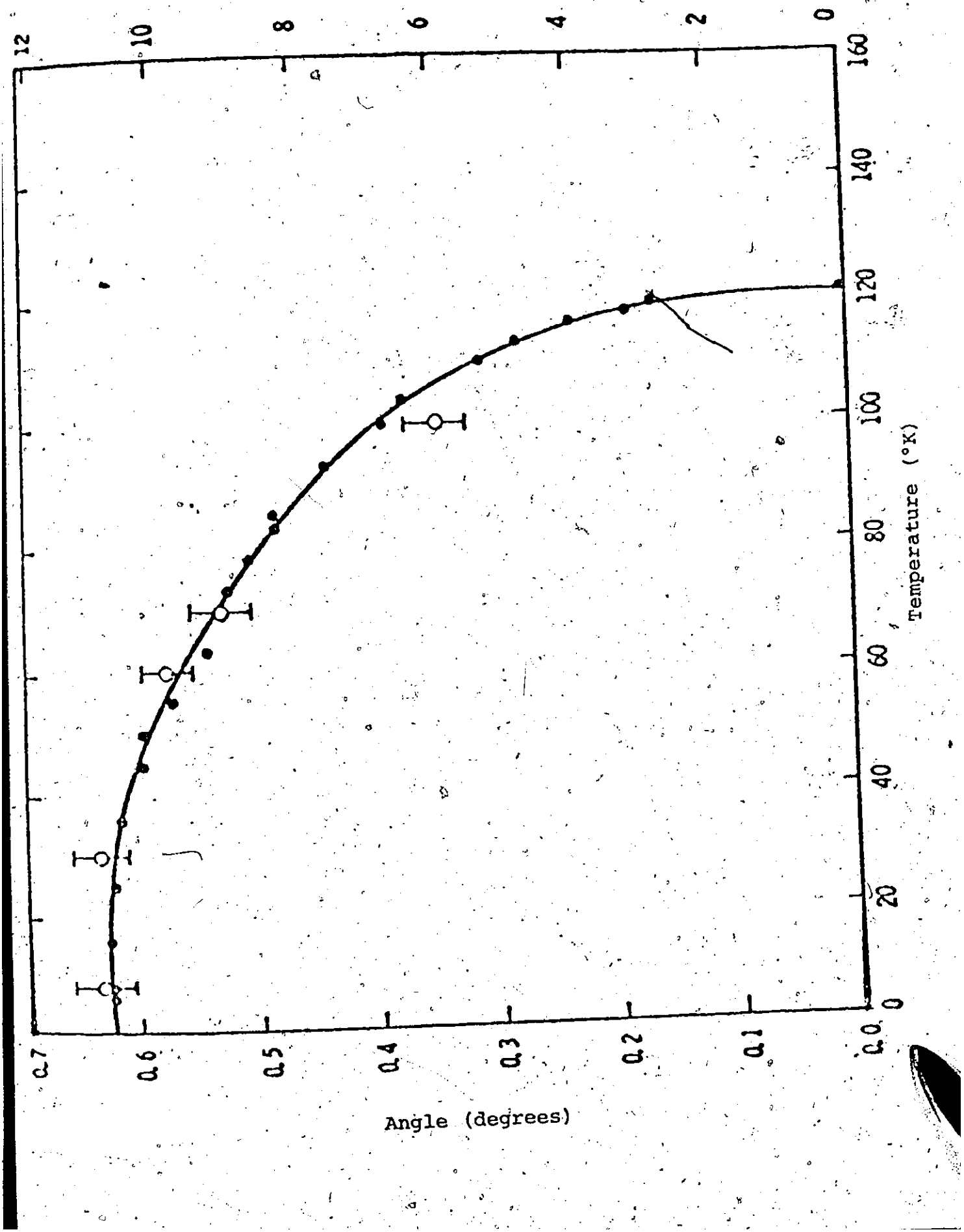
Angle (10^{-3} radians)
12
10
8
6
4
2
0
160
140
120
100
80
60
40
20
0
Temperature (°K)
0.7
0.6
0.5
0.4
0.3
0.2
0.1
0.0
Angle (degrees)

anisotropy will, in general, be small and arise dominantly from dipole-dipole interactions. For f.c.c. Type-II structures Kaplan showed that dipolar interactions would constrain the spins to lie in (111) planes. Keffer and O'Sullivan (1957) and Roth (1958) pointed out that this is true only if one disregards the possibility of multiaxial spin structures. They suggested, later confirmed by Nagamiya (1958), that it is the distortion which stabilizes the single spin structure in MnO. A very similar situation exists for NiO where the existence of single spin axis structure has also been confirmed (Roth and Slack, 1960).

The 'out of plane' dipolar anisotropy, which for MnO is only a few percent of the isotropic exchange energy, does not confine the spins to any particular direction within the (111) plane. There will be weaker 'in plane' anisotropic forces that fix the direction of the spin within the plane, though these are at least an order of magnitude weaker. The possible sources of these in-plane anisotropy forces are discussed by Keffer and O'Sullivan (1957).

Collins (1964) was first to measure the spin wave dispersion relationship in MnO using the inelastic neutron scattering techniques. The data were restricted to a rather small range of wavevector and energy. The values of exchange constants obtained were $J_1 = -0.33 \pm 0.04$ meV and $J_2 = -0.29 \pm 0.013$ meV. No distinction was possible between J_{1d} and J_{1s} because of the limited nature of the data.

Richards (1963) studied the $q = 0$ mode by AFMR, and Hughes (1971) studied it by infrared absorption.

Recently the measurements of the spin wave spectrum over the complete Brillouin zone were reported by us (Collins, Tondon and Buyers, 1973). Apart from our own work, two more groups, one from Saclay, France (Bonfante et al., 1972A) and the other from Tohoku University, Japan (Kohgi et al., 1972) have independently reported these measurements. Our results are in substantial agreement with these groups, but are believed to be more accurate. We have also treated dipole-dipole interactions and the effect of zero-point motion on the spin wave energy to a more complete extent. We describe the measurements of the spin wave spectrum in MnO in the next chapter.

CHAPTER VI

SPIN WAVE MEASUREMENTS IN MnO

The spin wave spectrum can be determined by measuring the one-magnon coherent neutron scattering cross-section from a single crystal as given by Eq. (II-67).

If a neutron of momentum $\hbar\underline{k}$ and energy $E = \hbar^2k^2/2m_n$ is scattered by a specimen with the creation of a magnon of energy $\hbar\omega$ to a momentum state $\hbar\underline{k}'$ and energy $E' = \hbar^2k'^2/2m_n$, the energy of the magnon $\hbar\omega$ and the momentum transfer $\underline{Q} = \underline{k} - \underline{k}'$ will be governed by the energy and momentum conservation laws as given by Eq. (II-63). The equations are

$$\hbar\omega = E - E' = \frac{\hbar^2k^2}{2m_n} - \frac{\hbar^2k'^2}{2m_n}$$

and (VI-1)

$$\underline{Q} = \underline{k} - \underline{k}' = \underline{q} + \underline{\tau}$$

where $\underline{\tau}$ is a reciprocal lattice vector and $\underline{q}$ is the reduced wavevector, namely the wavevector $\underline{Q}$ reduced to the first Brillouin zone. The magnon frequency ω satisfies the dispersion relation

$$\omega = \omega(\underline{q}) \quad . \qquad \text{(VI-2)}$$

All the measurements of the dispersion relations in MnO were done using the C5 triple axis spectrometer in the NRU reactor at AECL, Chalk River. A brief description of the spectrometer is given below (for detailed description, see P. K. Iyengar, 1965; Brockhouse, 1961). A schematic diagram of the apparatus and the corresponding reciprocal space diagram is given in Fig. VI-1. Neutrons of initial energy E are selected from the white spectrum of the reactor by Bragg reflection from the monochromating crystal X_M at a Bragg angle θ_M, and impinge on the specimen single crystal S set at an angle ψ with respect to the incident beam. The neutron beam is scattered by the specimen through an angle ϕ into the analyzer crystal X_A and detected by a BF_3 or He^3 counter at D after Bragg reflection at an angle θ_A from the analyzer crystal. The number of neutrons impinging on the specimen can be preset by the monitor fission counter. Soller collimators C_M and C_A determine the directions of neutrons. The instrumental resolution is determined by the mosaic spread of the monochromating and the analyzing crystals as well as by the amount of divergence tolerated by the collimators C_M and C_A. The variation in the magnitudes of $\underline{k}$ and $\underline{k}'$ are determined by the ranges of $2\theta_M$ and $2\theta_A$ and the $d_{hk\ell}$ spacings of the crystal planes $(hk\ell)$ used for X_M and X_A. In general, $2\theta_M$ and $2\theta_A$ are limited by the physical size of the instrument, the available neutron spectrum, etc.

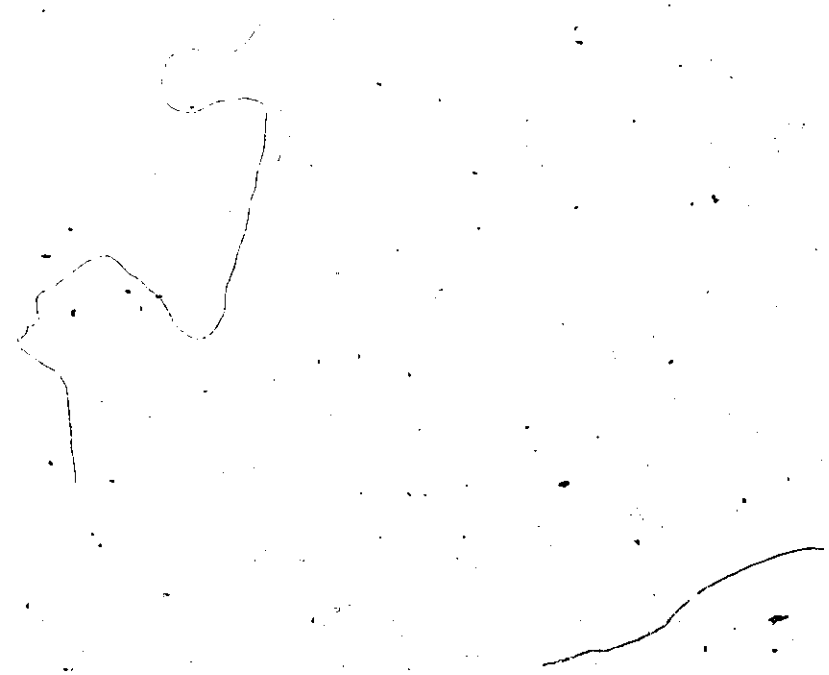

Fig. VI-1: A schematic drawing (i) of a triple axis spectrometer and (ii) the corresponding reciprocal space diagram.

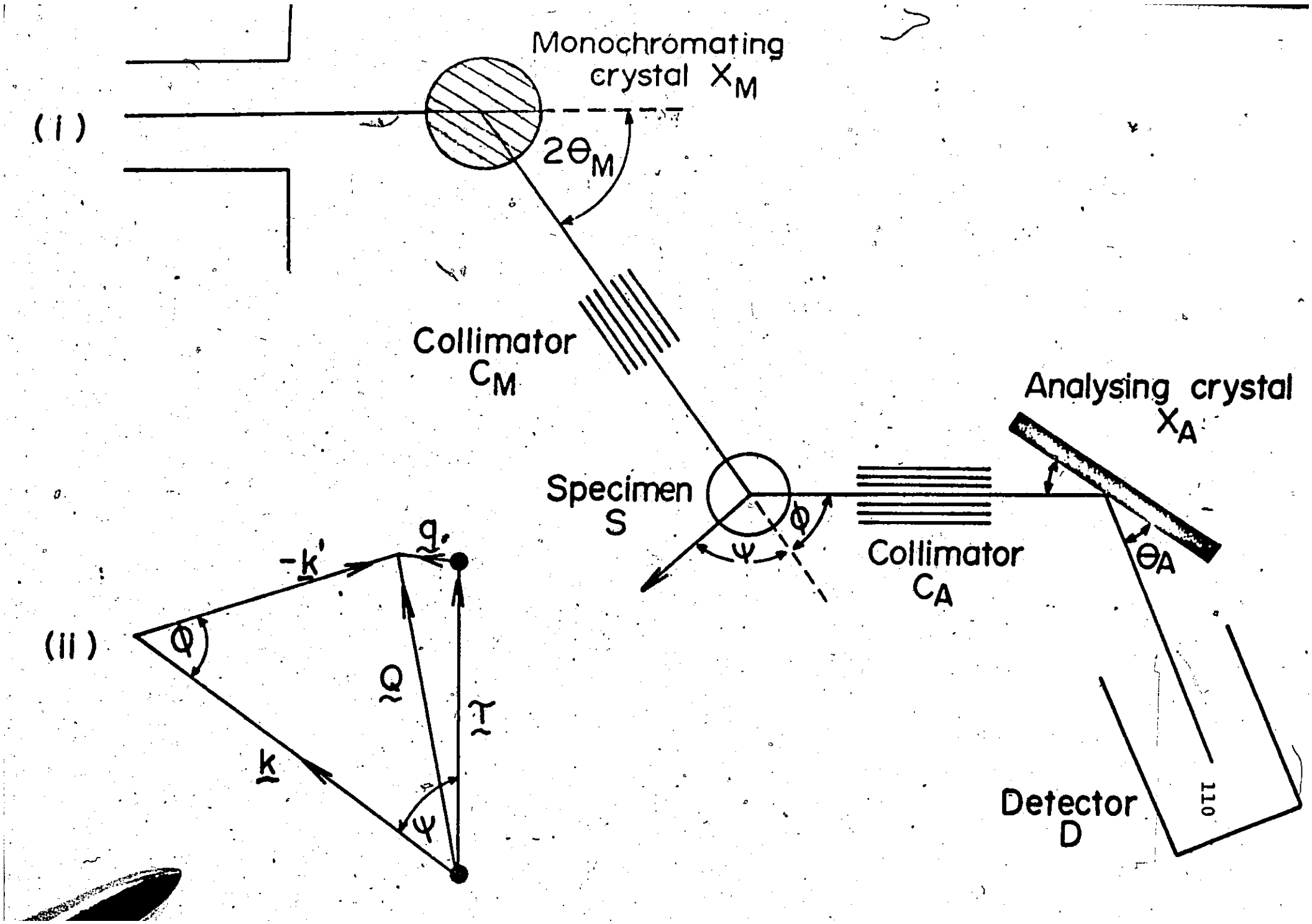
(I)
Monochromating crystal X_M
$2\theta_M$
Collimator C_M
Specimen S
ϕ
ψ
Analysing crystal X_A
Collimator C_A
θ_A
Detector D
110
(II)
$-k'$
q
ϕ
Q
τ
k
ψ

To follow any given path in $(\underline{Q},\omega)$ space, it is necessary to vary three of the four variables, ϕ, ψ, θ_M and θ_A (the values of θ_M and θ_A fix the value of $\underline{k}$ and $\underline{k}'$ respectively). In the set-up of an experiment either the incident neutron wave vector $\underline{k}$ or the scattered wave vector $\underline{k}'$ is kept fixed, which in turn implies keeping either θ_M or θ_A fixed. The specimen crystal is aligned so that one of its major symmetry planes is in the plane of the spectrometer, namely the plane determined by wave vectors $\underline{k}$ and $\underline{k}'$.

Since the whole dynamics of the scattering system can be described in terms of $\underline{Q}$, the momentum transfer and $\hbar\omega$, the energy transfer (see Eq. (II-61)), 'constant $\underline{Q}$' and 'constant E' are two common ways of scanning $(\underline{Q},\omega)$ space for the measurements of spin waves.

In the 'constant $\underline{Q}$' mode, the angles ϕ and ψ along with the angles θ_M or θ_A are varied in such a way so as to keep the terminus of the vector $-\underline{k}'$ at $\underline{Q}$, thereby keeping $\underline{Q}$ and hence $\underline{q}$ constant. The spectrometer is programmed to scan a predetermined frequency range for a preset monitor counts by changing these angles in suitable steps, thus producing a 'neutron group'. The frequency of the magnon of interest is then given by the peak of the neutron group, which occurs only when the frequency ω satisfies the dispersion relation (VI-2) for the set value of $\underline{q}$.

In the 'constant E' mode, the energy transfer is held constant and $\underline{Q}$ is allowed to vary along a predetermined

path in reciprocal space. This mode is normally used for measurements in the regions where the dispersion curve is rather steep.

At low temperatures, MnO can be described as a two sublattice antiferromagnet. As was discussed in the last chapter, apart from the dominant Heisenberg superexchange interaction between the spins, the magnetic dipole-dipole interactions are appreciable and indeed essential for describing the spin wave dispersions at small wave vectors.

The Hamiltonian for MnO can be written as

$$H_{MnO} = H_{ex} + H_{d-d} \qquad \text{(VI-3)}$$

where H_{ex} and H_{d-d} are as given by Eqs. (II-1) and (II-30) respectively. Since the measurements do not have sufficient sensitivity to render the in-plane terms significant, they have not been included in the Hamiltonian (VI-3).

The Hamiltonian was solved in the spin wave approximation. The mathematical details are given in Chapter II, and it is shown that the spin wave energies as given by solution of Eq. (II-50) are the eigenvalues of the Hamiltonian (VI-3). The numerical calculations of the dipole sums involved were performed using the Ewald technique discussed in Chapter II. The sums were evaluated for the distorted lattice of MnO using the lattice parameter of Morosin (1970). Calculations of the spin wave energies were made assuming Z

to be along either $[11\bar{2}]$ or $[1\bar{1}0]$, the differences in the dispersion curves were very small and less than experimental uncertainties.

The specimen consisted of two multi-domain single crystals of volume 1.4 cm^3. The crystals were grown by the Marabeni-Iida Company of Japan using the Verneuil technique and are black in colour. The density of the crystals was 5.36 ± 0.2, a value equal to the density calculated from the lattice parameters. The Néel temperature at 120 ± 3 K was within error of the conventional value for MnO. The Bragg reflection indicated a mosaic width of the order of 40' at room temperature. The crystals were aligned parallel to each other with the $[\bar{1}10]$ direction vertical to better than 6'. Except for a magnon at $\underline{q} = (\frac{1}{2}\ \frac{1}{2}\ \frac{1}{2})$, which was measured at various temperatures below T_N, all the measurements were done with the specimen maintained at the temperature 4.2 K in a Helium Cryostat.

It was necessary to make final alignment of the crystals at 4.2 K because of the rhombohedral distortion below the Néel temperature. The (111) nuclear reflection as measured with a neutron beam of wavelength 2.83 Å was then split up (see Fig. VI-2) into two components separated by 1.09°. The higher angle component, P, corresponds to the (111) reflection and the lower angle reflection, Q, which was found to be three times as intense, corresponds to the planes $(\bar{1}11)$, $(1\bar{1}1)$ and $(11\bar{1})$ in the multi-domain crystal.

Fig. VI-2: The splitting up of (111) nuclear reflection into two components in MnO. The higher angle component, P, corresponds to $(\bar{1}11)$ and the lower angle component, Q, to $(\bar{1}11)$, $(1\bar{1}1)$ and $(11\bar{1})$ reflections in a multidomain crystal of MnO.

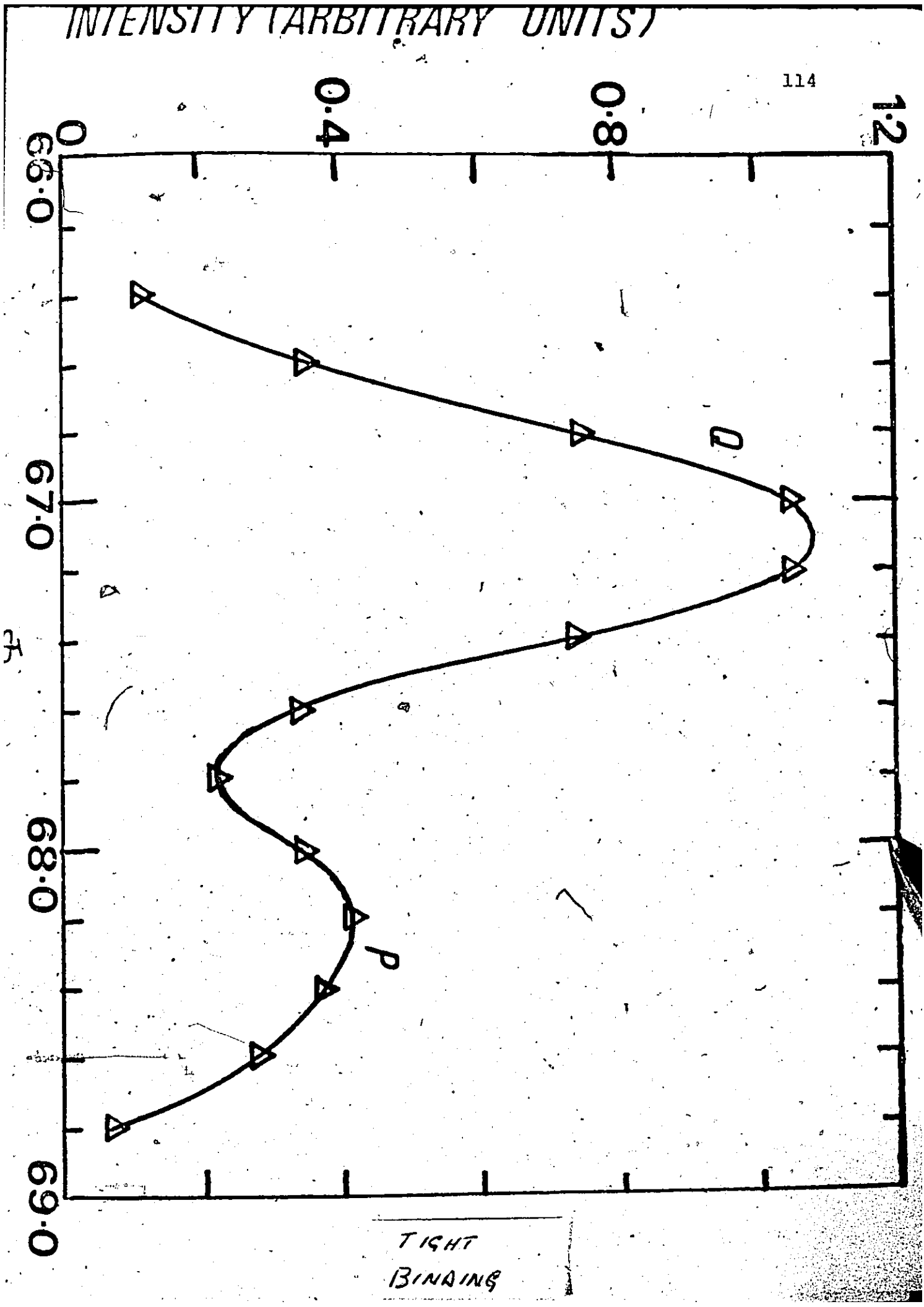
INTENSITY (ARBITRARY UNITS)
0
0.4
0.8
1.2
0.69
0.89
0.79
E
D
P
TIGHT
BINDING

The $(\frac{1}{2}\ \frac{1}{2}\ \frac{1}{2})$ magnetic reflection was not split and corresponds to peak P since the three other domains have zero magnetic structure factor. Analysis based on this data yields $a = 4.421$ Å for the cell edge and $\Delta = 0.61°$ for the small angle by which the axes depart from 90°. These values compare satisfactorily with Morosin's values of 4.4316 Å and 0.624° using X-rays. The wave vectors quoted in this experiment were obtained by aligning the crystal on the centre of gravity of the (111) reflection, the best single compromise when magnons are to be studied in a variety of magnetic and nuclear zones. The Brillouin zone scheme for the (111) domain is shown in Fig. VI-3.

All the measurements were done with the 'constant $\underline{Q}$' mode of operation. The spin waves were measured using a Germanium (220) plane as monochromator and either the pyrolytic graphite (002) or the Germanium (111) plane as the analyzer. The scattered neutron wave vector $\underline{k}'$ was kept fixed for all the measurements.

In Fig. VI-4 is shown some of the typical neutron groups obtained. The energy of the neutron group at $\underline{Q} = (\frac{1}{2}\ \frac{1}{2}\ \frac{3}{2})$ corresponding to $\underline{q} = (\frac{1}{2}\ \frac{1}{2}\ -\frac{1}{2})$ arises due to the distortion of the lattice below the Néel temperature and is proportional to $(J_{1d} - J_{1s})^{1/2}$. As pointed out by Lines and Jones (1965), this distortion lowers the total energy of the system at low temperatures and stabilises the spin system. Statistical errors on the location of the centre of the

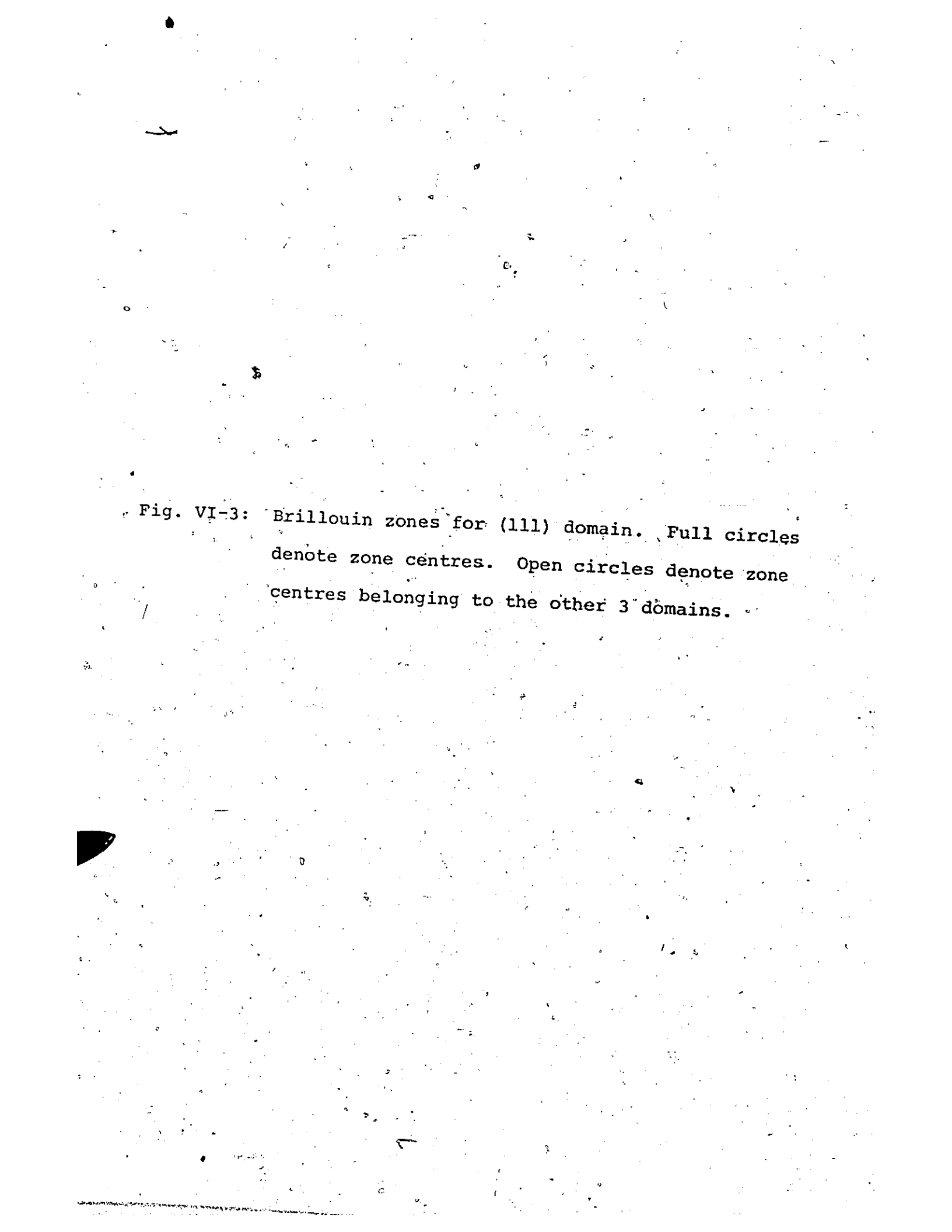

Fig. VI-3: Brillouin zones for (111) domain. Full circles denote zone centres. Open circles denote zone centres belonging to the other 3 domains.

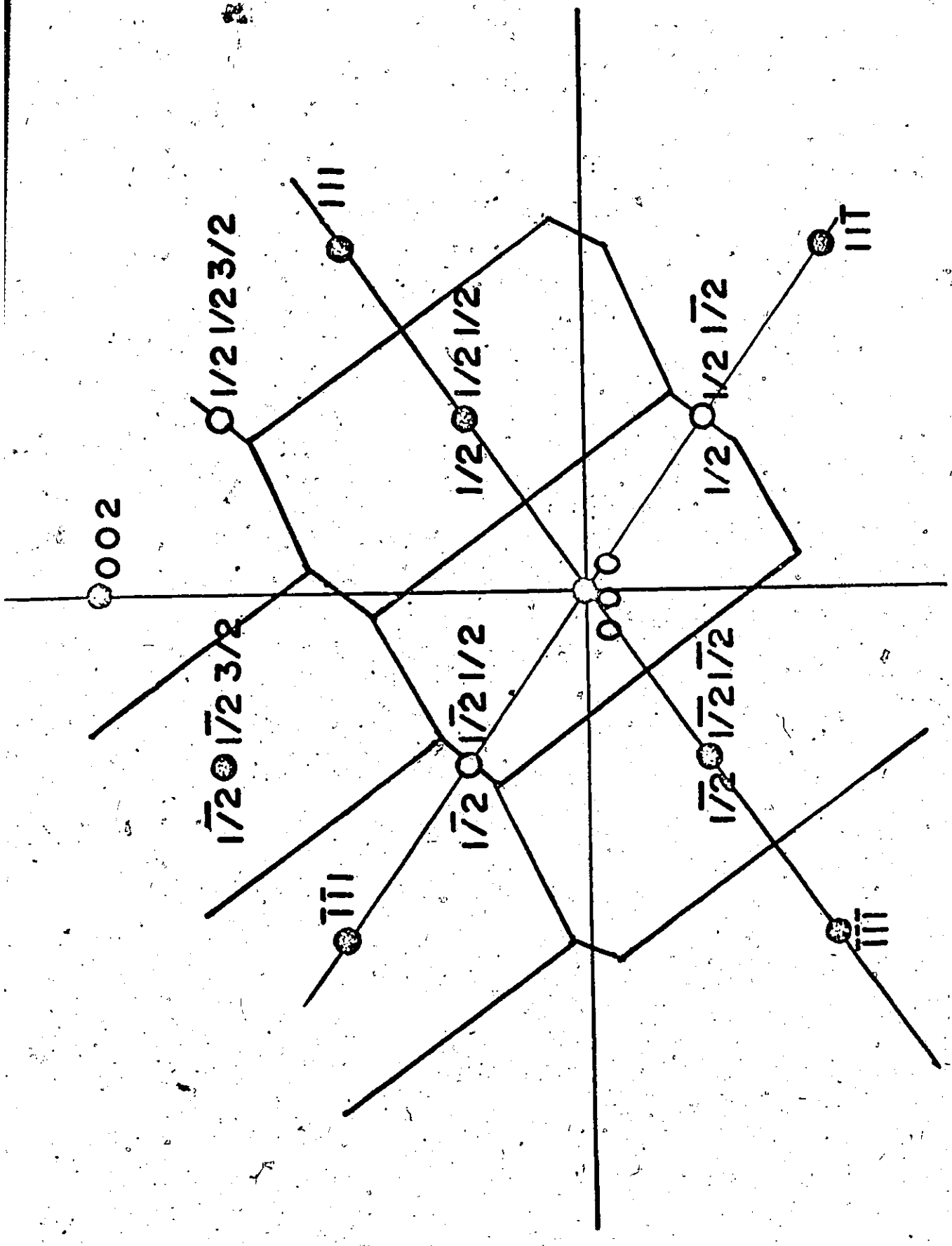
111
1/2 1/2 3/2
1/2 1/2 1/2
1/2 1/2 1̄/2
1̄T
002
1/2
1/2
1̄/2 0 1̄/2 3/2
1̄/2 1/2
1̄/2 1/2 1̄/2
1̄/2 0 1̄/2 1̄/2
1̄/2
1̄11
1̄1̄1

Fig. VI-4: Some typical neutron groups in MnO at 4.2K. The magnon at $\underline{Q} = (\frac{1}{2}\ \frac{1}{2}\ \frac{3}{2})$ corresponds to the zone centre magnon, whose energy arises from the distortion of the lattice below the Néel temperature.

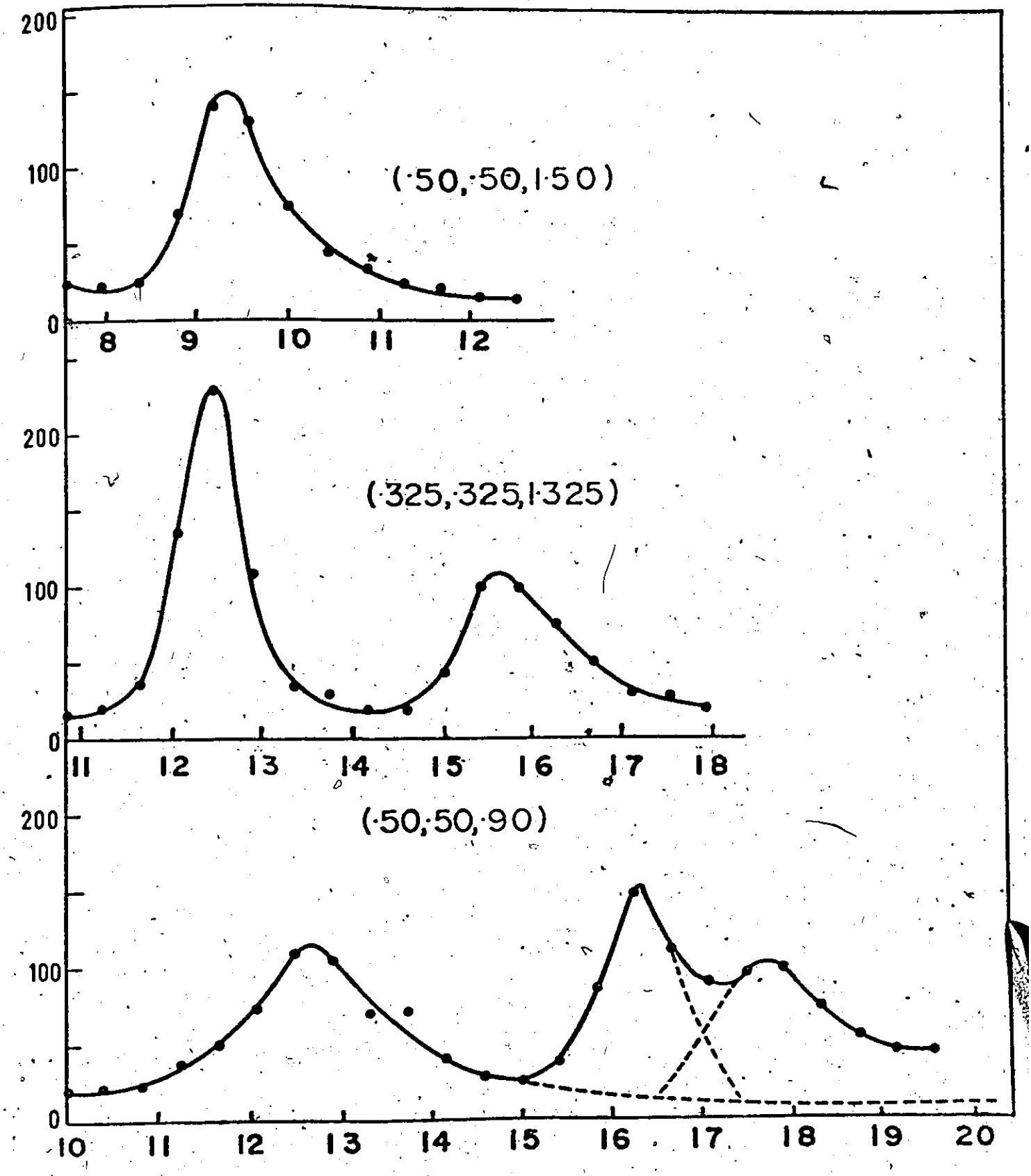

TIGHT BINAING

neutron group were of the order of ±1%. The difference in energy when the same group was observed at equivalent points in different zones was also of this order, except for the case of neutron groups of wave vector $\underline{q} = (-\frac{1}{2} + \rho, -\frac{1}{2} + \rho, \frac{1}{2} + \rho)$ with scattering vector $\underline{Q} = (\frac{3}{2} - \rho, \frac{3}{2} - \rho, \frac{3}{2} + \rho)$ and $\underline{Q} = (\frac{1}{2} - \rho, \frac{1}{2} - \rho, \frac{3}{2} - \rho)$. Differences in energies ranging from zero to 3% were observed for these groups. This may be a result of the multi-domain character of the specimen or of the compromise used in aligning the crystals. In all cases where measurements were taken at equivalent points in different zones average values were used as the quoted magnon energy. The uncertainties in most of our quoted energies are probably of the order of 2%. This represents a significant improvement over the data of Bonfante et al. (1972A), and Kohgi et al. (1972) who have also measured the dispersion relations more or less at the same time as our measurements.

In Figs. VI-5 and VI-6 are shown the dispersion curves obtained for the directions [111] and [001]. In Table VI-1 the experimentally observed magnon energies with their $\underline{q}$ vectors referred to (111) domain are listed. The branches are split by dipole-dipole interactions, but this splitting is important only at small wave vectors. The data are somewhat complicated by the fact that the crystal forms a multi-domain antiferromagnet, with sheets along [111], $[11\bar{1}]$, $[1\bar{1}1]$, $[\bar{1}11]$ directions occuring with approximately

Fig. VI-5: Dispersion relations for spin waves in MnO at 4.2K along the [111]-type directions. The reduced wavevectors, ρ, are referred to a (111) domain. Up to four of these sections of the dispersion relations may be seen at one scattering wavevector. The branches are split by dipole-dipole interactions, which are important mainly for small wavevectors and the splittings are too small to be shown elsewhere in the figure.

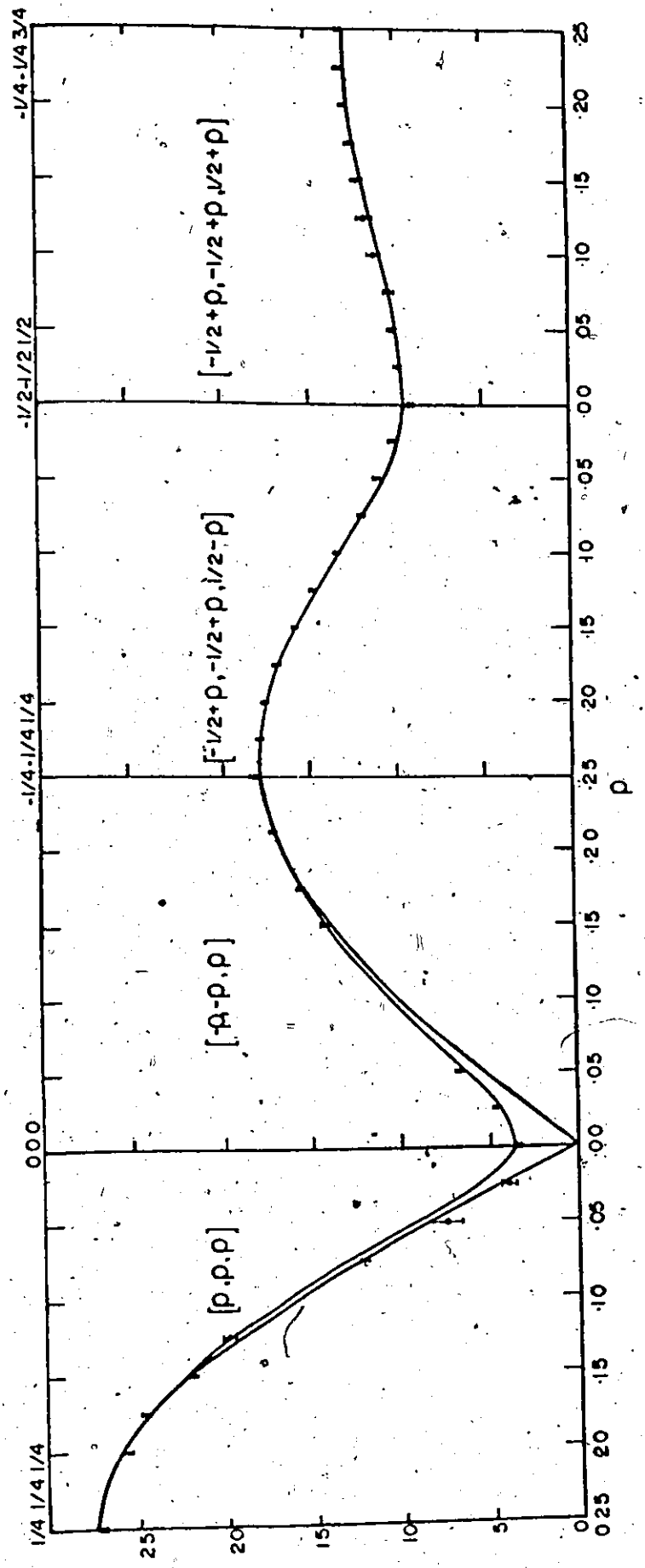
ENERGY (mev)
[ρ,ρ,ρ]
[ρ,ρ-ρ,ρ]
[-1/2+ρ,-1/2+ρ,1/2-ρ]
[-1/2+ρ,-1/2+ρ,1/2+ρ]
ρ
1/4 1/4 1/4
0 0 0
-1/4-1/4 1/4
-1/2-1/2 1/2
-1/4-1/4 3/4

Fig. VI-6: Dispersion relations for spin waves in MnO at 4.2K along [001]-type directions. Wavevectors are referred to a (111) domain. Up to two sections of the dispersion relations may be seen at any one scattering vector.

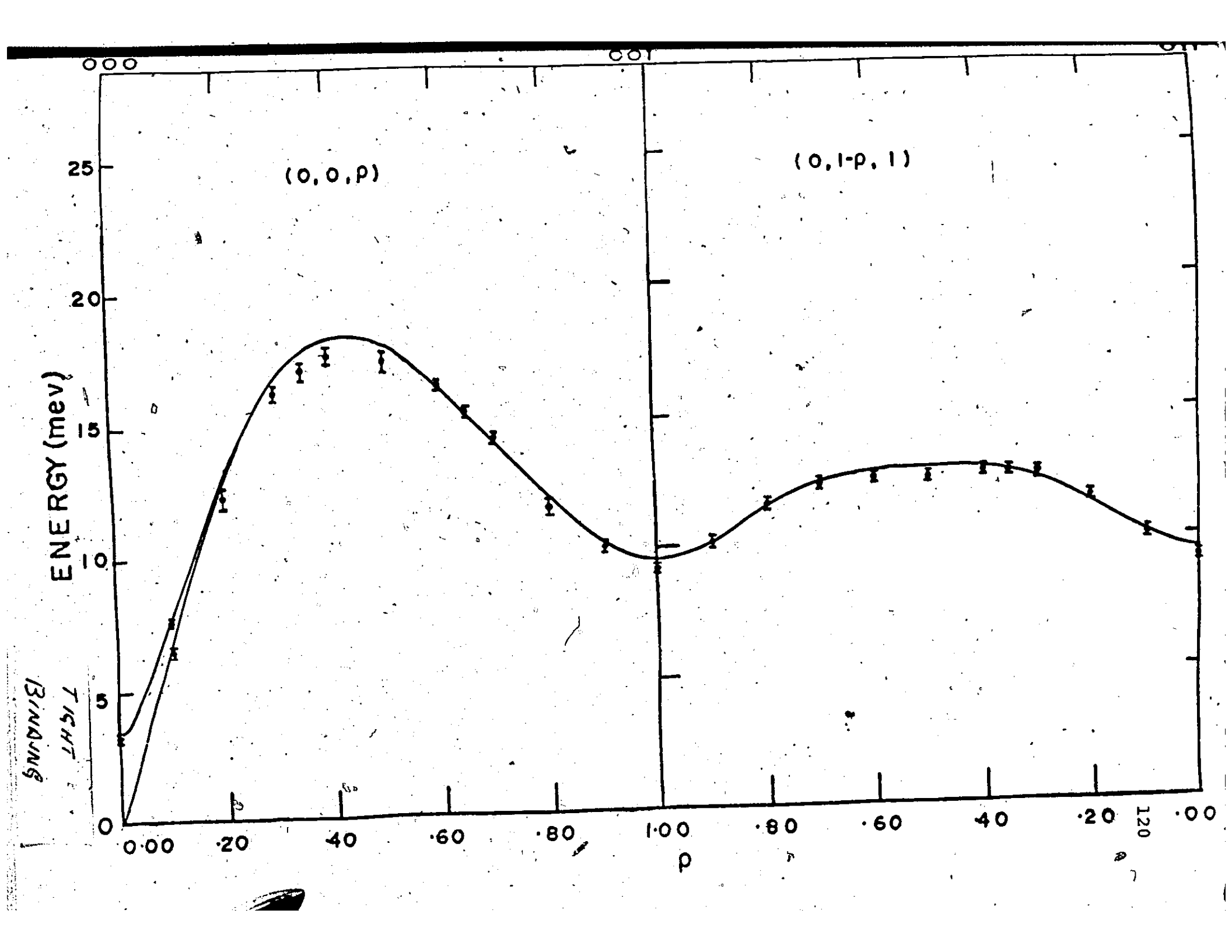
000
001
(0, 0, ρ)
(0, 1-ρ, 1)
ENERGY (mev)
25
20
15
10
5
0
0·00
·20
·40
·60
·80
1·00
·80
·60
·40
·20
·00
ρ
120
Binding
Trans

TABLE VI-1

THE EXPERIMENTALLY OBSERVED MAGNONS ENERGIES (meV) AT 4.2 K WITH $\underline{q}$, THE REDUCED WAVE VECTORS, IN TERMS OF ITS COMPONENTS ρ_x, ρ_y, ρ_z WHERE $\underline{q} \equiv 2\pi/a\ (\rho_x, \rho_y, \rho_z)$. THE WAVE VECTORS ARE REFERRED TO (111) DOMAIN

(i) Branch [ρρρ]

ρ_x	ρ_y	ρ_z	E (meV)	ΔE (meV)
.50	.50	.50	3.967	.165
.525	.525	.525	3.946	.413
.550	.550	.550	7.438	.826
.575	.575	.575	12.148	.165
.625	.625	.625	19.709	.206
.650	.650	.650	21.899	.206
.675	.675	.675	24.544	.124
.700	.700	.700	25.536	.248
.750	.750	.750	27.065	.330

(ii) Branch [ρρ$\bar{\rho}$]

ρ_x	ρ_y	ρ_z	E (meV)	ΔE (meV)
.525	.525	.475	4.545	.206
.55	.55	.45	6.652	.206
.575	.575	.425	9.049	.289

TABLE VI-1 - continued

(ii) Branch $[\rho\rho\bar{\rho}]$

ρ_x	ρ_y	ρ_z	E(meV)	ΔE(meV)
.65	.65	.35	14.214	.206
.675	.675	.325	15.495	.165
.70	.70	.30	16.941	.124
.725	.725	.275	17.106	.124

(iii) Branch $[\frac{1}{2}+\rho, \frac{1}{2}+\rho, -\frac{1}{2}-\rho]$

ρ_x	ρ_y	ρ_z	E(meV)	ΔE(meV)
.50	.50	-.50	9.214	.124
.525	.525	-.525	9.999	.165
.550	.550	-.550	10.908	.124
.575	.575	-.575	11.776	.083
.60	.60	-.60	13.264	.124
.625	.625	-.625	14.668	.124
.650	.650	-.650	15.743	.083
.675	.675	-.675	16.693	.124
.70	.70	-.70	17.437	.124
.725	.725	-.725	17.809	.165
.750	.750	-.750	18.015	.206

TABLE VI-1 - continued

(iv) Branch $[\frac{1}{2} + \rho, -\frac{1}{2} + \rho, -\frac{1}{2} + \rho]$

ρ_x	ρ_y	ρ_z	E(meV)	ΔE(meV)
.525	-.475	-.475	9.669	.165
.550	-.450	-.450	10.041	.206
.575	-.425	-.425	10.165	.289
.60	-.40	-.40	11.074	.330
.625	-.375	-.375	11.569	.413
.650	-.350	-.350	11.941	.330
.675	-.325	-.325	12.396	.248
.70	-.30	-.30	12.726	.206
.725	-.275	-.275	12.974	.165
.750	-.250	-.250	12.933	.165

(v) Branch $[\frac{1}{2}, \frac{1}{2}, \frac{1}{2} - \rho]$

ρ_x	ρ_y	ρ_z	E(meV)	ΔE(meV)
.50	.50	.40	7.851	.124
.50	.50	.40	6.528	.248
.50	.50	.30	12.313	.413
.50	.50	.20	16.197	.248
.50	.50	.15	17.065	.330
.50	.50	.10	17.602	.372
.50	.50	.00	17.354	.330
.50	.50	-.10	16.404	.206

TABLE VI-1 - continued

(v) Branch $[\frac{1}{2}, \frac{1}{2}, \frac{1}{2} - \rho]$

ρ_x	ρ_y	ρ_z	E(meV)	ΔE(meV)
.50	.50	-.15	15.247	.165
.50	.50	-.20	14.338	.124
.50	.50	-.30	11.611	.165
.50	.50	-.40	10.165	.165

(vi) Branch $[\frac{1}{2}, \frac{1}{2} - \rho, -\frac{1}{2}]$

ρ_x	ρ_y	ρ_z	E(meV)	ΔE(meV)
.50	.20	-.50	12.231	.083
.50	.10	-.50	12.437	.124
.50	.00	-.50	12.478	.124
.50	-.10	-.50	12.685	.124
.50	-.15	-.50	12.603	.124
.50	-.20	-.50	12.644	.124

equal probability. Because of this multi-domain nature, in [111]-type directions up to four sections of these dispersion relations can be seen at any one scattering vector. For [001]-type directions two such sections of the dispersion relations can be seen. We believe that we have disentangled the domain problem unambiguously for all our data with the exception of a few points located close to the branch crossings. The positions in the reciprocal space where the magnons are observed are given in Table VI-2.

In general, our results are in satisfactory agreement with those of Bonfante et al. (1972A) and Kohgi et al. (1972). In the [001] direction Kohgi et al. have not observed the $[\frac{1}{2}, \frac{1}{2} - \rho, -\frac{1}{2}]$ branch and in the [111] direction have not observed the $[-\frac{1}{2} + \rho, \frac{1}{2} + \rho, \frac{1}{2} + \rho]$ branch, while Bonfante et al. do have measurements for all the branches. In [001] our measurements of magnon energies are in good agreement with both of these groups. In the [111] direction, as compared to Bonfante, we have better agreement with Kohgi's data. Bonfante's measurements for the $[\rho\rho\rho]$ branch are systematically lower than ours by about 5%, and that of Kohgi's lie in between two measurements (~3% higher values than Bonfante's). Our value of 3.6 ± 0.3 meV for the out-of-plane zone centre mode is in agreement with the values from AFMR experiments of 3.42 ± .01 meV obtained by Richards (1963) and of 3.44 meV obtained by Hughes (1971). The out-of-plane character of the mode was verified by noting that it was

TABLE VI-2

RECIPROCAL SPACE POSITIONS Q, WHERE NEUTRON GROUPS OF FIGS. (VI-5) AND (VI-6) WERE OBSERVED REFERRED TO A (111) DOMAIN

Wave Vectors	Scattering Wave Vector Q	Reciprocal Lattice Point	Domain
(ρ,ρ,ρ)	$(\frac{1}{2}+\rho,\frac{1}{2}+\rho,\frac{1}{2}+\rho)$	$(\frac{1}{2},\frac{1}{2},\frac{1}{2})$	(111)
	$(\frac{1}{2}-\rho,\frac{1}{2}-\rho,\frac{3}{2}+\rho)$	$(\frac{1}{2},\frac{1}{2},\frac{3}{2})$	$(\bar{1}\bar{1}1)$
$(-\rho,-\rho,\rho)$	$(\frac{1}{2}-\rho,\frac{1}{2}-\rho,\frac{1}{2}+\rho)$	$(\frac{1}{2},\frac{1}{2},\frac{1}{2})$	$(11\bar{1})$
$(-\frac{1}{2}+\rho,-\frac{1}{2}+\rho,\frac{1}{2}-\rho)$	$(\frac{1}{2}+\rho,\frac{1}{2}+\rho,\frac{1}{2}+\rho)$	(1,1,1)	$(\bar{1},\bar{1},1)$
	$(\frac{1}{2}-\rho,\frac{1}{2}-\rho,\frac{3}{2}+\rho)$	(0,0,2)	(1,1,1)
$(-\frac{1}{2}+\rho,-\frac{1}{2}+\rho,\frac{1}{2}+\rho)$	$(\frac{1}{2}-\rho,\frac{1}{2}-\rho,\frac{3}{2}-\rho)$	(0,0,2)	(1,1,1)
	$(\frac{3}{2}-\rho,\frac{3}{2}-\rho,\frac{3}{2}+\rho)$	(1,1,1)	$(\bar{1},\bar{1},1)$

continued...

TABLE VI-2 - continued

Wave Vectors	Scattering Wave Vector, Q	Reciprocal Lattice Point	Domain
(0,0,ρ)	$(\frac{1}{2},\frac{1}{2},\frac{3}{2}+\rho)$	$(\frac{1}{2},\frac{1}{2},\frac{3}{2})$	$(\bar{1}\bar{1}1)$
	$(\frac{1}{2},\frac{1}{2},\frac{1}{2}+\rho)$	$(\frac{1}{2},\frac{1}{2},\frac{1}{2})$	(111)
(0,1-ρ,1)	$(\frac{1}{2},\frac{1}{2},\frac{3}{2}+\rho)$	$(\frac{1}{2},\frac{1}{2},\frac{3}{2})$	$(\bar{1},1,1)$
	$(\frac{1}{2},\frac{1}{2},\frac{1}{2}+\rho)$	$(\frac{1}{2},\frac{1}{2},\frac{1}{2})$	$(\bar{1},1,1)$

absent for $\underline{Q}$ along [111]. The in-plane mode was not observed down to the lowest frequencies available in the infra-red experiments, and the present neutron experiments are consistent with the conclusion that its frequency is zero and its value is certainly less than 0.30 meV. In the vicinity of the 1.8 meV energy quoted by Bonfante et al. (1972B) for the in-plane mode, no evidence was found for the existence of a spin wave mode when due allowance was made for the vertical resolution of the spectrometer and the mosaic spread of the crystal.

The spin wave energies as given by the solution of Eq. (II-50) have been fitted by the method of least squares to the data together with the AFMR value of 3.42 ± 0.01 meV for the $\underline{q} = 0$ out-of-plane mode. The exchange constants have been treated as the adjustable parameters in comparing the experimental results to the calculated magnon energies. The resultant exchange parameters were corrected for the effect of zero-point motion. The effect has been discussed in Chapter IV. From Eq. (IV-17) one can see that the apparent (fitted) exchange parameters are related to exchange constants J_i for a given atom i by

$$J_i^{APP} = J_i(1 + c_i/2S) \quad . \qquad \text{(VI-4)}$$

The values of c_2, c_{1s} and c_{1d} can be read from Table IV-1. The corrected values (the correction is of the order of 1%)

are listed in Table VI-3. As can be seen in Figs. VI-5 and VI-6, the overall fit with the theory is good but for one or two regions (e.g., the region around (0,0,.4) small systematic discrepancies remain). Exchange to third nearest neighbours was not found to be significantly different from zero, a physically reasonable result.

For comparison we have included the exchange constants determined by Bonfante et al, corrected for the zero-point effects using the theory of Chapter IV (Collins and Tondon 1972). The values obtained by Kohgi et al. (1972) are not included in Table VI-3, since they were obtained by treating the dipole-dipole interactions in the Hamiltonian in an approximate way that was outlined in Section 2 Chapter II. There appears to be a typographical error in Bonfante's paper (corrected in Table VI-3) since they quote J_{1s} as being greater in magnitude than J_{1d} and this is not consistent with stability. We have assumed that in fact J_{1d} and J_{1s} are for antiparallel and parallel nearest neighbours. The overall agreement is not good in view of the errors quoted; Bonfante et al. seem to have systematically lower values of exchange than us, even though much of the data of Bonfante et al. is in agreement with ours. Part of the difference may come from the different way they have treated spin wave interactions and dipole terms.

We have calculated the density of states for MnO using our fitted exchange constants as given in Column 2 of

TABLE VI-3

VALUES OF THE EXCHANGE CONSTANTS (IN meV) FOR MnO

	Exchange Constants - This Work		
	Third Neighbours Included in Fit	Third Neighbours Excluded from Fit	Bonfante et al.
J_{1d}	-0.452 ± .009	-0.464 ± .009	-0.428 ± .014
J_{1s}	-0.361 ± .005	-0.367 ± .005	-0.328 ± .014
J_2	-0.437 ± .003	-0.434 ± .003	-0.422 ± .036
J_{3d}	0.006 ± .003	-	-
J_{3s}	0.007 ± .002	-	-

Table VI-3. The curve obtained is shown in Fig. VI-7. Due to limitations in computer time, dipole-dipole interactions have been neglected in the calculations. This amounts to an error of the order of 0.1 to 0.2 meV in the frequency scale, which will not modify the form of the curve significantly. The calculations are based on the method of Gilat and Raubenheimer (1966), modified to take into account the trigonal symmetry. A noteworthy feature of the density of states curve is the very sharp rise near 10 meV, this might be expected to show up clearly in infra-red or light scattering experiments.

In Table VI-4 are given a set of apparent exchange constants J^{APP} and constant out-of-plane anisotropy, H_A, that will reproduce approximately the observed spin wave frequencies from the formula

$$h^2\omega^2(\underline{q}) = [H_A - 2SJ_{1s}(0) + 2SJ_{1s}(\underline{q}) + 2SJ_{1d}(0) + 2SJ_2(0)]^2 - [2SJ_{1d}(\underline{q}) + 2SJ_2(\underline{q})]^2 \quad \text{(VI-5)}$$

where for $\underline{q} = 2\pi(x,y,z)/a$,

$$J_1(\underline{q}) = 2J_1[\cos\pi(x\pm y) + \cos\pi(x\pm z) + \cos\pi(y\pm z)] \quad \text{(VI-6)}$$

with the upper (lower) signs referring to d (s),

Fig. VI-7: Density of states in MnO. Dipole-dipole interactions have been ignored in the calculation.

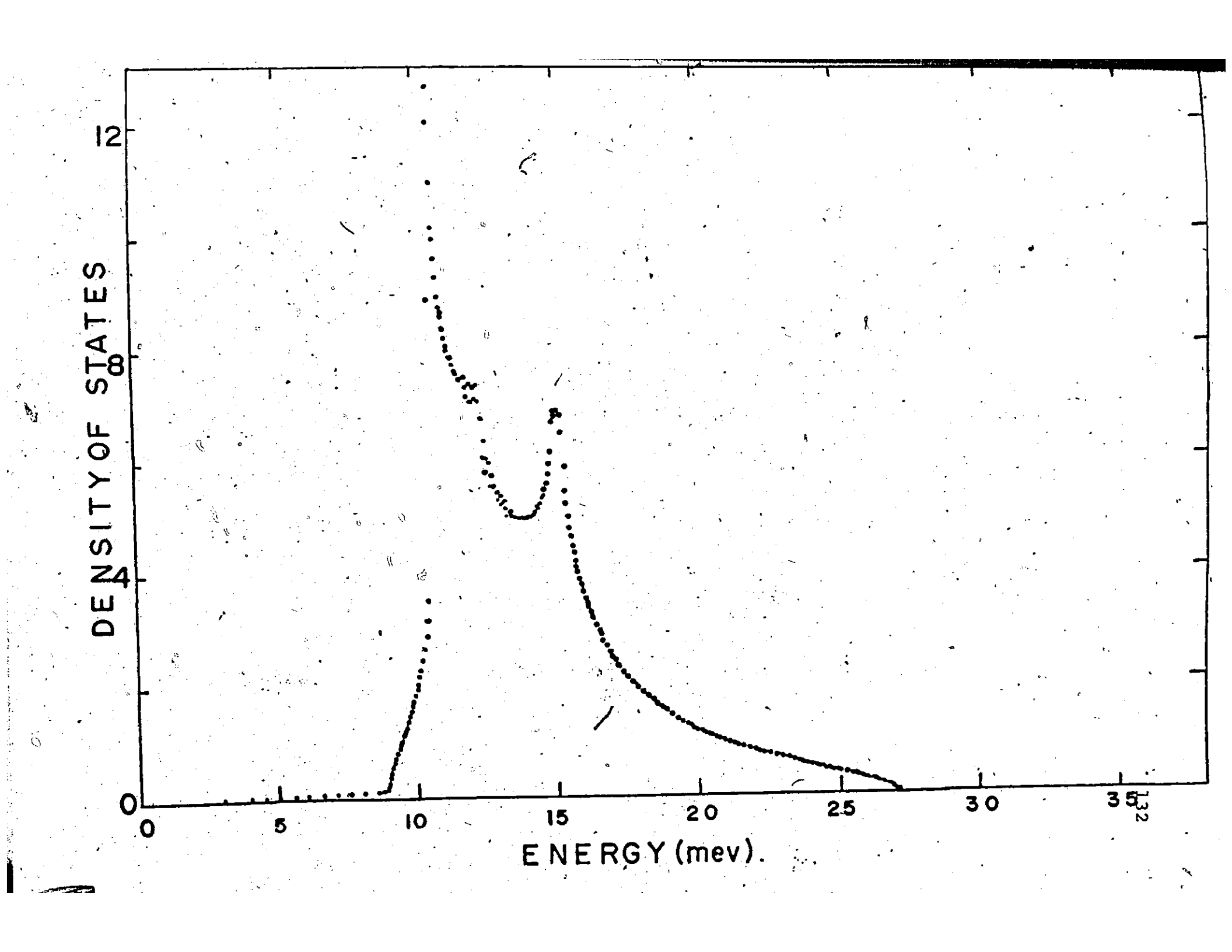
DENSITY OF STATES
0
4
8
12
0
5
10
15
20
25
30
35
ENERGY (mev).

TABLE VI-4

APPARENT EXCHANGE CONSTANTS

AND EFFECTIVE ANISOTROPY

(IN meV)

J_{1d}^{APP}	-0.466
J_{1s}^{APP}	-0.361
J_{2}^{APP}	-0.438
H_A(out)	0.2156
H_A(in)	0

$$J_2(q) = 2J_2[\cos(2\pi x) + \cos(2\pi y) + \cos(2\pi z)] \qquad \text{(VI-7)}$$

and $H_A = 0$ for the in-plane mode.

Our value of $H_A = 0.2156$ meV, which corresponds to $D_1 = 0.043$ meV ($H_A = 2SD_1$), agrees well with the Kohgi's value of $D_1 = 0.043 \pm .002$ meV. The value of D_1 as calculated by using Eq. (II-56) for $K_1 = 1.64 \times 10^7$ ergs/c.c. (Kaplan, 1954; Keffer and O'Sullivan, 1957) and $K_1 = (1.16 \pm .08) \times 10^7$ ergs/c.c. (Lines and Jones, 1965) are 0.055 meV and $0.039 \pm .002$ meV respectively.

The splitting of the nearest neighbour exchange constants in MnO gives us information about the way the exchange interaction varies with the bond angle and the bond length. Let us make the assumption that the exchange splitting arises from the change of interatomic distances only and not from the change of bond angle. Using the value of Δ as given by Fig. V-3 to get the value of r as defined by Eq. (V-1) and our values of exchange constants, we get (see Eq. (V-2) for the definition of ϵ)

$$\epsilon = -21 \pm 1 \quad . \qquad \text{(VI-8)}$$

The value is in satisfactory agreement with the value of -23 of Morosin (1970) and the value -19 of Harris (1972) in view of the uncertainties involved. The agreement and the approximate equality of J_1 and J_2 indicate that the exchange

is rather insensitive to the bond angle at the oxygen atom in MnO.

CHAPTER VII

SPIN WAVES AT FINITE TEMPERATURE

In this chapter we shall describe the experimentally-observed features of spin waves at finite temperature in antiferromagnets. Then we give a review of the present day status of the theories that have been put forward to explain some of the features.

Spin wave modes that are well defined when observed at temperatures very low as compared to the Néel temperature become increasingly degraded at higher temperatures. The energies of the spin wave modes decrease, their line widths increase and they lose their individual character in a growing continuous spectrum of frequencies characteristic of the disorder of the paramagnetic phase. Figure VII-1, which is the measurement of a spin wave mode in MnO at different temperatures (Collins, Tondon and Buyers, unpublished work) up to the Néel temperature of 120K, helps to illustrate these points.

Measurements of spin wave dispersion relations at finite temperature have so far been reported in three simple Heisenberg three-dimensional antiferromagnets: MnF_2, MnO and $RbMnF_3$.

MnF_2 was the first antiferromagnet in which finite temperature measurements were made (Turberfield, Okazaki and

Fig. VII-1: The degrading of spin waves with the increasing temperature. The magnon peaks shown are of MnO at $\underline{q} = (\frac{1}{2}\ \frac{1}{2} - \frac{1}{2})$.

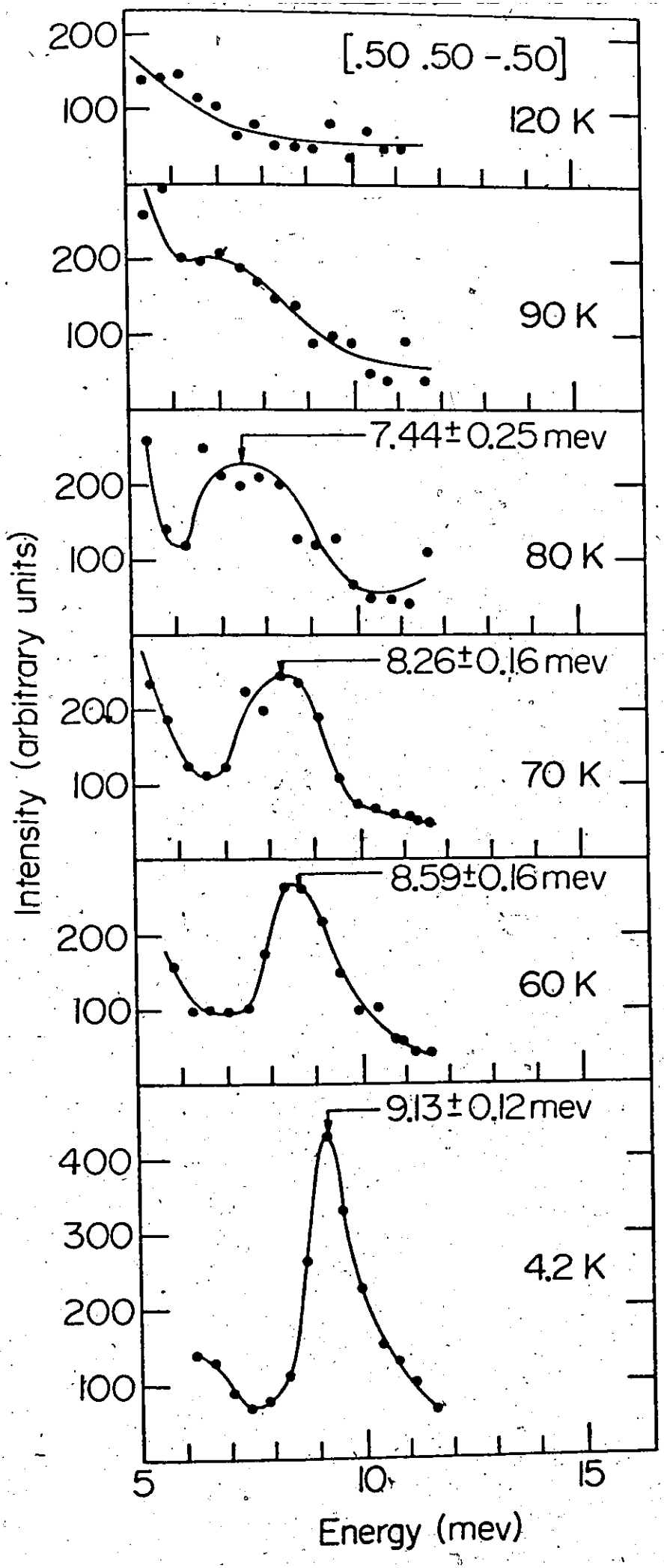
[.50 .50 -.50]
120 K
90 K
7.44±0.25 mev
80 K
8.26±0.16 mev
70 K
8.59±0.16 mev
60 K
9.13±0.12 mev
4.2 K
200
100
400
300
5
10
15
Intensity (arbitrary units)
Energy (mev)

Stevenson, 1965). The magnetic structure of MnF_2 is known from neutron diffraction experiments by Erickson (1953). The crystal structure is of the rutile type with the Mn ions lying on a body-centred tetragonal lattice. In the antiferromagnetic state two sets of antiparallel spins are aligned along the c-axis. These may be regarded as belonging to two interpenetrating simple tetragonal sublattices. This form of antiferromagnetic structure is usually described as CsCl type. The dominant exchange interaction is between an ion and its eight nearest neighbours on the other sublattice. The exchange constant corresponding to this interaction is denoted as J_2, while J_1 signifies the interactions between nearest neighbour ions which lie along the c-axis and on the same sublattice. The various magnetic properties of MnF_2, along with the experimental values of exchange constants and the effective anisotropy field, are summarized in Table VII-1. The zero temperature dispersion curves were obtained by Low et al. (1964), using inelastic neutron scattering techniques.

Turberfield et al. (1965) studied the behaviour of spin wave excitations in MnF_2 at temperatures in the range of 49.5 to 70.0K, i.e., in the antiferromagnetic region $0.75 < T/T_N < 1$, and in the paramagnetic region $1 < T/T_N < 1.2$. The experiments were performed using the twin rotor neutron time-of-flight spectrometer on the Pluto reactor at Harwell. They obtained complete dispersion curves in the [001] direction at 49.5K and 62K. Along with decreasing energy,

TABLE VII-1

THE MAGNETIC PROPERTIES OF MnF_2

Structure: Rutile type in paramagnetic and Cs Cl type in antiferromagnetic phase

Magnetic Ion: Mn^{+2}, spin 5/2 in S state

Neighbours	Spin	Type	Number	Position h=±1,k=±1/2	Exchange Constant (meV)
1	||	s	2	(0,0,h)	J_1=0.027
2	anti||	d	8	{k,k,k}	J_2=-.151
3	||	s	4	(h,0,0) and (0,h,0)	J_3=0.0

Néel Temperature: 67K

The Effective Anisotropy Field: H_A = 0.091 meV.

they observed line broadening of the peaks with the increase of temperature.

These effects become extremely significant as the temperature approaches the Néel temperature. The accelerating decrease in energy with the increasing temperature is much more marked at small wave vectors. As we proceed we will see that this experimentally observed wave vector dependence of the fractional decrease in magnon energy is not unique to MnF_2.

The measurements of spin waves at finite temperatures in $RbMnF_3$ were also done at Harwell by Saunderson, Windsor et al. (1972).

In the paramagnetic phase the magnetic Mn^{+2} ions lie on a simple cubic lattice in $RbMnF_3$. On passing below the Néel temperature ($T_N \doteq 83K$) the crystal undergoes an antiferromagnetic phase transition without loss of cubic symmetry. In the ordered phase the spins on adjacent Mn^{+2} ions along cube axes align antiferromagnetically such that the ions of each sublattice now form a face-centred cubic lattice with double the paramagnetic lattice parameter. The spin wave dispersion curves measured at 4.2K by Windsor and Stevenson (1966) and confirmed by measurements of Saunderson, Windsor et al. (1972) indicate that only the nearest neighbour exchange interaction is important. The second and third nearest neighbour exchanges are not significantly different from zero. The value of the anisotropy is also

very small (4.5 gauss) thus making it one of the simplest of magnetic salts. The magnetic properties of $RbMnF_3$ are summarized in Table VII-2.

The data of finite temperature measurements in $RbMnF_3$ by Saunderson et al. (1972) are rather extensive. The dispersion curve measurements along [001] were made at five temperatures, from .38 T_N to .80 T_N, for sixteen values of the wave vector. As in MnF_2, the decrease in energy at a particular temperature is observed not to be the same at all wave vectors but to be more at smaller wave vectors. At temperatures close to the Néel temperature, there is an almost 20% greater reduction in the energy of spin waves at small wave vector than of the spin waves at the zone boundary.

Finite temperature measurements in MnO have been reported by Bonfante et al. (1972B). Very recently Kohgi et al. (1973) have also reported similar measurements. The magnetic properties of MnO have been already discussed in Chapters V and VI and summarized in Tables V-1 and VI-3.

Bonfante et al. measured dispersion curves at two temperatures: 88.75K (.75 T_N) and 114.75K (.95 T_N). While the 114.75K data is confined to measurements along the [001] direction only, the 88.75K data is along both the [001] and [111] directions. Also they studied a particular magnon mode (0,0,.1) up to temperatures very close to the Néel temperature. Kohgi et al. have measured complete dispersion

TABLE VII-2

THE MAGNETIC PROPERTIES OF $RbMnF_3$

Structure: Simple cubic, in antiferromagnetic phase spins alternate along the cube edges

Magnetic Ion: Mn^{+2}, spin 5/2 in S state

Neighbours	Spin	Type	Number	Position h=±1	Exchange Constant (meV)
1	anti||	d	6	{h,0,0}	J_1=-0.292
2	||	s	12	{h,h,0}	J_2= 0.0
3	anti||	d	8	{h,h,h}	J_3= 0.0

Néel Temperature: 83K

curves at 60K (.50 T_N), 78K (.65 T_N) and 100K (.83 T_N) for both [001] and [111] directions. Besides they attempted measurements at 115K also. At this temperature, however, they could make only limited measurements confined to low energy excitations because of the highly damped nature of spin waves at large q. However, the spin waves with low energy and small q seem to be well defined even at high temperature. In both of these papers, no mention is made of the q dependence of the fractional decrease in magnon energy with temperature, although the experimental data does indicate such a dependence at least for the [001] direction. In the [111] direction, the dependence does not seem significant up to .75 T_N.

NiO has the same magnetic structure as MnO (Type II f.c.c.). Although dispersion curve measurements have been made at low temperatures (Hutchings et al., 1973), no finite temperature measurements have been reported. In Table VII-3 the magnetic properties of NiO are summarized.

In the past few years, several experimental measurements have been made on the shift of the energy of magnon sidebands with temperature (Sell, 1968). The magnon sidebands are caused by the simultaneous creation of an exciton and a magnon by light absorption, and their shift with temperature is related to the temperature dependence of the magnon energy. Experiments on Raman scattering by magnons in various antiferromagnets (Fleury, 1970) also show that the

TABLE VII-3

THE MAGNETIC PROPERTIES OF NiO

Structure: Type II f.c.c. (same as of MnO)

Magnetic Ion: Ni^{+2}, spin 1 in S state

Neighbours	Spin	Type	Number	Position h=±1/2,k=±1	Exchange Constant (meV)
1	anti||	d	6	{h,h,0}	J_{1d}=0.674
1	||	s	6	{h,-h,0}	J_{1s}=0.692
2	anti||	d	6	{k,0,0}	J_2=-9.497

Néel Temperature: 523K

decrease in magnon energy has wave vector dependence with short wavelength magnons persisting even above T_N. This phenomenon is most marked in systems of low dimensionality (Skalyo, 1969; Birgeneau, 1969), where all but the very long-wavelength spin waves are found to be essentially temperature independent in excess of transition temperature, although the zero wave vector (zone-centre) magnons have energies going to zero at the transition temperature.

In order to study the magnetic properties at a finite temperature and in particular to calculate the decrease in the magnon energy with temperature, one needs to take the interactions between the spin waves of a system into consideration. We shall not concern ourselves with the calculations of the life time that accounts for the broadening of the magnon peaks.

In the spin wave approximation one assumes that for small values of total spin deviations the difference in energy between a state with n spin deviations and the completely parallel one can be regarded as approximately equal to the sum of n rigorously computed differences for unit deviations, i.e., one makes the assumption of additivity about the spin reversals. However, actually speaking even if there are just two spin deviations present, the energy of the system would depend on whether the deviations are present on the same atom (for $S > 1/2$), on different atoms that are coupled, or on more distant atoms

not coupled by the Hamiltonian. Since at a finite temperature there are large number of spin deviations present, the concept of superposition of spin waves breaks down, i.e., the spin waves start interacting.

Dyson (1956) in his two classic papers gave a general theory of spin wave interactions in ferromagnets. He categorised the interactions as of two types: kinematical and dynamical. Of the two, dynamical interaction is the dominant one.

The kinematical interaction may physically be interpreted as due to the fact that the number of spin deviations at any lattice site cannot exceed 2S, because of the spin conservation. However, the boson operators into which spin operators are transformed by the H-P transformation do not obey any such restriction, the boson space being infinite dimensional as compared to (2S+1) dimensional space of spin. Thus, the transformation to bosons introduces non-physical states. It should be noted, however, that this is not due to H-P transformation as given by Eq. (II-9), which maintains the separability of the two spaces (Eq. (II-9) yields zero when $a^{\dagger}a = 2S$). These nonphysical states are introduced when a simplification is made such as say by restricting to linear approximation (see Eq. (II-15)). In any case, these states are not likely to give any contribution as long as the temperature of the system is not high enough to have more than 2S spin deviations per atom, on the average.

This is known to happen only for temperatures within a few degrees of the critical temperature. Low (1964) estimates that for S = 5/2, kinematical effects will be important only within 1% or so of the Néel temperature. We shall neglect the effect of kinematical interactions on magnon energy in the calculations.

Physically speaking, dynamical interactions arise because it costs less energy for a spin to suffer a deviation if the spins with which it directly interacts have already undergone deviations from their fully aligned state. This interaction is the one primarily responsible for the experimentally observed decrease in magnon energy with temperature. Dynamical interaction represents the nondiagonal part of the Hamiltonian in Dyson's basic set of states.

Dyson's results extrapolated to high temperatures suggested that magnon-magnon interactions in ferromagnets may be relatively weak even near the curie temperature. This prompted Michelene Bloch (1962) to explore the possibility of treating ferromagnets and antiferromagnets (M. Bloch, 1963) as a gas of weakly interacting magnons. She examined the Heisenberg exchange Hamiltonian in H-P formalism, obtained by truncating the square root expansion after the first term in boson operators (see Eq. (IV-3)) and then retaining only terms involving occupation numbers of a pair of spin waves, for the purpose of calculating the temperature dependence of the magnon energy and the magnetization. It is assumed that

this truncated Hamiltonian remains valid through the entire temperature range. Bloch's paper was limited to simple cubic ferromagnets and simple cubic and Cs Cl type antiferromagnets with just one exchange interaction. The Hamiltonian H^B, for a cubic ferromagnet is

$$H^B = \sum_{\underline{k}} n_k E_k - \left(\frac{Z}{NJ}\right) \sum_{\underline{k}\underline{k}'} n_k n_{k'} (\gamma_0 + \gamma_{k-k'} - \gamma_k - \gamma_{k'}) \qquad \text{(VII-1)}$$

where

$$E_k = 2JSZ(\gamma_0 - \gamma_k) \quad , \quad \gamma_k = \sum_{\delta} \exp i(\underline{k}\cdot\underline{\delta})/Z \quad . \qquad \text{(VII-2)}$$

Here $\underline{\delta}$ denotes vectors to nearest neighbours, and n_k is the number operator.

For a simple cubic lattice, H^B can be rewritten as

$$= \sum_k E_k n_k - \left(\frac{1}{4JNZS^2}\right) \sum_{kk'} E_k E_{k'} n_k n_{k'} \qquad \text{(VII-3)}$$

Z being the number of nearest neighbours and N, the total number of atoms. In going from Eq. (VII-1) to Eq. (VII-3), one makes use of (Semura, 1972)

$$\sum_k \gamma_{k-k'} n_k = \gamma_{k'} \sum_k \gamma_k n_k \quad . \qquad \text{(VII-4)}$$

By using a variational approach, i.e., minimizing the free energy of the system with respect to $\langle n_k \rangle$, the

average occupation number, one gets an expression for the energy $E_k(T)$ of a quasimagnon of wave vector $\underline{k}$ at the temperature T as

$$E_k(T) = E_k\{1 - (2ZJNS^2)^{-1} \sum_{k'} [<n_{k'}>E_{k'}]\} \qquad \text{(VII-5)}$$

where $<n_k>$, the boson population factor, is given as

$$<n_k> = 1/[\exp(E_k(T)/k_BT) - 1] \qquad \text{(VII-6)}$$

Thus, the magnon energy at zero temperature E_k is renormalised to $E_k(T)$ at temperature T, and the renormalisation factor $\alpha^F(T)$ for a ferromagnet is

$$\alpha^F(T) = E_k(T)/E_k = 1 - (2ZJNS^2)^{-1}[\sum_{k'} <n_{k'}>E_{k'}] \qquad \text{(VII-7)}$$

The similar expression for the renormalisation of a simple antiferromagnet (Bloch, 1963) is

$$\alpha^A(T) = 1 + C/2S - [(JNZS^2)^{-1} \sum_{k'} <n_{k'}>E_{k'}] * \qquad \text{(VII-8)}$$

where C is as given by (III-5) and

---

* These expressions are written with N as the total number of atoms, Bloch's expressions are with N as the number of primitive cells in the crystal.

$$E_k = 2JSZ(1 - \gamma_k^2)^{1/2} \quad . \qquad \text{(VII-9)}$$

Since spin wave interactions result in renormalising the spin wave energy by a certain factor, the interaction theories are also commonly referred to as renormalisation theories.

Following Bloch, we summarise below the main properties of $\alpha(T)$:

(1) $\alpha(T)$, as derived by Bloch, is the same for all magnon modes (independent of $\underline{k}$) at a given temperature T. This simplification is a result of the above expressions being restricted to the simple cases of just one exchange constant, and is not true in general.

(2) The expression for $\alpha(T)$ is an implicit equation since $\langle n_k \rangle$ on the right hand side of Eqs. (VII-7) and (VII-8) is itself $\alpha(T)$ dependent. Thus, the equation needs to be solved in a self-consistent fashion in order to evaluate $\alpha(T)$.

(3) There exists a maximum temperature T_M (T_M' for an antiferromagnet) above which no self-consistent solution of Eqs. (VII-7) and (VII-8) can be found and this temperature is close to experimental values of the transition temperature.

(4) In a domain of temperatures $(0, T_M)$ Eqs. (VII-7) and

(VII-8) have two roots α_1 and α_2 at each temperature T, of which the larger corresponds in the low temperature limit to the standard results of the spin wave theory. The two roots at zero temperature are 1 and 0, as can be seen by examining the low temperature limit of Eq. (VII-7).

(5) At T_M, the reduced magnetization does not reduce to zero but has a finite value of about 0.25.

Since the appearing of these two papers of M. Bloch (Bloch, 1962, 1963) on spin wave renormalisation, a rather large number of authors have referred to this work. Even previous to Bloch; Oguchi and Honma (1961) had studied the temperature dependence of spin wave energy. Their theory, however, considers only the spin waves with infinite wavelength, that is, the ferromagnetic and antiferromagnetic resonance frequencies. Kanamori and Tachiki (1962) had given a general description of temperature dependence of spin waves with finite wavelength. Also, Bloch's expression for the renormalisation was known in the long wavelength approximation (Keffer and Loudon, 1961).

The approximation under which Bloch obtained the renormalisation expression is usually referred to as the 'magnon renormalisation approximation' (MRA) or as 'self consistent renormalisation' (SCR). Low (1963) used Bloch's approach to calculate thermodynamic properties of ferro and antiferromagnets. In particular, he calculated (Low, 1964)

dispersion curves at finite temperature for MnF_2 and compared the calculations with experimental data of Turberfield et al. (1965). While we only mention it here, in the next chapter Low's calculation will be discussed in more detail.

Nagai in a series of papers (O. Nagai, 1969A 1969B; Nagai and Tanaka, 1969; 1970) develops the theory of temperature dependent magnon energies in antiferromagnets, in which the spin wave interaction terms are treated by the random phase approximation (RPA). Nagai (1969A) suggests another temperature T_0, lower than T_M', defined as the temperature at which the energy of a magnon with infinite wavelength ($\underline{q} = 0$) becomes zero, may be the maximum temperature instead of T_M' above which MRA cannot be valid. Nagai and Tanaka (1969) use RPA as well as the MRA approach to compute the temperature dependence of the AFMR, sublattice magnetization and magnetic specific heat of MnF_2 and FeF_2. They find that the experimental data mostly lie between these two approximate calculations.

Using standard Green's function techniques, the renormalised magnon energies of Bloch (Loly, 1968) appear as a solution of the one-particle Dyson equation with the first order self-energy calculated self-consistently. Further energy shifts as well as an energy width appear as the real and imaginary part of the second order self-energy. Loly (1971) also examines for $S = 1/2$ the double valued solution of the renormalisation factor and concludes that the lower

branch of α gives a higher free energy and is, therefore, inconsistent with minimization of the free energy.

Liu (1966) solved the Hamiltonian for a simple antiferromagnet within the random phase approximation by using a formalism similar to the Gorkov theory of superconductivity, and got results analogous to Bloch (1963). Flax (1970) used this approach for an anisotropic Heisenberg antiferromagnet with spin 1/2.

Bonfante et al. (1972B) calculate dispersion curves in MnO at finite temperature using Green's functions. The calculations use a decoupling scheme due to Callen (1963), adapted following Lines (1964) to type II f.c.c. like MnO. The agreement of the calculations with the experimental data is rather good. The Néel temperature yielded by the Callen decoupling method is about 135K.

Kohgi et al. (1973) calculate dispersion curves in MnO at finite temperatures using an extension of the RPA approach of Harada et al. (1972) and compare it with their experimental data. They obtain satisfactory agreement with observed spin wave energies even at T = 100K (.83 T_N).

We have discussed earlier in this chapter that the renormalisation of magnon energy is experimentally observed to be wave vector dependent, a phenomenon more pronounced in systems of low dimensionality. Since second order magnetic phase transitions affect only long-wavelength magnons significantly, Lines (1971) in advancing his new approach to

Green's function decoupling emphasises the importance of having theories to calculate wave vector dependent renormalisation. Harada et al. (1972) point out, however, that the results of Lines' phenomenological treatment cannot be compared directly with the spin wave interaction theory. Yelon (1971) studied the renormalisation of large wave vector magnons in ferromagnetic $CrBr_3$, and concluded that the wave vector dependence of the energy loss gives evidence for observation of the effect of correlation between spin waves.

In general, it appears (Low, 1963; Loly, 1971) that the predictions of all the renormalisation theories cannot be expected to be reliable much above 80% of the transition temperature.

CHAPTER VIII

FORMAL THEORY OF SPIN WAVES AT FINITE TEMPERATURE AND IT'S APPLICATION TO ANTIFERROMAGNETS

In this chapter the extension of Bloch's theory (Bloch, 1962, 1963) to an arbitrary range of exchange interaction is undertaken and the theory applied to various antiferromagnets.

The Hamiltonian describing the dynamical interaction between a pair of spin waves is as given by Eq. (IV-7). We use the Bogoliubov transformation to get terms quartic in the α and β operators. The constant and the quadratic terms, which respectively contribute to the ground state energy (Eq. (IV-13)) and the spin wave energy (Eq. (IV-17)), have been discussed earlier in the thesis. Bloch's approximation consists in retaining only those quartic terms in α and β operators that represent a direct interaction between a pair of spin waves. Such terms, being expressible in terms of occupation numbers, are the ones that are expected to contribute to the free energy of the system. The resulting interaction Hamiltonian, with terms like $\alpha_{q_1}\beta_{q_1}\alpha_{q_2}\beta_{q_2}$, $\alpha^{\dagger}_{q_1}\beta^{\dagger}_{q_1}\alpha^{\dagger}_{q_2}\beta^{\dagger}_{q_2}$ or $\alpha^{\dagger}_{q_1}\beta^{\dagger}_{q_1}\beta^{\dagger}_{q_2}\beta_{q_2}$ etc. ignored, can be written as

$$H_{int} = \sum_{q_1 q_2} \alpha^{\dagger}_{q_1}\alpha_{q_1}\alpha^{\dagger}_{q_2}\alpha_{q_2} \{(\tfrac{4}{N})\, J_d(0)\cosh^2\theta_{q_1}\sinh^2\theta_{q_2}$$

$$+ (\tfrac{1}{N})\, J_d(q_2-q_1)\sinh 2\theta_{q_1}\sinh 2\theta_{q_2} - (\tfrac{2}{N})\,[J_s(0) + J_s(q_1-q_2)$$

$$- J_s(q_1) - J_s(q_2)][\cosh^2\theta_{q_1}\cosh^2\theta_{q_2} + \sinh^2\theta_{q_1}\sinh^2\theta_{q_2}]$$

$$- (\tfrac{3}{2N})\, J_d(q_1)\sinh 2\theta_{q_1}\sinh^2\theta_{q_2} - (\tfrac{1}{2N})\, J_d(q_1)\sinh 2\theta_{q_1}$$

$$\times \cosh 2\theta_{q_2} - (\tfrac{3}{2N})\, J_d(q_2)\sinh 2\theta_{q_2}\cosh^2\theta_{q_1}\}$$

$$+ \sum_{q_1 q_2} \beta^{\dagger}_{q_1}\beta_{q_1}\beta^{\dagger}_{q_2}\beta_{q_2} \{(\tfrac{4}{N})\, J_d(0)\sinh^2\theta_{q_1}\cosh^2\theta_{q_2}$$

$$+ (\tfrac{1}{N})\, J_d(q_2-q_1)\sinh 2\theta_{q_1}\sinh 2\theta_{q_2} - (\tfrac{2}{N})[J_s(0) + J_s(q_1-q_2)$$

$$- J_s(q_1) - J_s(q_2)][\sinh^2\theta_{q_1}\sinh^2\theta_{q_2} + \cosh^2\theta_{q_1}\cosh^2\theta_{q_2}]$$

$$- (\tfrac{3}{2N})\, J_d(q_1)\sinh 2\theta_{q_1}\cosh^2\theta_{q_2} - (\tfrac{1}{2N})\, J_d(q_1)\sinh 2\theta_{q_1}$$

$$\times \cosh 2\theta_{q_2} - (\tfrac{3}{2N})\, J_d(q_2)\sinh^2\theta_{q_1}\sinh 2\theta_{q_2}\}$$

$$+ \sum_{q_1 q_2} \alpha^{\dagger}_{q_1}\alpha_{q_1}\beta^{\dagger}_{q_2}\beta_{q_2} \{(\tfrac{4}{N})\, J_d(0)\cosh^2\theta_{q_1}\cosh^2\theta_{q_2} + (\tfrac{1}{N})$$

$$\times J_d(q_2-q_1)\sinh 2\theta_{q_1}\sinh 2\theta_{q_2} - (\tfrac{3}{2N})\, J_d(q_1)\sinh 2\theta_{q_1}\cosh^2\theta_{q_2}$$

$$- (\tfrac{1}{2N})\, J_d(q_1)\sinh 2\theta_{q_1}\cosh 2\theta_{q_2} - (\tfrac{3}{2N})\, J_d(q_2)\cosh^2\theta_{q_1}$$

$$\times \sinh 2\theta_{q_2} - \left(\frac{2}{N}\right)[J_s(0) + J_s(q_1-q_2) - J_s(q_1) - J_s(q_2)]$$

$$\times [\cosh^2\theta_{q_1}\sinh^2\theta_{q_2} + \sinh^2\theta_{q_1}\cosh^2\theta_{q_2}]\}$$

$$+ \sum_{q_1 q_2} \beta^\dagger_{q_1}\beta_{q_1}\alpha^\dagger_{q_2}\alpha_{q_2}\{\left(\frac{4}{N}\right) J_d(0)\sinh^2\theta_{q_1}\sinh^2\theta_{q_2}$$

$$+ \left(\frac{1}{N}\right) J_d(q_2-q_1)\sinh 2\theta_{q_1}\sinh 2\theta_{q_2} - \left(\frac{1}{2N}\right) J_d(q_1)$$

$$\times \sinh 2\theta_{q_1}\cosh 2\theta_{q_2} - \left(\frac{3}{2N}\right) J_d(q_1)\sinh 2\theta_{q_1}\sinh^2\theta_{q_2}$$

$$- \left(\frac{3}{2N}\right) J_d(q_2)\sinh 2\theta_{q_2}\sinh^2\theta_{q_1} - \left(\frac{2}{N}\right)[J_s(0) + J_s(q_1-q_2)$$

$$- J_s(q_1) - J_s(q_2)][\sinh^2\theta_{q_1}\cosh^2\theta_{q_2} + \cosh^2\theta_{q_1}\sinh^2\theta_{q_2}]\}. \tag{VIII-1}$$

In order to simplify the Hamiltonian, let us rearrange terms and write it with all the d terms and the s terms collected separately, as

$$H_{int} = \left(\frac{1}{N}\right) \sum_{q_1 q_2} J_d(q_2-q_1)[\alpha^\dagger_{q_1}\alpha_{q_1} \sinh 2\theta_{q_1} \alpha^\dagger_{q_2}\alpha_{q_2} \sinh 2\theta_{q_2}$$

$$+ \beta^\dagger_{q_1}\beta_{q_1} \sinh 2\theta_{q_1} \beta^\dagger_{q_2}\beta_{q_2} \sinh 2\theta_{q_2} + \alpha^\dagger_{q_1}\alpha_{q_1} \sinh 2\theta_{q_1}$$

$$\times \beta^\dagger_{q_2}\beta_{q_2} \sinh 2\theta_{q_2} + \beta^\dagger_{q_1}\beta_{q_1} \sinh 2\theta_{q_1} \beta^\dagger_{q_2}\beta_{q_2} \sinh 2\theta_{q_2}]$$

$$- \left(\frac{1}{2N}\right) \sum_{q_1 q_2} J_d(q_1)[\alpha^\dagger_{q_1}\alpha_{q_1} \cosh 2\theta_{q_1} \alpha^\dagger_{q_2}\alpha_{q_2} \cosh 2\theta_{q_2}$$

$$+ \beta^{\dagger}_{q_1}\beta_{q_1} \cosh 2\theta_{q_1}\, \beta^{\dagger}_{q_2}\beta_{q_2} \cosh 2\theta_{q_2} + \alpha^{\dagger}_{q_1}\alpha_{q_1} \cosh 2\theta_{q_1}$$

$$\times \beta^{\dagger}_{q_2}\beta_{q_2} \cosh 2\theta_{q_2} + \beta^{\dagger}_{q_1}\beta_{q_1} \cosh 2\theta_{q_1}\, \alpha^{\dagger}_{q_2}\alpha_{q_2} \cosh 2\theta_{q_2}]$$

$$+ \left(\frac{4}{N}\right) \sum_{q_1 q_2} J_d(0)[\alpha^{\dagger}_{q_1}\alpha_{q_1} \cosh^2\theta_{q_1}\, \alpha^{\dagger}_{q_2}\alpha_{q_2} \sinh^2\theta_{q_2}$$

$$+ \beta^{\dagger}_{q_1}\beta_{q_1} \sinh^2\theta_{q_1}\, \beta^{\dagger}_{q_2}\beta_{q_2} \cosh^2\theta_{q_2} + \alpha^{\dagger}_{q_1}\alpha_{q_1} \cosh^2\theta_{q_1}$$

$$\times \beta^{\dagger}_{q_2}\beta_{q_2} \cosh^2\theta_{q_2} + \beta^{\dagger}_{q_1}\beta_{q_1} \sinh^2\theta_{q_1}\, \alpha^{\dagger}_{q_2}\alpha_{q_2} \sinh^2\theta_{q_2}]$$

$$- \left(\frac{3}{2N}\right) \sum_{q_1 q_2} J_d(q_1)[\alpha^{\dagger}_{q_1}\alpha_{q_1} \cosh 2\theta_{q_1}\, \alpha^{\dagger}_{q_2}\alpha_{q_2} \sinh^2\theta_{q_2}$$

$$+ \alpha^{\dagger}_{q_1}\alpha_{q_1} \cosh 2\theta_{q_1}\, \beta^{\dagger}_{q_2}\beta_{q_2} \cosh^2\theta_{q_2} + \beta^{\dagger}_{q_1}\beta_{q_1} \cosh 2\theta_{q_1}$$

$$\times \alpha^{\dagger}_{q_2}\alpha_{q_2} \sinh^2\theta_{q_2} + \beta^{\dagger}_{q_1}\beta_{q_1} \cosh 2\theta_{q_1}\, \beta^{\dagger}_{q_2}\beta_{q_2} \cosh^2\theta_{q_2}]$$

$$- \left(\frac{3}{2N}\right) \sum_{q_1 q_2} J_d(q_2)[\alpha^{\dagger}_{q_1}\alpha_{q_1} \cosh^2\theta_{q_1}\, \alpha^{\dagger}_{q_2}\alpha_{q_2} \cosh 2\theta_{q_2}$$

$$+ \alpha^{\dagger}_{q_1}\alpha_{q_1} \cosh^2\theta_{q_1}\, \beta^{\dagger}_{q_2}\beta_{q_2} \cosh 2\theta_{q_2} + \beta^{\dagger}_{q_1}\beta_{q_1} \sinh^2\theta_{q_1}$$

$$\times \alpha^{\dagger}_{q_2}\alpha_{q_2} \cosh 2\theta_{q_2} + \beta^{\dagger}_{q_1}\beta_{q_1} \sinh^2\theta_{q_1}\, \beta^{\dagger}_{q_2}\beta_{q_2} \cosh 2\theta_{q_2}]$$

$$- \left(\frac{2}{N}\right) \sum_{q_1 q_2} [J_s(0) + J_s(q_1 - q_2) - J_s(q_1) - J_s(q_2)]$$

$$\times [\alpha^{\dagger}_{q_1}\alpha_{q_1} \cosh^2\theta_{q_1}\, \alpha^{\dagger}_{q_2}\alpha_{q_2} \cosh^2\theta_{q_2} + \alpha^{\dagger}_{q_1}\alpha_{q_1} \sinh^2\theta_{q_1}$$

$$\times \alpha^{\dagger}_{q_2}\alpha_{q_2} \sinh^2\theta_{q_2} + \beta^{\dagger}_{q_1}\beta_{q_1} \sinh^2\theta_{q_1}\, \beta^{\dagger}_{q_2}\beta_{q_2} \sinh^2\theta_{q_2}$$

$$+ \beta^{\dagger}_{q_1}\beta_{q_1} \cosh^2\theta_{q_1}\, \beta^{\dagger}_{q_2}\beta_{q_2} \cosh^2\theta_{q_2} + \alpha^{\dagger}_{q_1}\alpha_{q_1} \cosh^2\theta_{q_1}$$

$$\times \beta^{\dagger}_{q_2}\beta_{q_2} \sinh^2\theta_{q_2} + \alpha^{\dagger}_{q_1}\alpha_{q_1} \sinh^2\theta_{q_1}\, \beta^{\dagger}_{q_2}\beta_{q_2} \cosh^2\theta_{q_2}$$

$$+ \beta^{\dagger}_{q_1}\beta_{q_1} \sinh^2\theta_{q_1}\, \alpha^{\dagger}_{q_2}\alpha_{q_2} \cosh^2\theta_{q_2} + \beta^{\dagger}_{q_1}\beta_{q_1} \cosh^2\theta_{q_1}$$

$$\times \alpha^{\dagger}_{q_2}\alpha_{q_2} \sinh^2\theta_{q_2}] \qquad \text{(VIII-2)}$$

It is possible to separate the q_1 and q_2 terms by recalling the transforms of exchange constants as given by Eq. (IV-11). Moreover, since q_1 and q_2 may be interchanged in the sums, terms such as, e.g.,

$$\sum_{q_1}\sum_{q_2} [(\alpha^{\dagger}_{q_1}\alpha_{q_1} + \beta^{\dagger}_{q_1}\beta_{q_1})\cos \underline{q}_1\cdot\underline{d} \sinh 2\theta_{q_1}]$$

$$\times [(\alpha^{\dagger}_{q_2}\alpha_{q_2} + \beta^{\dagger}_{q_2}\beta_{q_2})\cos \underline{q}_2\cdot\underline{d} \sinh 2\theta_{q_2}]$$

can be rewritten as

$$[\sum_{q} (\alpha^{\dagger}_{q}\alpha_{q} + \beta^{\dagger}_{q}\beta_{q})\cos \underline{q}\cdot\underline{d} \sinh 2\theta_{q}]^2$$

The interaction Hamiltonian is, then

$$H_{int} = \sum_d J_d \{ (\tfrac{1}{N}) [\sum_q (\alpha_q^\dagger \alpha_q + \beta_q^\dagger \beta_q) \cos \underline{q}\cdot\underline{d} \sinh 2\theta_q]^2$$

$$- (\tfrac{1}{2N}) [\sum_q (\alpha_q^\dagger \alpha_q + \beta_q^\dagger \beta_q) \sinh 2\theta_q \cos \underline{q}\cdot\underline{d}] [\sum_q (\alpha_q^\dagger \alpha_q + \beta_q^\dagger \beta_q)$$

$$\times \cosh 2\theta_q] + (\tfrac{4}{N}) [\sum_q (\alpha_q^\dagger \alpha_q \cosh^2\theta_q + \beta_q^\dagger \beta_q \sinh^2\theta_q)]$$

$$\times [\sum_q (\alpha_q^\dagger \alpha_q \sinh^2\theta_q + \beta_q^\dagger \beta_q \cosh^2\theta_q)] - (\tfrac{3}{2N}) [\sum_q (\alpha_q^\dagger \alpha_q$$

$$+ \beta_q^\dagger \beta_q) \sinh 2\theta_q \cos \underline{q}\cdot\underline{d}] [\sum_q (\alpha_q^\dagger \alpha_q \sinh^2\theta_q + \beta_q^\dagger \beta_q \cosh^2\theta_q)]$$

$$- (\tfrac{3}{2N}) [\sum_q (\alpha_q^\dagger \alpha_q \cosh^2\theta_q + \beta_q^\dagger \beta_q \sinh^2\theta_q)] [\sum_q (\alpha_q^\dagger \alpha_q + \beta_q^\dagger \beta_q)$$

$$\times \sinh 2\theta_q \cos \underline{q}\cdot\underline{d}]\} + \sum_s J_s \{ (-\tfrac{2}{N}) \sum_q (\alpha_q^\dagger \alpha_q \sinh^2\theta_q + \beta_q^\dagger \beta_q$$

$$\times \cosh^2\theta_q)]^2 - (\tfrac{2}{N}) [\sum_q (\alpha_q^\dagger \alpha_q \cosh^2\theta_q + \beta_q^\dagger \beta_q \sinh^2\theta_q)]^2$$

$$- (\tfrac{2}{N}) [\sum_q \cos \underline{q}\cdot\underline{s} (\alpha_q^\dagger \alpha_q \sinh^2\theta_q + \beta_q^\dagger \beta_q \cosh^2\theta_q)]^2$$

$$- (\tfrac{2}{N}) [\sum_q \cos \underline{q}\cdot\underline{s} (\alpha_q^\dagger \alpha_q \cosh^2\theta_q + \beta_q^\dagger \beta_q \sinh^2\theta_q)]^2$$

$$+ (\tfrac{4}{N}) [\sum_q \cos \underline{q}\cdot\underline{s} (\alpha_q^\dagger \alpha_q \sinh^2\theta_q + \beta_q^\dagger \beta_q \cosh^2\theta_q)]$$

$$\times [\sum_q (\alpha_q^\dagger \alpha_q \sinh^2\theta_q + \beta_q^\dagger \beta_q \cosh^2\theta_q)] + (\tfrac{4}{N}) [\sum_q \cos \underline{q}\cdot\underline{s}$$

$$\times (\alpha_q^\dagger \alpha_q \cosh^2\theta_q + \beta_q^\dagger \beta_q \sinh^2\theta_q)] [\sum_q (\alpha_q^\dagger \alpha_q \cosh^2\theta_q$$

$$+ \beta_q^\dagger \beta_q \sinh^2\theta_q)]\} \qquad \text{(VIII-3)}$$

The total Hamiltonian is

$$H_{TOT} = \text{constant terms} + H_{\text{spin wave}} + H_{int} \qquad \text{(VIII-4)}$$

where H_{int} is as given by Eq. (VIII-3), and $H_{\text{spin wave}}$ and the constant terms are as given by Eqs. (IV-17) and (IV-13) respectively.

Using the approach outlined in Chapter VII, let the average occupancies $\langle n_q \rangle$ be as given by

$$\langle n_q \rangle = \langle \alpha_q^\dagger \alpha_q \rangle = \langle \beta_q^\dagger \beta_q \rangle \qquad \text{(VIII-5)}$$

The internal energy U of the system, ignoring constant terms, since they are independent of occupation numbers, is

$$U = \sum_d J_d \{ (\tfrac{4}{N}) \sum_q (\langle n_q \rangle \cos \underline{q}\cdot\underline{d} \sinh 2\theta_q)^2$$

$$- (\tfrac{2}{N}) [(\sum_q \langle n_q \rangle \sinh 2\theta_q \cos \underline{q}\cdot\underline{d}) (\sum_q \langle n_q \rangle \cosh 2\theta_q)]$$

$$+ (\tfrac{4}{N}) (\sum_q \langle n_q \rangle \cosh 2\theta_q)^2 - (\tfrac{6}{N}) [(\sum_q \langle n_q \rangle \sinh 2\theta_q$$

$$\times \cos \underline{q}\cdot\underline{d}) (\sum_q \langle n_q \rangle \cosh 2\theta_q)] \} + \sum_s J_s \{ (-\tfrac{4}{N}) (\sum_q \langle n_q \rangle$$

$$\times \cosh 2\theta_q)^2 - (\tfrac{4}{N}) (\sum_q \langle n_q \rangle \cosh 2\theta_q \cos \underline{q}\cdot\underline{s})^2$$

$$+ \left(\frac{8}{N}\right)\left[\left(\sum_q \langle n_q\rangle \cosh 2\theta_q \cos \underline{q}\cdot\underline{s}\right)\left(\sum_q \langle n_q\rangle \cosh 2\theta_q\right)\right]$$

$$+ 2 \sum_q E_q \langle n_q\rangle \quad . \qquad \text{(VIII-6)}$$

The entropy S of an assembly of harmonic oscillators, each with average occupancy $\langle n_q\rangle$, is the sum of the entropy of the individual oscillators. The entropy S_q of an individual oscillator (see, e.g., Eq. (15-14) of Thermal Physics by Kittel (1969)) is given by

$$S_q = - k_B[\langle n_q\rangle \ln(\langle n_q\rangle) - (\langle n_q\rangle + 1)\ln(\langle n_q\rangle + 1)] \qquad \text{(VIII-7a)}$$

with $S = \sum_q S_q$.

Our system can be regarded as an assembly of harmonic oscillators labelled q with average occupancy $\langle n_q\rangle$ and since we have two identical systems because of the equality introduced by Eq. (VIII-5) for the occupancy number, the entropy of the system is

$$S = - 2k_B \sum_q [\langle n_q\rangle \ln(\langle n_q\rangle) - (\langle n_q\rangle + 1)\ln(\langle n_q\rangle + 1)] \quad . \qquad \text{(VIII-7b)}$$

The free energy F of this system at a temperature T is

$$F = U - TS \qquad \text{(VIII-8)}$$

with U and S as given by Eqs. (VIII-6) and (VIII-7b). Equating the extremum of the free energy with respect to the average occupation number for a certain wavevector $\underline{k}$

$$\frac{\partial F}{\partial \langle n_k \rangle} = \sum_d J_d \{ (\tfrac{4}{N}) [(\sum_q \langle n_q \rangle \cos \underline{q}\cdot\underline{d} \sinh 2\theta_q) \times (\cos \underline{k}\cdot\underline{d} \sinh 2\theta_k)] - (\tfrac{1}{N}) [(\sum_q \langle n_q \rangle \sinh 2\theta_q \times \cos \underline{q}\cdot\underline{d}) (\cosh 2\theta_k)] - (\tfrac{1}{N}) [(\sum_q \langle n_q \rangle \cosh 2\theta_q) \times (\sinh 2\theta_k \cos \underline{k}\cdot\underline{d})] + (\tfrac{4}{N}) [(\sum_q \langle n_q \rangle \cosh 2\theta_q) \times (\cosh 2\theta_k)] - (\tfrac{3}{N}) [(\sum_q \langle n_q \rangle \sinh 2\theta_q \cos \underline{q}\cdot\underline{d}) \times (\cosh 2\theta_k)] - (\tfrac{3}{N}) [(\sum_q \langle n_q \rangle \cosh 2\theta_q) \times (\sinh 2\theta_k \cos \underline{k}\cdot\underline{d})] \} + \sum_s J_s (-\tfrac{4}{N}) [(\sum_q \langle n_q \rangle \cosh 2\theta_q) (\cosh 2\theta_k)] - (\tfrac{4}{N}) [(\sum_q \langle n_q \rangle \cosh 2\theta_q \times \cos \underline{q}\cdot\underline{s}) (\cosh 2\theta_k \cos \underline{k}\cdot\underline{s})] + (\tfrac{4}{N}) [(\sum_q \langle n_q \rangle \times \cosh 2\theta_q \cos \underline{q}\cdot\underline{s}) (\cosh 2\theta_k)] + (\tfrac{4}{N}) [(\sum_q \langle n_q \rangle \times \cosh 2\theta_q) (\cosh 2\theta_k \cos \underline{k}\cdot\underline{s})] \} + E_k$$

$$+ k_B T \ln[\langle n_k \rangle / (\langle n_k \rangle + 1)] = 0 \quad . \qquad \text{(VIII-9)}$$

Since the average occupancy $\langle n_k \rangle$ for a magnon of energy $E_k'(T)$ at a temperature T is given by

$$\langle n_k \rangle = 1/[\exp(E_k(T)/k_B T) - 1] \qquad \text{(VIII-10)}$$

it is possible to rewrite Eq. (VIII-9) in a form that gives the ratio of the magnon energy of wavevector $\underline{k}$ for temperature T, $E_k(T)$, to the zero temperature energy E_k. This ratio $E_k(T)/E_k$, which tells us the factor by which the energy of a magnon is renormalised at the temperature T, is the so-called renormalisation factor $\alpha_k(T)$. So that, one writes

$$\begin{aligned} \alpha_k(T) &= E_k(T)/E_k \\ &= 1 - \left(\frac{4}{N}\right)\left(\frac{1}{E_k}\right) \sum_d J_d \{[\cosh 2\theta_k - \cos \underline{k}\cdot\underline{d} \sinh 2\theta_k] \\ &\quad \times \left(\sum_q \langle n_q \rangle (\cos \underline{q}\cdot\underline{d} \sinh 2\theta_q - \cosh 2\theta_q)\right]\} \\ &\quad + \left(\frac{4}{N}\right)\left(\frac{1}{E_k}\right) \sum_s J_s \{[\cosh 2\theta_k - \cos \underline{k}\cdot\underline{s} \cosh 2\theta_k] \\ &\quad \times [\sum_q \langle n_q \rangle (\cos \underline{q}\cdot\underline{s} \cosh 2\theta_q - \cosh 2\theta_q)]\} \quad . \end{aligned} \qquad \text{(VIII-11)}$$

Thus, at a temperature T the zero-temperature energy $E_{\underline{k}}$ of a magnon of wavevector $\underline{k}$ is renormalised by a factor $\alpha_{\underline{k}}(T)$ to

$$E_{\underline{k}}(T) = \alpha_{\underline{k}}(T) E_{\underline{k}} \quad . \qquad \text{(VIII-12)}$$

$\alpha_{\underline{k}}(T)$, the renormalisation factor, as given by Eq. (VIII-11), is wavevector dependent.

Using Eq. (VIII-12) one can write $\langle n_k \rangle$ also as

$$\langle n_k \rangle = 1/[\exp(\alpha_k(T) E_k / k_B T) - 1] \quad . \qquad \text{(VIII-13)}$$

In the limit of the temperature of the system approaching zero, $\langle n_k \rangle$ also approaches towards the value zero. From Eq. (VIII-11) one can see that then $\alpha_k(T)$ will be equal to 1, as expected.

Next it is shown that in the special case of just one exchange constant, the renormalisation factor $\alpha_k(T)$ as given by Eq. (VIII-11) reduces to the wavevector independent form given by Bloch.

(i) Simple ferromagnet with just one exchange constant

For a ferromagnet on a Bravais lattice with a single exchange constant, J, it can be shown that the analogous form to Eq. (VIII-11) is

$$\alpha_k^F(T) = 1 + \left(\frac{2}{N}\right)\left(|J|/E_k\right) \sum_s \{[1 - \cos \underline{k}\cdot\underline{s}]$$

$$\times [\sum_q \langle n_q \rangle (\cos \underline{q}\cdot\underline{s} - 1)]\} \qquad \text{(VIII-14)}$$

The zero temperature energy E_k^F of a magnon for a ferromagnet is

$$E_k^F = 2S|J|Z_s(1 - \gamma_k)$$

$$= 2S|J|[Z_s - (\sum_s \cos \underline{k}\cdot\underline{s})] \qquad \text{(VIII-15)}$$

where γ_k is as given by Eq. (III-6). Noting that $\sum_q \cos \underline{q}\cdot\underline{s}$ can be written as $\sum_q [(\sum_s \cos \underline{q}\cdot\underline{s})/Z_s]$, Eq. (VIII-14) reduces to Bloch's expression for a cubic ferromagnet (Eq. (VII-7)).

(ii) Simple antiferromagnet with one exchange constant

Putting all J_s terms equal to zero and $J_d = -|J|$, Eq. (VIII-11) becomes

$$\alpha_k(T) = 1 + \left(\frac{4}{N}\right)\left(|J|/E_k\right) \sum_d \{[\cosh 2\theta_k - \cos \underline{k}\cdot\underline{d} \sinh^2 \theta_k]$$

$$\times [\sum_q \langle n_q \rangle (\cos \underline{q}\cdot\underline{d} \sinh 2\theta_q - \cosh 2\theta_q)]\} \qquad \text{(VIII-16)}$$

The T = 0K energy of a magnon of wavevector $\underline{k}$ for the case of $J_s = 0$ and $J_d = -|J|$ is

$$E_k = 2S|J_0|[z_d \cosh 2\theta_k - (\sum_d \cos \underline{k}\cdot\underline{d}) \sinh 2\theta_k] \quad . \qquad \text{(VIII-17)}$$

Again noting that $\sum_q \cos \underline{q}\cdot\underline{d} = \sum_q [(\sum_d \cos \underline{q}\cdot\underline{d})/z_d]$, Eq. (VIII-16) reduces in a straightforward manner to Bloch's expression for a cubic antiferromagnet (Eq. (VII-8)).

Summarising one can say that the renormalisation factor of a magnon of wavevector $\underline{k}$ at the temperature T depends both on the wavevector $\underline{k}$ as well as the temperature T, in general. Bloch studied the simple cases in which, as we saw, the factor at any temperature T depends only on that temperature and is independent of the wavevector of the magnon. We shall use the general formula (Eq. (VIII-11)) in the calculations of the renormalisation.

We will apply the theory to calculate the dispersion curves of MnF_2, $RbMnF_3$, MnO and NiO at finite temperature. A comparison of the calculations of the temperature dependence of the magnon energy with the data obtained from inelastic neutron scattering experiments is one of the most sensitive tests of spin wave theory at finite temperature. We will also calculate the temperature dependence of the sublattice magnetization and compare it with the experimental data. The examination of the temperature dependence of magnetization and of other similar magnetic properties such as specific heat are a less demanding approach to an investigation of spin wave theory as they involve a summation

over all the magnon modes present, in contrast to the neutron experiments which are capable of measuring the properties associated with a small group of magnon modes (Low, 1963). Finally, T_M', the temperature beyond which the self-consistent solution of $\alpha_k(T)$ does not exist will be compared with the experimental value of T_N.

The antiferromagnetic structure of these compounds have already been discussed in earlier chapters. The number and types of neighbours and the magnitudes of the exchange constants, etc., is the type of information that is needed to write down the explicit expression for various summations that appear in Eq. (VIII-11) and to evaluate them. This information is summarised in Table VII-1 for $RbMnF_3$, Table VII-2 for MnF_2, Table V-1 and VI-4 for MnO and in Table VII-3 for NiO. The explicit expressions for the summations have been put together in Table VIII-1. The zero temperature energy E_k is calculated using Eq. (II-59), which treats the anisotropy in an approximate way as a parameter, H_A. In general, H_A is a function of both temperature and the wavevector. In MnF_2, the $\underline{q}$ dependence of H_A (Low, 1964) is known to be associated entirely with the magnitude of q_z and amounts to a maximum of a 1% reduction in spin wave energy when q_z has its maximum value. For MnO, the $\underline{q}$ dependence of H_A amounts to even less than a 1% reduction in spin wave energy at the zone boundary. In view of this, we have ignored the $\underline{q}$ dependence of H_A. The temperature

TABLE VIII-1

THE CALCULATION OF RENORMALISATION OF SPIN WAVES

The general expression for $\alpha_k(T)$ is

$$\alpha_k(T) = 1 - \left(\frac{4}{N}\right)\left(\frac{1}{E_k}\right) \sum_d J_d \{[\cosh 2\theta_k - \cos \underline{k}\cdot\underline{d} \sinh 2\theta_k] \times \{\sum_q \langle n_q \rangle (\cos \underline{q}\cdot\underline{d} \sinh 2\theta_q - \cosh 2\theta_q)]\}$$

$$+ \left(\frac{4}{N}\right)\left(\frac{1}{E_k}\right) \sum_s J_s \{[\cosh 2\theta_k - \cos \underline{k}\cdot\underline{s} \cosh 2\theta_k] \times \{\sum_q \langle n_q \rangle (\cos \underline{q}\cdot\underline{s} \cosh 2\theta_q - \cosh 2\theta_q)]\}$$

with

$$E_k = (A_k'^2 - B_k^2)^{1/2} ,$$

$$\cosh 2\theta_k = A_k'/E_k ,$$

$$\sinh 2\theta_k = B_k/E_k ,$$

and $\langle n_k \rangle = 1/[\exp[(\alpha_k(T)E_k)/k_BT] - 1]$.

TABLE VIII-1 - continued

THE CALCULATION OF RENORMALISATION OF SPIN WAVES

(i) MnF_2

1. $J_s(k) = \sum_s J_s \cos \underline{k}\cdot\underline{s} = 2J_1 \cos z_k + 2J_3[\cos Y_k + \cos X_k]$

$J_s(0) = 2J_1 + 4J_3$

2. $J_d(k) = \sum_d J_d \cos \underline{k}\cdot\underline{d} = 8J_2 \cos(X_k/2)\cos(Y_k/2)\cos(Z_k/2)$

$J_d(0) = 8J_2$

3. $A'_k = -5\{[8J_2 - 4J_1 \sin^2(Z_k/2)] - 4J_3[\sin^2(X_k/2) + \sin^2(Y_k/2)]\} + H_A$

$B_k = -40J_2 \cos(X_k/2)\cos(Y_k/2)\cos(Z_k/2)$

4. $\sum_d J_d \cos(\underline{k}\cdot\underline{d})\cos(\underline{q}\cdot\underline{d})$

$= 2J_2[\cos((X_k+Y_k+Z_k)/2)\cos((X_q+Y_q+Z_q)/2)$

$+ \cos((X_k+Y_k-Z_k)/2)\cos((X_q+Y_q-Z_q)/2)$

$+ \cos((X_k-Y_k+Z_k)/2)\cos((X_q-Y_q+Z_q)/2)$

$+ \cos((-X_k+Y_k+Z_k)/2)\cos((-X_q+Y_q+Z_q)/2)]$

TABLE VIII-1 - continued

THE CALCULATION OF RENORMALISATION OF SPIN WAVES

5. $\sum_s J_s \cos(\underline{k}\cdot\underline{s})\cos(\underline{q}\cdot\underline{s}) = 2J_1[\cos Z_k \cos Z_q]$

$$+ 2J_3[\cos X_k \cos X_q + \cos Y_k \cos Y_q]$$

(ii) $RbMnF_3$

1. $J_s(k) = \sum_s J_s \cos \underline{k}\cdot\underline{s} = 2J_2 BB_k$; $J_s(0) = 12J_2$

where $BB_k = \cos(X_k+Y_k) + \cos(Y_k+Z_k) + \cos(Z_k+X_k)$

$$+ \cos(X_k-Y_k) + \cos(Y_k-Z_k) + \cos(Z_k-X_k)$$

2. $J_d(k) = \sum_d J_d \cos \underline{k}\cdot\underline{d} = 2J_1 AA_k + 2J_3 CC_k$;

$J_d(0) = 6J_1 + 8J_3$

where $AA_k = \cos X_k + \cos Y_k + \cos Z_k$

$CC_k = \cos(X_k+Y_k+Z_k) + \cos(X_k+Y_k-Z_k)$

$$+ \cos(X_k-Y_k+Z_k) + \cos(-X_k+Y_k+Z_k)$$

3. $\Lambda'_k = -5[6J_1 + 8J_3 - 12J_2 + 2J_2 BB_k]$

TABLE VIII-1 - continued

THE CALCULATION OF RENORMALISATION OF SPIN WAVES

$$B_k = -5[2J_1 AA_k + 2J_3 CC_k]$$

4. $\sum_d J_d \cos(\underline{k}\cdot\underline{d})\cos(\underline{q}\cdot\underline{d})$

$$= 2J_1[\cos X_k \cos X_q + \cos Y_k \cos Y_q + \cos Z_k \cos Z_q]$$

$$+ 2J_3[\cos(X_k+Y_k+Z_k)\cos(X_q+Y_q+Z_q)$$

$$+ \cos(X_k+Y_k-Z_k)\cos(X_q+Y_q-Z_q)$$

$$+ \cos(X_k-Y_k+Z_k)\cos(X_q-Y_q+Z_q)$$

$$+ \cos(-X_k+Y_k+Z_k)\cos(-X_q+Y_q+Z_q)]$$

5. $\sum_s J'_s \cos \underline{k}\cdot\underline{s} \cos \underline{q}\cdot\underline{s}$

$$= 2J_2[\cos(X_k+Y_k)\cos(X_q+Y_q) + \cos(Y_k+Z_k)\cos(Y_q+Z_q)$$

$$+ \cos(Z_k+X_k)\cos(Z_q+X_q) + \cos(X_k-Y_k)\cos(X_q-Y_q)$$

$$+ \cos(Y_k-Z_k)\cos(Y_q-Z_q) + \cos(Z_k-X_k)\cos(Z_q-X_q)]$$

TABLE VIII-1 - continued

THE CALCULATION OF RENORMALISATION OF SPIN WAVES

(iii) MnO and NiO

1. $J_s(k) = \sum_s J_s \cos \underline{k}\cdot\underline{s} = 2J_{1s}BB_k \quad ; \quad J_s(0) = 6J_{1s}$

where $BB_k = \cos[(X_k-Y_k)/2] + \cos[(Y_k-Z_k)/2] + \cos[(Z_k-X_k)/2]$

2. $J_d(k) = \sum_d J_d \cos \underline{k}\cdot\underline{d} = 2J_{1d}CC_k + 2J_2AA_k$

where $CC_k = \cos[(X_k+Y_k)/2] + \cos[(Y_k+Z_k)/2] + \cos[(Z_k+X_k)/2]$

and $AA_k = \cos X_k + \cos Y_k + \cos Z_k$

3. $A'_k = -2S[6(J_2+J_{1d}-J_{1s}) + 2J_{1s}BB_k] + H_A$

$B_k = -2S[2(J_{1d}CC_k + J_2AA_k)]$

with $S = 5/2$ for MnO and $S = 1$ for NiO

4. $\sum_d J_d \cos(\underline{k}\cdot\underline{d})\cos(\underline{q}\cdot\underline{d})$

$= 2J_{1d}\{\cos[(X_k+Y_k)/2]\cos[(X_q+Y_q)/2] + \cos[(Y_k+Z_k)/2]$

$\times \cos[(Y_q+Z_q)/2] + \cos[(Z_k+X_k)/2]\cos[(Z_q+X_q)/2]\}$

TABLE VIII-1 - continued

THE CALCULATION OF RENORMALISATION OF SPIN WAVES

$$+ 2J_2\{[\cos X_k \cos X_q] + [\cos Y_k \cos Y_q] + [\cos Z_k \cos Z_q]\}$$

5. $\sum_s J_s \cos(\underline{k}\cdot\underline{s})\cos(\underline{q}\cdot\underline{s})$

$$= 2J_{1s}\{\cos[(X_k-Y_k)/2]\cos[(X_q-Y_q)/2]$$

$$+ \cos[(Y_k-Z_k)/2]\cos[(Y_q-Z_q)/2]$$

$$+ \cos[(Z_k-X_k)/2]\cos[(Z_q-X_q)/2]\}$$

For all these expressions, we have

$$X_q = 2\pi\rho_x^q \quad , \quad Y_q = 2\pi\rho_y^q \quad , \quad Z_q = 2\pi\rho_z^q$$

where $\underline{q} = (2\pi/a)(\rho_x^q, \rho_y^q, \rho_z^q)$.

dependence of H_A is taken care of by fitting it to the experimental values of the $q = 0$ magnon energy at that temperature. For MnO, the AFMR frequency was used for this purpose (Sievers et al., 1963).

The summations over q can be performed by 'brute' force' methods using N×N×N mesh as discussed in Chapter IV. In this case, however, because of the implicit nature of $\alpha_k(T)$, the Eq. (VIII-11) needs to be solved by an iterative procedure and this restricts the mesh size that can be used without spending excessive computer time. A mesh size of 6×6×6 was the maximum that was used. This mesh size which asks for the evaluation of α_q for 6^3 wavevectors takes 220 secs. for a single iteration, since every single evaluation of α_q in turn needs a summation over 6^3 wavevectors amounting to a summation over 6^6 wavevectors in all. A change in mesh size did not alter the average value of α_q by more than a percent or so, provided the mesh size was at least 4×4×4.

In view of the large number of different values of α_q involved and with their values changing in no simple pattern with q, an extrapolation to $N = \infty$ mesh size was not found to be feasible. A mesh size of 5×5×5 was used for most of the calculations. To start with one assumes the same value of α_q (say, 1) for all the wavevectors. The first iteration generates a set of values of α_q which is, now,

different for every value of q. The process is reiterated until consistency is found between the values of α_q before and after an iteration. A maximum of three iterations was found to be sufficient to give values of α_q which were within 1% of their values from the previous iteration. Having got a set of values of α_q for the whole of the Brillouin zone at a temperature T_1, it can be used to calculate the dispersion curves in a desired symmetry direction at that temperature. In order to calculate the $\{\alpha_q\}$ set at another temperature T_2 close to T_1, set $\{\alpha_q\}_{T_2}$ forms a better starting approximation for the calculation than the zero-temperature set.

The calculated dispersion curves for MnF_2 at temperatures 49.5K (.74 T_N), 62K (.92 T_N), and also at 4.2K, along with the experimental data of Turberfield et al. (1965) in the [001] direction are shown in Fig. VIII-1. These calculations are essentially a repetition of Low's work (Low, 1964), apart from the fact that the present calculations include both J_1 and J_2 in the evaluation of the $\alpha_k(T)$. The renormalisation factor calculated by Low corresponds to Eq. (VIII-11) applied to MnF_2 with the J_s terms equated to zero. Our calculated energies check with Low's calculations.

The agreement of the calculated energies with the experimental values is good at 49.5K which is 75% of T_n. At

Fig. VIII-1: The calculated spin wave dispersion curves in MnF_2 at various temperatures in the [001] direction. Experimental data are from Turberfield et al. (1965).

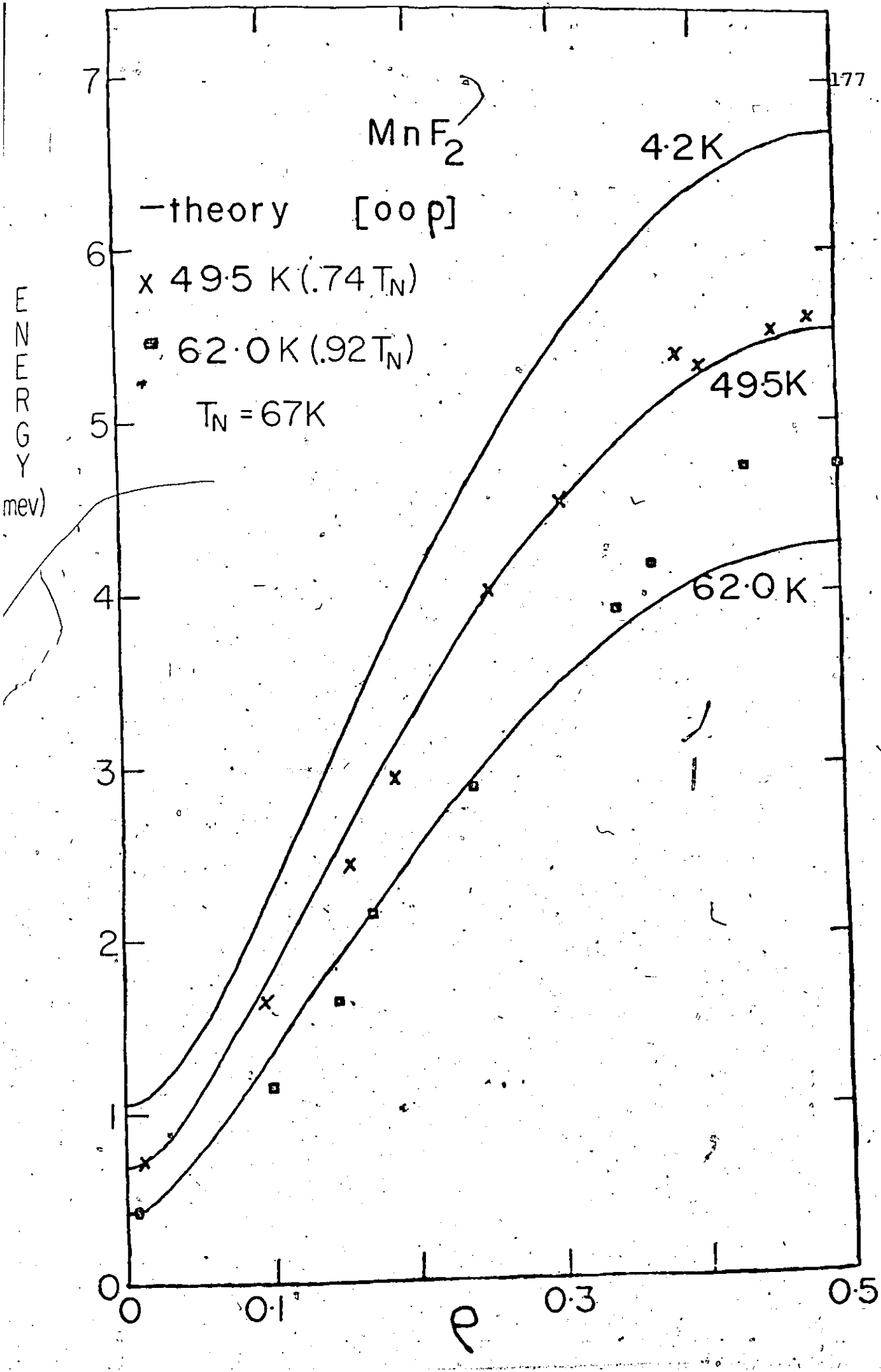
MnF2
4·2K
—theory [oop]
x 49·5 K (.74 TN)
62·0 K (.92 TN)
TN = 67K
49·5K
62·0 K
ENERGY
mev)
0
1
2
3
4
5
6
7
0
0·1
0·3
0·5
ρ

62K (92% T_N) the calculated energies are lower by a few percent near the zone boundary. The overall agreement is, however, better than the one obtained by Low, and corresponds to an increase in spin wave renormalisation of 5% over his calculations. This arises from the inclusion of the effect of two exchange parameters.

In Fig. VIII-2, the calculated dispersion curves for $RbMnF_3$ in the [001] direction are shown along with the extensive experimental data of Saunderson et al. (1972). $RbMnF_3$, being one of the simplest of all magnetic compounds (only one exchange constant and no anisotropy), should be a crucial test for the theory. The calculated dispersion curves are compared with the experimental data from 50% of T_N to 80% T_N. Again, agreement is good except near the zone boundaries where the calculated energies are systematically lower than the experimental ones by a few percent.

As was mentioned in the last chapter, the renormalisation factor α_k at a particular temperature is experimentally observed to be a wavevector dependent quantity. In Fig. VIII-3 typical plots, one each for MnF_2 and $RbMnF_3$, are shown of the calculated and the experimental values of α_k against $\underline{k}$ in the [001] direction. For $RbMnF_3$, the calculated α_k does not show any wavevector dependence and corresponds to the special simple case considered by Bloch. Thus the wavevector dependent interaction that decreases the energy of

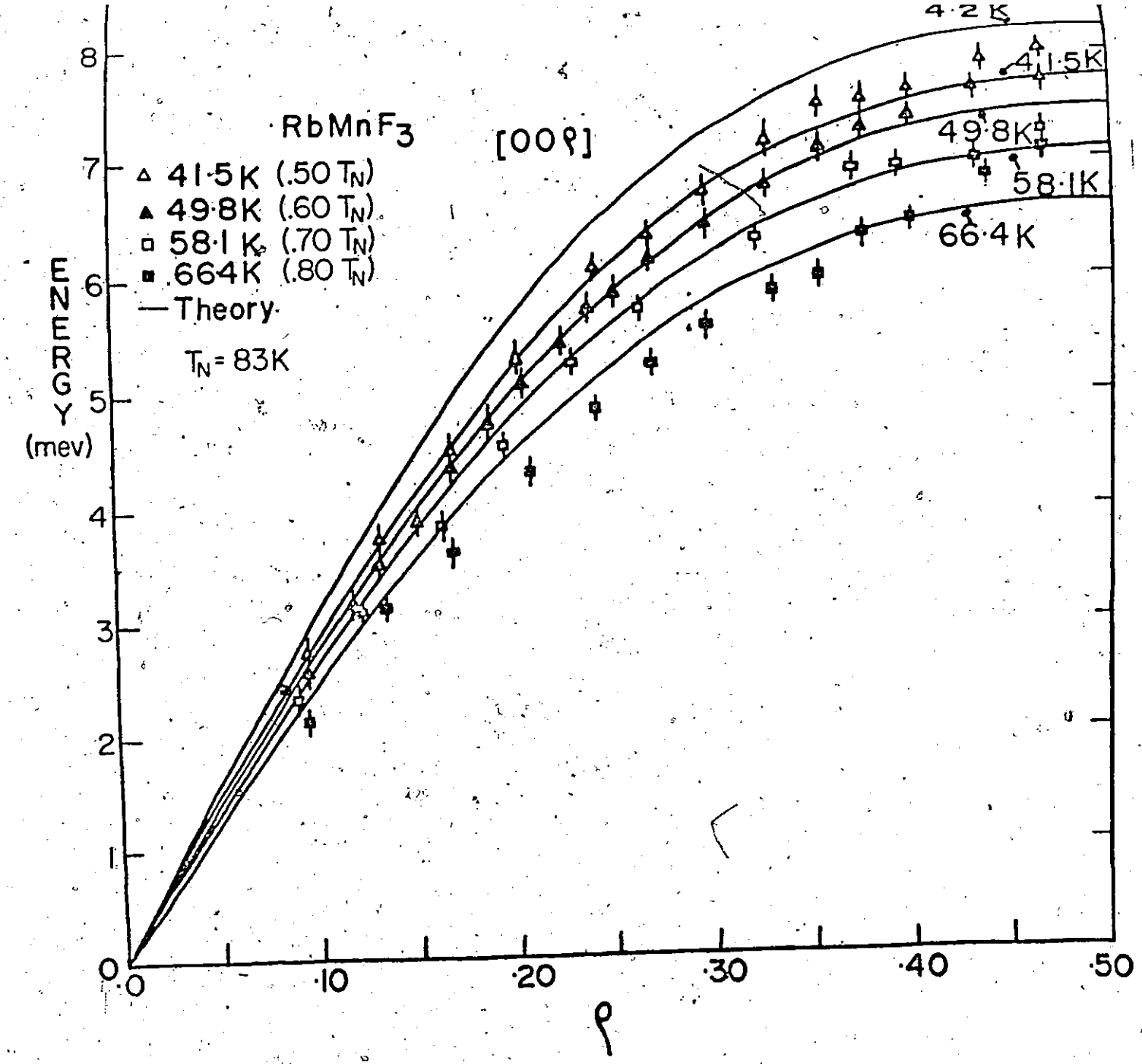
RbMnF3
[00ρ]
△ 41·5K (.50 TN)
▲ 49·8K (.60 TN)
□ 58·1 K (.70 TN)
■ 66·4K (.80 TN)
—Theory
TN = 83K
ENERGY (mev)
4·2K
41·5K
49·8K
58·1K
66·4K
0·0
·10
·20
·30
·40
·50
ρ

Fig. VIII-3: The wave vector dependence of the renormalisation factor in the [001] direction in MnF_2 and $RbMnF_3$. For MnF_2 the experimental data are from Okazaki et al. (1964) and for $RbMnF_3$ from Saunderson et al. (1972).

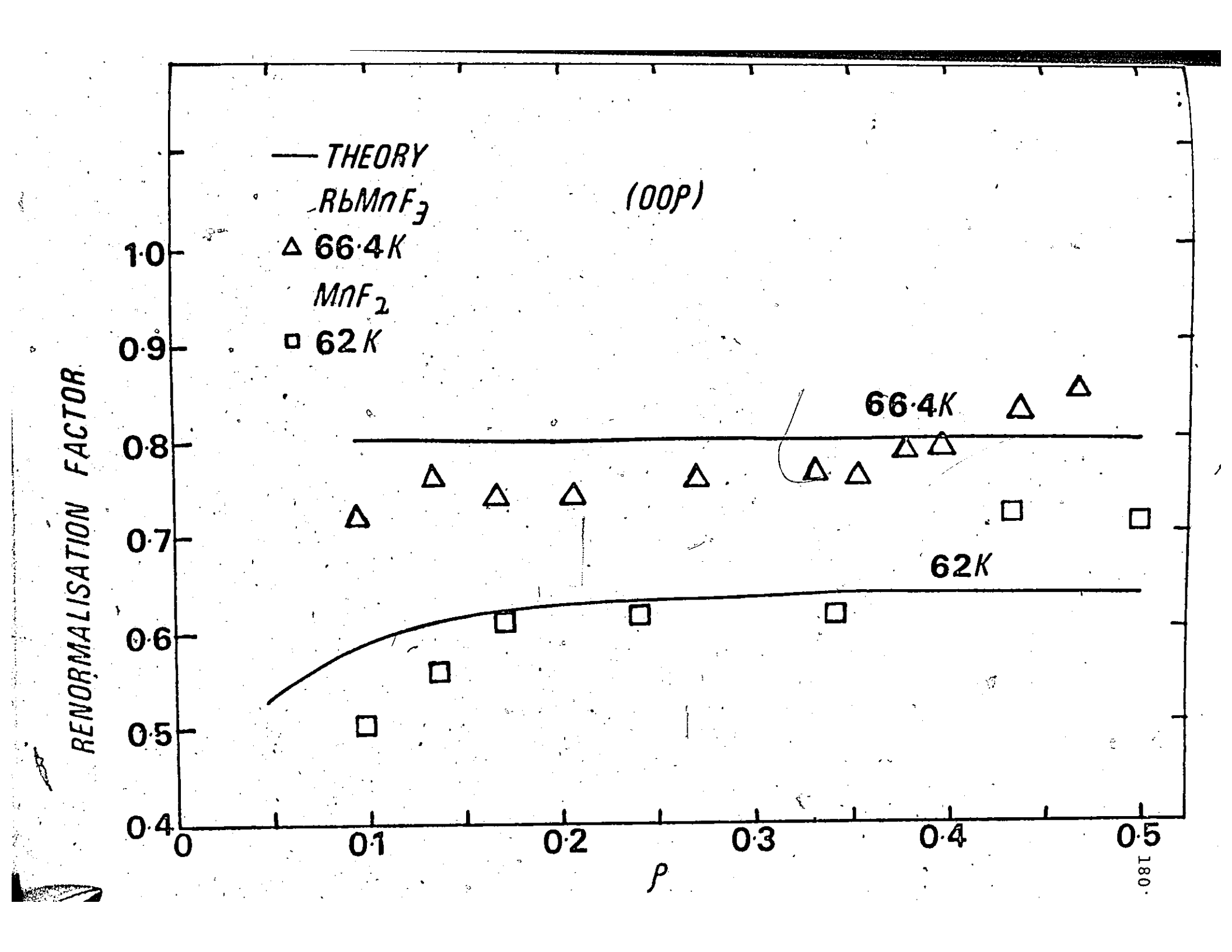
THEORY
RbMnF3
(OOP)
66·4K
MnF2
62K
66·4K
62K
RENORMALISATION FACTOR
1·0
0·9
0·8
0·7
0·6
0·5
0·4
0
0·1
0·2
0·3
0·4
0·5
ρ
180

low $\underline{k}$ magnons faster with temperature in $RbMnF_3$ does not seem to be calculable by our theory.

For MnF_2, the calculated renormalisation factor shows insignificant dependence upon the wavevector, if one does not include the variation of H_A with temperature. The dependence arises from the presence of J_1 which is an order of magnitude smaller than J_2. The calculated α_k, with H_A altered for the effect of temperature, shows a reasonable agreement with the experimental values for MnF_2. Moreover, the observation that the magnons with low $\underline{k}$ show greater fractional loss with temperature, is understandable in this case, since the energy of a $\underline{k} = 0$ magnon is due to the presence of anisotropy which arises from dipole-dipole interactions and these interactions are long range in nature.

As compared with $RbMnF_3$ and MnF_2, the case of MnO is rather complicated. It has three exchange constants J_{1d}, J_{1s} and J_2, all of which are of about equal importance in describing the system adequately. The temperature dependence of the distortion presents yet another problem in MnO. Equations (V-1) and (V-2) along with the values of the distortion, Δ, as given by Fig. V-3 are used (Morosin, 1970) to calculate the values of J_{1d} and J_{1s} at different temperatures below T_N. The final form of the equation used is

$$J_{1d}(T) = J_1(T_N)\exp[-\varepsilon \ell n(1 - \Delta/2)]$$

$$J_{1s}(T) = J_1(T_N)\exp[-\varepsilon \ell n(1 + \Delta/2)]$$

with $\varepsilon = 21$. (VIII-18)

The values of J_{1d} and J_{1s} at the Néel temperature were calculated using known values of the Δ and exchange constants at 4.2K. The values of the J_{1d} and J_{1s} along with the values of Δ at different temperatures are given in Table VIII-2. In Fig. VIII-4 the calculated dispersion curves in the [111]-type directions and in Fig. VIII-5 in the [001] direction at various temperatures are compared with the experimental data for MnO. As discussed in Chapter VI, the data at 4.2K are from three groups (Kohgi et al., 1972; Collins and Tondon et al., 1973; Bonfante et al., 1972A). The data at 60K, 78K and 100K are from Kohgi et al. (1973) and at 88.75K and 114.75K from Bonfante et al. (1972B). The agreement of the calculated energies at 60K (.50 T_N) in the [111] and at 78K (.65 T_N) in the [001] direction is quite good. At 88.75K (.74 T_N) in the [111]-type directions the agreement is still good except for two regions. For the [ρρρ] branch, near the zone boundary the calculated energies are higher by a few percent as compared to the data of Bonfante et al. However, at 4.2K itself our calculated energies are higher by almost the

TABLE VIII-2

THE VARIATION OF THE NEAREST NEIGHBOUR EXCHANGE CONSTANT WITH THE DISTORTION Δ IN MnO

T(K)	Δ (radians)	J_{1d} (meV)	J_{1s} (meV)
4.2	0.011	-0.466	-0.361
20	0.011	-0.466	-0.361
60	0.010	-0.461	-0.365
80	0.009	-0.456	-0.369
88.75	0.008	-0.452	-0.373
100	0.007	-0.448	-0.376
110	0.005	-0.440	-0.383
114.75	0.004	-0.434	-0.387
120	0.000	-0.411	-0.411

Fig. VIII-4: The calculated spin wave dispersion curves in MnO at various temperatures in the [111]-type directions. The data points O, O and Θ are all at 4.2K and were measured by Kohgi et al. (1972), Bonfante et al. (1972A) and Collins and Tondon et al. (1973) respectively. The experimental data at 60K and 100K are from Kohgi et al. (1973) and at 88.75K from Bonfante et al. (1972B).

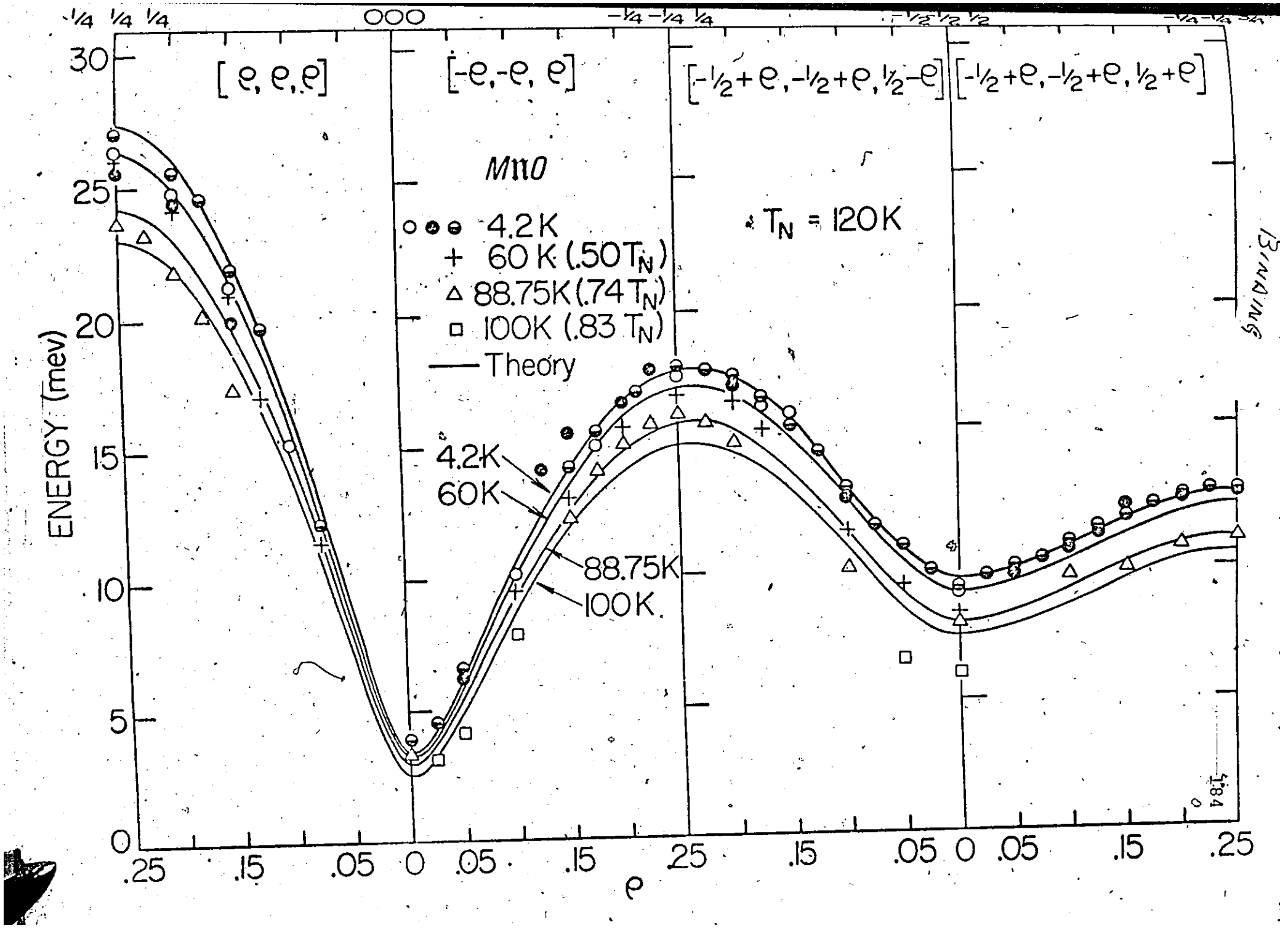
-¼ ¼ ¼
000
-¼ -¼ ¼
-½ ½ ½
-¼ -¼ ¼
[e, e, e]
[-e, -e, e]
[-½+e, -½+e, ½-e]
[-½+e, -½+e, ½+e]
MnO
4.2K
60K (.50 T_N)
88.75K (.74 T_N)
100K (.83 T_N)
Theory
T_N = 120K
4.2K
60K
88.75K
100K
ENERGY (mev)
30
25
20
15
10
5
0
.25
.15
.05
0
.05
.15
.25
.15
.05
0
.05
.15
.25
e
Brandis
1.84

Fig. VIII-5: The calculated spin wave dispersion curves in MnO at various temperatures in the [001] direction. The data points O, Δ, □ are all at 4.2K and were measured by Kohgi et al. (1972), Collins and Tondon et al. (1973) and Bonfante et al. (1972A) respectively. The data at 78K and 100K are from Kohgi et al. (1973) and at 114.75K from Bonfante et al. (1972B).

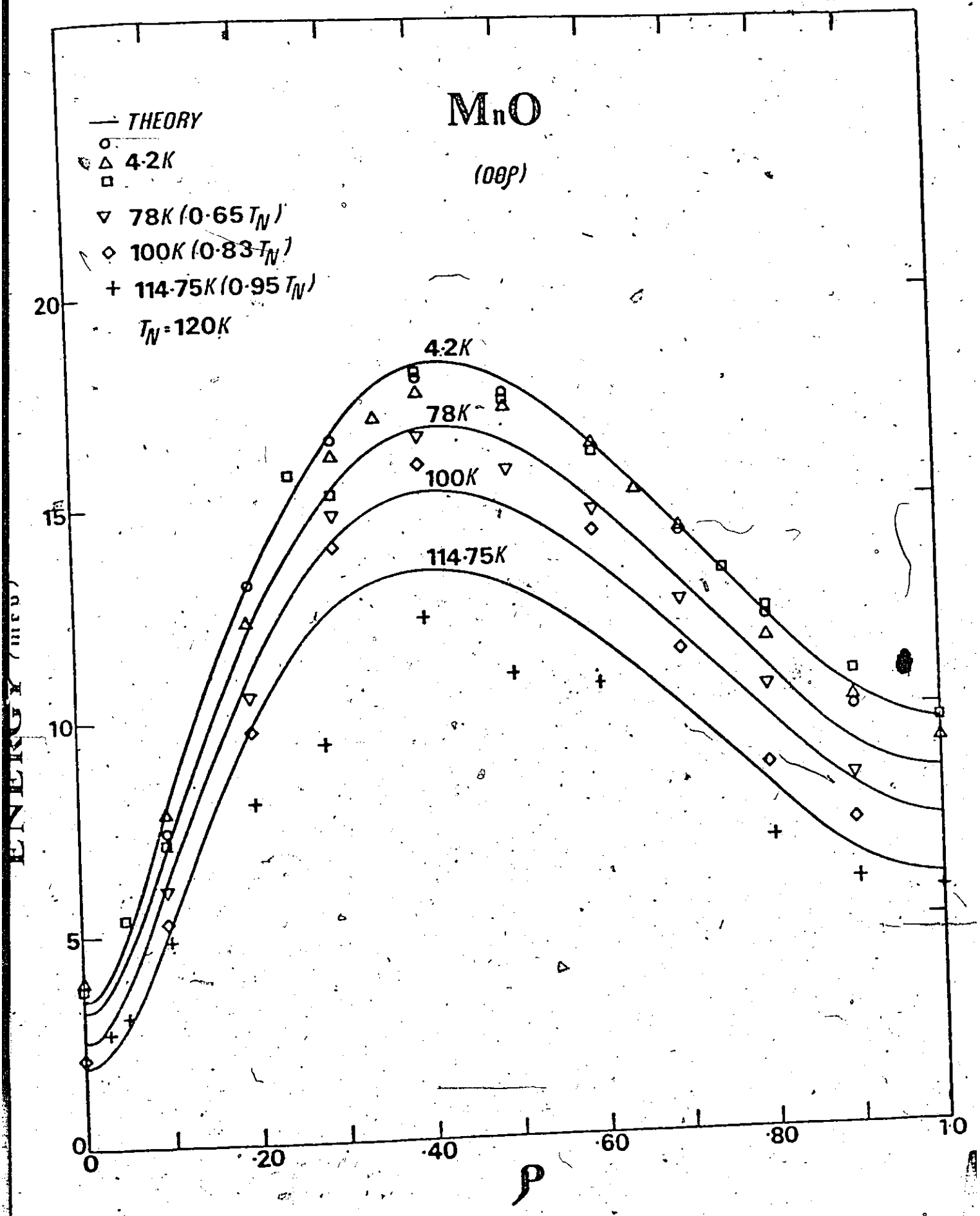
MnO
(0θρ)
THEORY
4·2K
78K (0·65 T_N)
100K (0·83 T_N)
114·75K (0·95 T_N)
T_N = 120K
4·2K
78K
100K
114·75K
20
15
10
5
0
0
·20
·40
·60
·80
1·0
ρ

same percentage as compared to their data and this disagreement appears to be merely a reflection of this experimental inconsistency. The other region of disagreement is in the vicinity of $\underline{q} = (\frac{1}{2}\ \frac{1}{2} - \frac{1}{2})$. The calculated energies are higher even at 60K (.50 T_N). We recall, that the magnon at $\underline{q} = (\frac{1}{2}\ \frac{1}{2} - \frac{1}{2})$ is a rather special one as it's energy arises from the distortion of MnO below T_N. In the renormalisation calculations for MnO we have taken into account the variation of J_{1d} and J_{1s} with the temperature using Eq. (VIII-18). We cannot be certain whether the problem lies in Eq. (VIII-18) or in our spin wave renormalisation theory, though we would be more disposed to guess that the former of these is the source of discrepancy. In the [001] direction, at 100K (.83 T_N) the calculated energies are higher by $\sim$ 8% in the vicinity of $\underline{q} = (\frac{1}{2}\ \frac{1}{2} - \frac{1}{2})$, otherwise the agreement is not bad. However, at T = 114.75K (.92 T_N), the agreement is poor. The discrepancy is a maximum for intermediate wave-vectors, where the calculated energies are high by up to 15%. At 4.2K our calculated energies are high by a few percent in this region and this might make some contribution towards the discrepancy but would not remove it altogether. It is apparent that beyond .80 T_N our calculations of dynamical interactions between pair of spin waves are insufficient to account completely for the experimentally observed lowering of energy. Although, we have not included the

effect of the kinematical interactions in our calculations, we know that these are important only when one is very close to T_N. A more complete treatment of the terms contributing to the dynamical interaction appears to be required.

In Fig. VIII-6 some typical plots of the renormalisation factor against wavevector for the [001] and in Fig. VIII-7 for the [111]-type directions at various temperatures along with it's experimental values are shown for MnO. Both in the [001] and the [111] directions the overall agreement with the experimental value is good. In the [001] direction, the theory with H_A altered for the effect of temperature, does show the experimentally observed features namely the zone centre and the magnons around $\underline{q} = (\frac{1}{2}\ \frac{1}{2} - \frac{1}{2})$ lose energy faster with temperature than the intermediate wavevector magnons. In the [111]-type directions experimentally α_k appears to have rather insignificant dependence upon the wavevector and this agrees with the calculations.

We have seen in Chapter V that the anisotropy field in MnO is due to dipole-dipole interactions. By analogy with MnF_2, it is not surprising that one finds the zone centre magnons suffering the greatest fractional loss in energy in the [001] direction. The energy of the magnon at $\underline{q} = (\frac{1}{2}\ \frac{1}{2} - \frac{1}{2})$, as was mentioned earlier, is due to the lattice distortion below T_N and is proportional to $(J_{1d} - J_{1s})^{1/2}$. The difference $(J_{1d} - J_{1s})$ is a temperature

Fig. VIII-6: The wave vector dependence of the renormalisation factor in the [001] direction in MnO. The experimental data at 88.75K and 114.75K are from Bonfante et al. (1972B) and at 78K and 100K are from Kohgi et al. (1973).

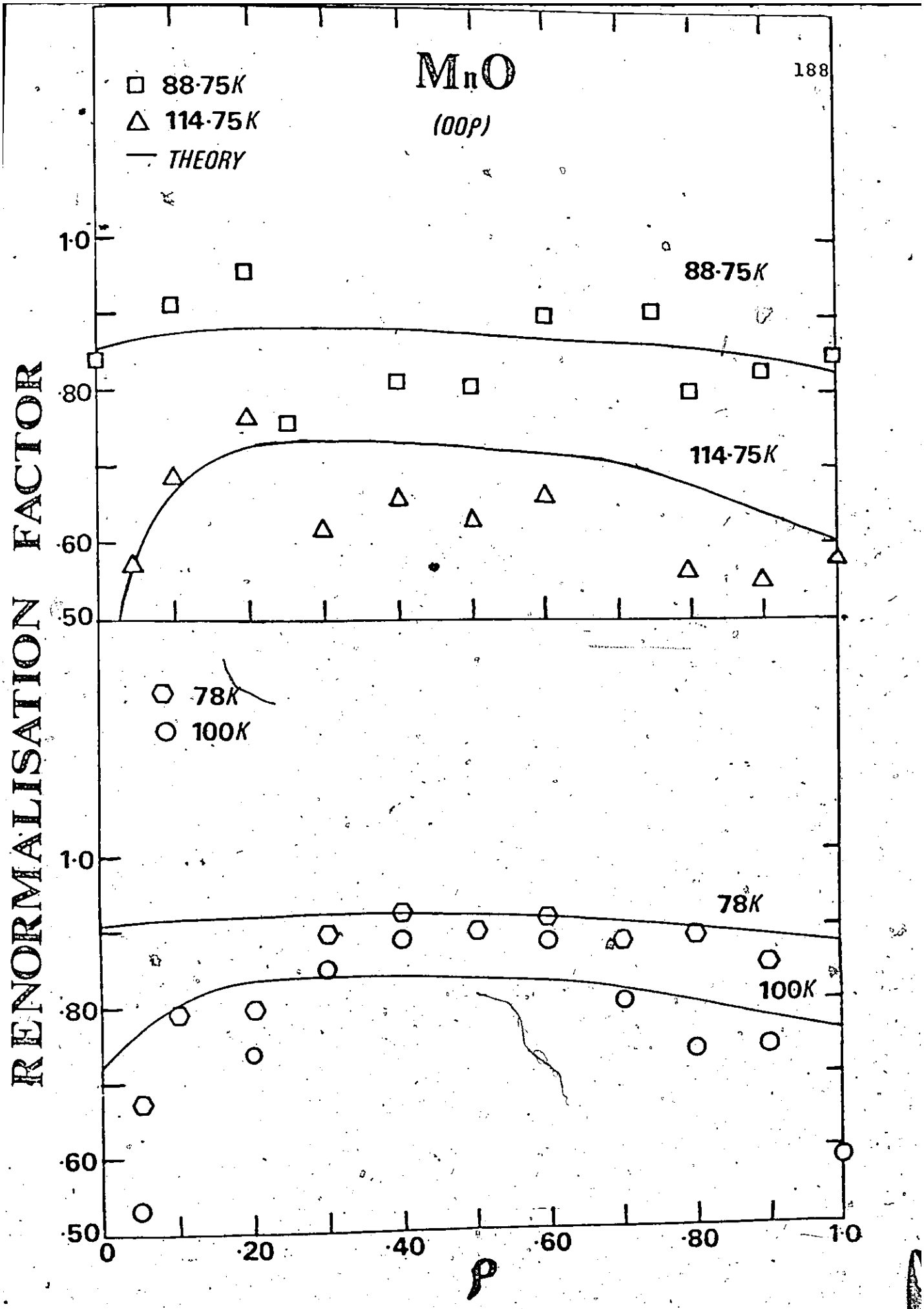
MnO
(00P)
88·75K
114·75K
THEORY
88·75K
114·75K
78K
100K
78K
100K
RENORMALISATION FACTOR
1·0
·80
·60
·50
0
·20
·40
·60
·80
1·0
ρ

Fig. VIII-7: The wave vector dependence of the renormalisation factor in the [111]-type directions in MnO. The experimental data at 60K are from Kohgi et al. (1973) and at 88.75K from Bonfante et al. (1972B).

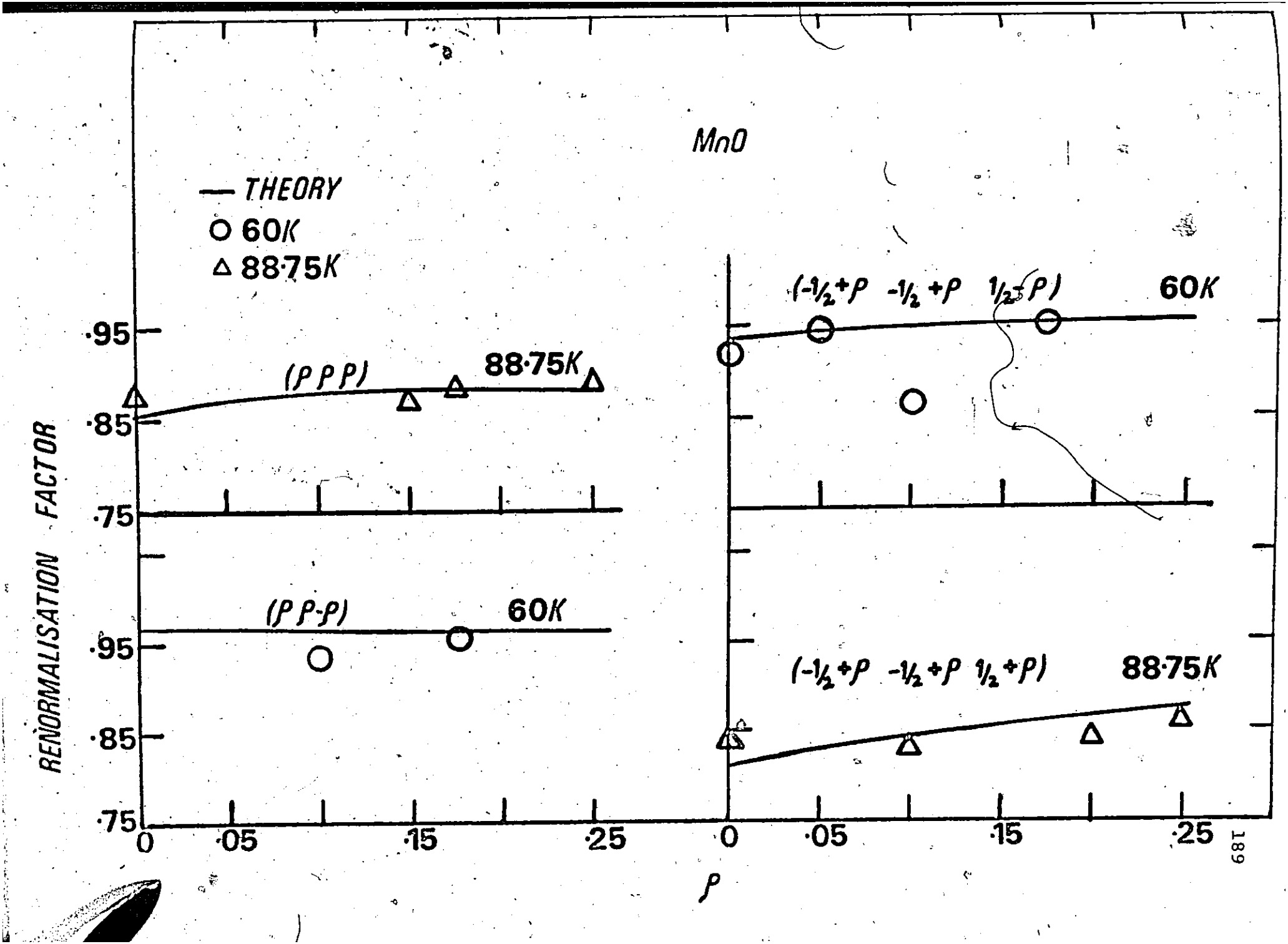
MnO
— THEORY
O 60K
Δ 88·75K
(P P P)
88·75K
(P P -P)
60K
(-½+P -½+P ½+P)
60K
(-½+P -½+P ½+P)
88·75K
·95
·85
·75
·95
·85
·75
0
·05
·15
·25
0
·05
·15
·25
RENORMALISATION FACTOR
P
189

dependent quantity and decreases to zero as the temperature approaches T_N. Thus, magnons in the vicinity of $\underline{q} = (\frac{1}{2}\ \frac{1}{2} - \frac{1}{2})$ have, in addition, to the usual spin wave interactions, another factor that decreases their energy and, as a result, they might be expected to suffer a greater fractional loss of energy in the [001] direction as the temperature rises. In the [111]-type directions up to T = 88.75K these features are not apparent, and at higher temperatures there is insufficient data. Kohgi et al. (1973) report difficulty in observing the spin waves at high temperatures due to their highly damped nature.

In Fig. VIII-8 the calculated dispersion curves for NiO are shown at different temperatures. As yet, the experimental data exist only at 78K (.15 T_N). Although NiO has the same magnetic structure as MnO (Type-II f.c.c.), its nearest neighbour exchange constant, J_1, is an order of magnitude smaller than its second neighbour exchange constant J_2. This results in its dispersion curves at zero temperature being very similar in all symmetry directions. In fact, because of the small value of J_1, its lattice can be approximated by four independent interpenetrating simple cubic sublattices similar to $RbMnF_3$ (see, e.g., discussion in Section 3 of Chapter IV). Hence, one may expect NiO to show trends similar to $RbMnF_3$ at higher temperatures.

The sublattice magnetization can be calculated using Eq. (IV-19) which, if non-diagonal terms in α and β

Fig. VIII-8: The calculated spin wave dispersion curves in NiO at various temperatures in the [001] direction.

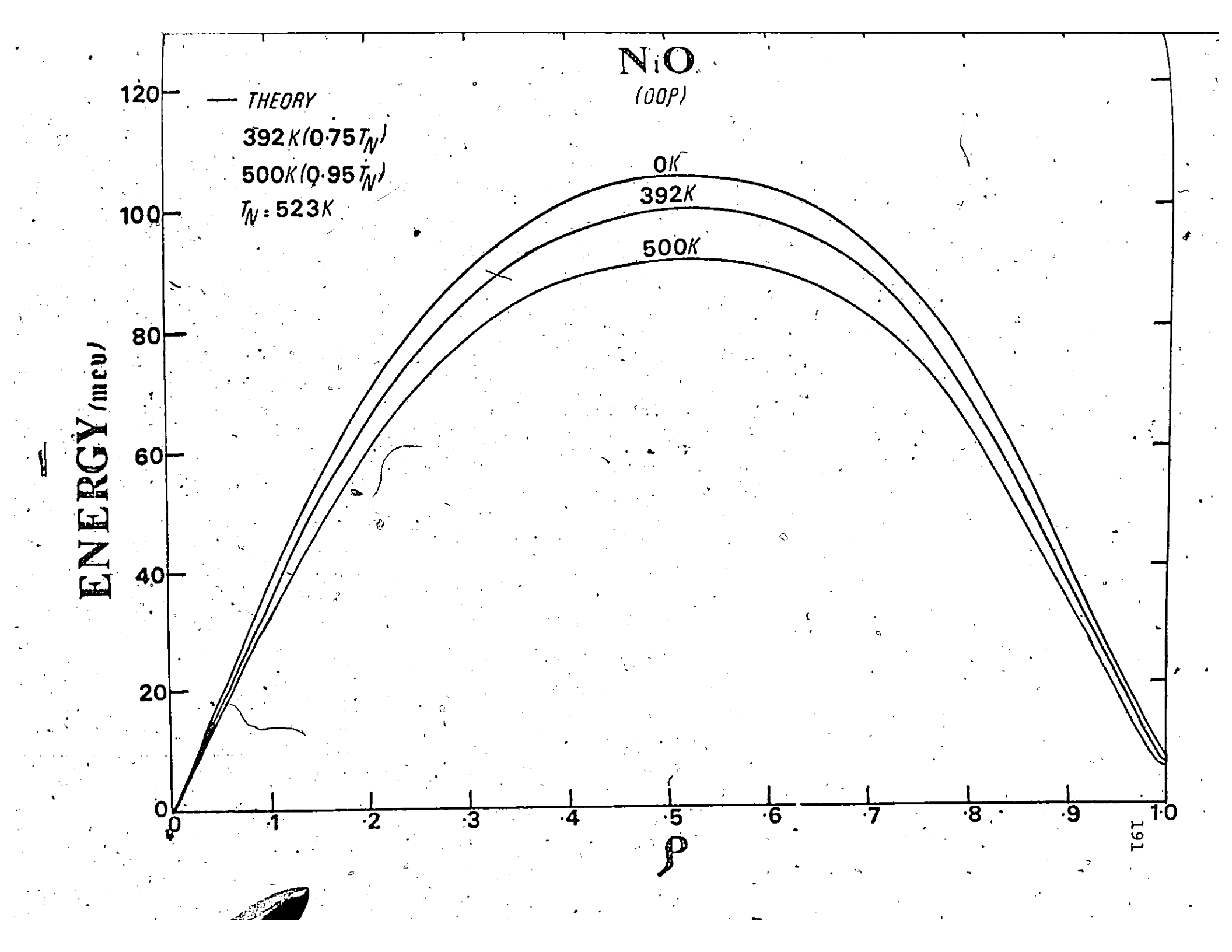
NiO
(00P)
— THEORY
392K (0·75 T_N)
500K (0·95 T_N)
T_N : 523K
0K
392K
500K
ENERGY (meV)
120
100
80
60
40
20
0
·0
·1
·2
·3
·4
·5
·6
·7
·8
·9
1·0
ρ
191

are neglected, reduces to

$$M_{s-\ell}(T) = NS/2 - \sum_q \sinh^2\theta_q - \sum_q \langle n_q \rangle \cosh 2\theta_q \quad . \qquad \text{(VIII-19)}$$

As this equation indicates, the calculation of magnetization at any temperature T involves knowing the magnon population factor, $\langle n_q(T) \rangle$, and this can be derived from the same calculations that were used earlier in this chapter to give spin-wave renormalisation as a function of temperature.

Figure VIII-9 compares the calculated sublattice magnetization with the experimental data for MnO and MnF_2. The experimental data for MnF_2 are from the NMR measurements of F^{19} nuclei (Jaccarino et al., 1959; Heller et al., 1962) and the data for MnO are from Shull et al. (1951). For MnF_2, the calculated sublattice magnetization shows good agreement with the data and goes to zero at a temperature very close to the Néel temperature of 67K. For MnO, the agreement with the data is good only up to about .80 T_N.

T_M', the temperature above which the self-consistent solution of Eq. (VIII-11) does not exist is found to be around 65K and 82K for MnF_2 and $RbMnF_3$. This is within five percent of their Néel temperatures of 67K and 83K respectively. For MnO, T_M', without and with the anisotropy field is found to be around 135K and 140K. Hence, the

Fig. VIII-9: The variation of fractional sublattice magnetization with temperature for MnO and MnF_2. The experimental data for MnO are from Shull et al. (1951) and for MnF_2 from Jaccarino et al. (1959) and Heller et al. (1962).

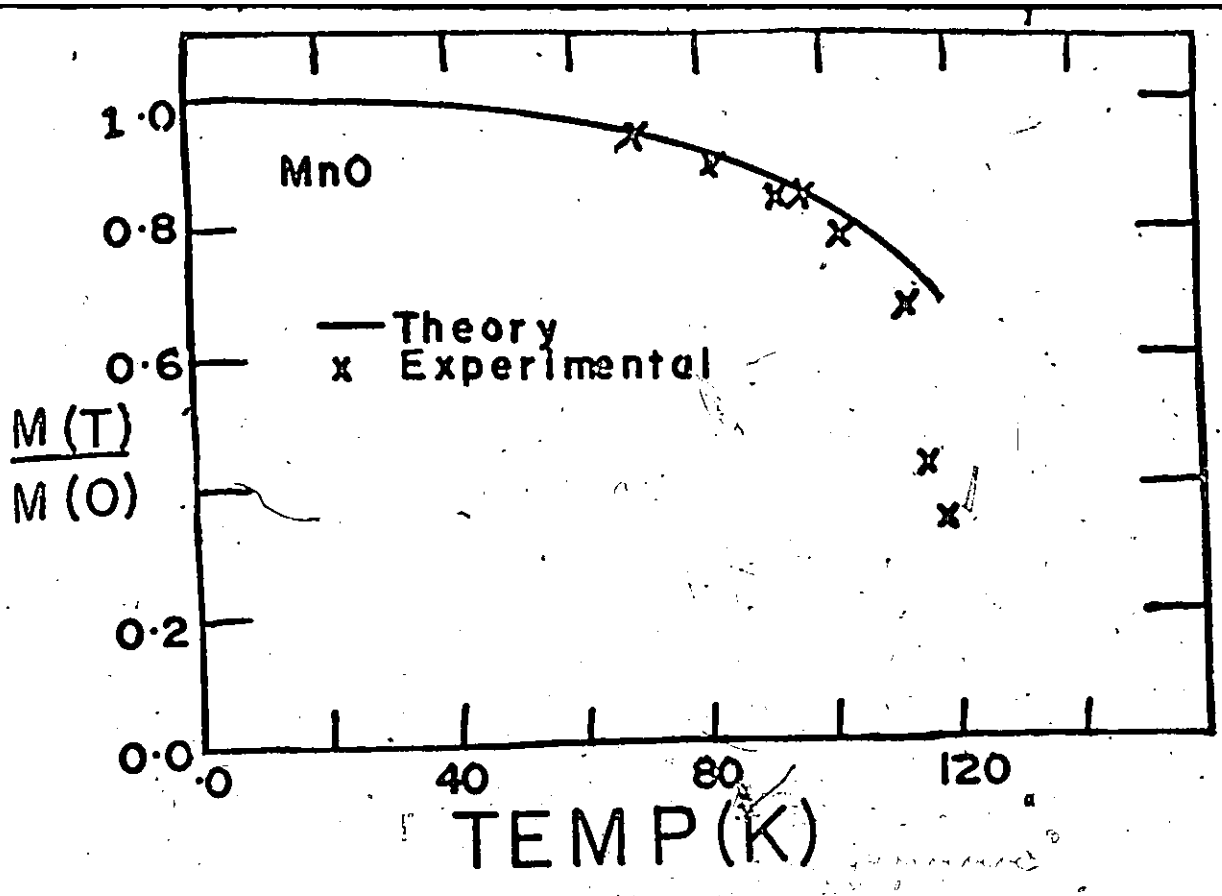
MnO
Theory
x Experimental
M(T)/M(O)
1·0
0·8
0·6
0·2
0·0
0
40
80
120
TEMP(K)

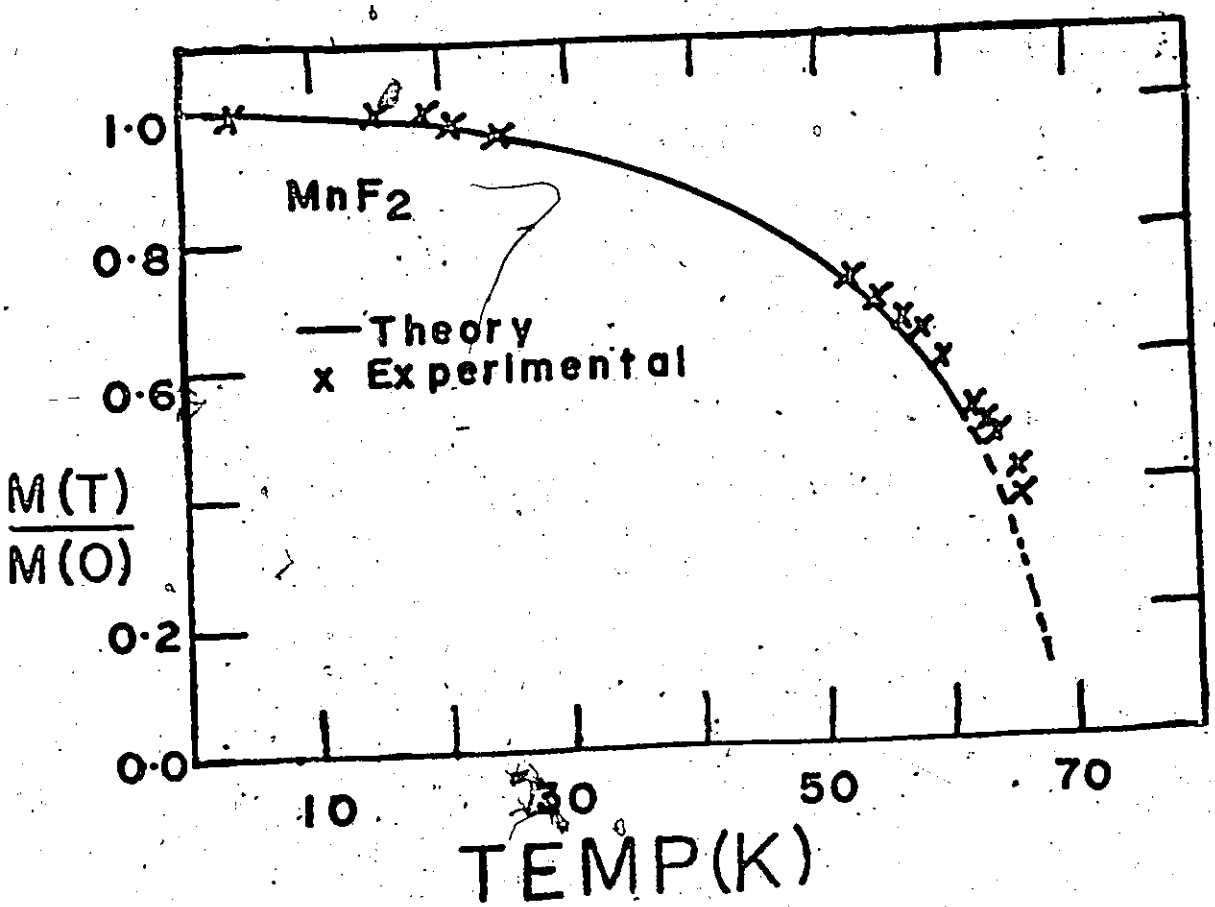
MnF2
Theory
x Experimental
M(T)/M(O)
1·0
0·8
0·6
0·2
0·0
10
30
50
70
TEMP(K)

anisotropy does seem to increase T_M'. However, Nagai observes that T_0 (T_0 has a different definition from T_M', see Chapter VII) decreases with the inclusion of uniaxial anisotropy. T_M' for NiO is found to be about 620K. Thus, T_M' for both NiO and MnO are $\sim$ 20% higher than their Néel temperatures (523K and 120K).

CHAPTER IX

CONCLUDING REMARKS

Generally speaking, we have looked into three aspects of antiferromagnets in this thesis:-

(i) The calculation of the effect of zero-point spin deviations on various properties of antiferromagnets at the absolute zero of temperature.

(ii) The experimental measurements of the dispersion curves in MnO at 4.2K.

(iii) The calculation of renormalisation of the energy of magnons at finite temperatures.

Spin wave theory, which has localized spin as its basic assumptions, is the common theme that interlinks the various aspects of this thesis.

The presence of spin deviations, even at the absolute zero of temperature in an antiferromagnet, make a finite contribution to its various properties such as the spin wave energy, the sublattice magnetization, etc.. One needs, in order to calculate this contribution, to go beyond the approximation of the linear spin wave theory. The contribution is dependent on the magnitude of spin, and is more for systems with small values of atomic spin. In

Chapter IV, we have seen how the earlier approaches to calculating this contribution can be extended to the case of an arbitrary range of exchange interaction in a rather simple way. The effect, though small, should be detectable experimentally for systems of low spin S. Unfortunately, no experimental data appears to exist for three-dimensional systems with $S = 1/2$. The calculations are useful for the determination of covalency parameters from neutron diffraction data, for calculation of Néel temperature using series techniques, etc.. The effect has another significance from a fundamental point of view since it's existence is entirely due to the quantum nature of spin.

In Chapter VI, we saw that the agreement of calculated dispersion curves using spin wave theory with our inelastic neutron scattering data was quite good for MnO. In view of the complicated, though seemingly well understood, nature of the magnetic interactions in MnO, the agreement speaks well for spin wave theory as applied to antiferromagnetic insulators. The values of the exchange constants that we have derived can be used reliably for calculations of the magnetic properties of MnO.

At finite temperature when the magnons start losing energy and having finite life times, spin wave theory still works satisfactorily as we saw in the last two chapters. Of course, now one has to take spin wave interactions into

account for calculation of the magnon energy. In the last chapter it was shown how an extension of Bloch's theory to a system with more than just one exchange interaction results in a wavevector dependent renormalisation factor for magnon energy. The theory works reasonably well for simple antiferromagnets like $RbMnF_3$ and MnF_2. However, the renormalisation factor for $RbMnF_3$, which according to the theory should be wavevector independent, shows significant dependence on wavevector experimentally. The overall calculations of the theory are satisfactory up to about $0.75\ T_N$ for the less simple case of MnO. The wavevector dependence of the renormalisation factor is experimentally found to be insignificant in the [111]-type directions up to $0.75\ T_N$ and the calculations agree with it.

Finite temperature experimental data on other antiferromagnets especially NiO would be helpful as a further check of the thoery. NiO being similar to $RbMnF_3$, it would be interesting to study the wavevector dependence of the renormalisation factor in it. A detailed knowledge of the pattern of the wavevector dependence of this factor in antiferromagnets at different temperatures may give a better insight into magnetic phase transitions.

BIBLIOGRAPHY

Alperin, H. A., J. Phys. Soc. Jap. 17 Suppl. B111, 12 (1962).

Anderson, P. W., Phys. Rev. 86, 694 (1952).

Anderson, P. W., Phys. Rev. 115, 2 (1959).

Armour, E. A. G., Physica 53, 304 (1971).

Bacon, G. E., "Neutron Diffraction", Oxford, 1962.

Bethe, H. A., Z. Physik 21, 205 (1931).

Birgeneau, R. J., Guggenheim, H. J. and Shirane, G., Phys. Rev. Lett. 22, 720 (1969).

Bizette, H., Squire, C. F. and Tsai, B., C. R. Acad. Sci. Paris 207, 449 (1938).

Bizette, H., Ann. de Phys. 1, 87 (1946).

Bloch, F., Z. Phys. 61, 206 (1930).

Bloch, M., Phys. Rev. Lett. 9, 286 (1962).

Bloch, M., J. Appl. Phys. 34, 1151 (1963).

Bloch-Nauciel, M., Ann. Phys. 5, 139 (1970).

Bonfante, M., Hennion, B., Moussa, F. and Pepy, G., Sol. St. Comm. 10, 553 (1972A).

Bonfante, M., Hennion, B., Moussa, F. and Pepy, G., Neutron Inelastic Scattering Symp., Grenoble, IAEA, Vienna, 1972B.

Born, M. and Huang, K., "Dynamical Theory of Crystal Lattices", Oxford Univ. Press, 1954.

Brockhouse, B. N., In. Scat. of Neutrons in Solids and Liquids, IAEA, 113 (1961).

Callen, M. B., Phys. Rev. 130, 890 (1963).

Casselman, T. N. and Keffer, F., Phys. Rev. 4, 498 (1960).

Collins, M. F., Proc. Int. Conf. Magn., 319 (1964).

Collins, M. F. and Tondon, V. K., Can, J. Phys. 50, 2991 (1972).

Collins, M. F., Tondon, V. K. and Buyers, W. J. L., Intern. J. Mag. 4, 17 (1973).

Corliss, L. M., Elliott, N. and Hastings, J. M., Phys. Rev. 104, 924 (1956).

Davis, H. L., J. Phys. Chem. Solids 23, 1348 (1962).

Dembinski, S. T., Physica 30, 1217 (1964).

Dyson, J. F., Phys. Rev. 102, 1217 (1956).

Erickson, R. A., Phys. Rev. 90, 779 (1953).

Fender, B. E. F., Jacobsen, A. J. and Wedgewood, F. A., J. Chem. Phys. 48, 990 (1968).

Flax, L. and Raich, J. C., Phys. Rev. B 2, 1338 (1970).

Fleury, P. A., Phys. Rev. Lett. 24, 1346 (1970).

Gilat, G. and Raubenheimer, L. J., Phys. Rev. 144, 390 (1966).

Halpern, O. and Johnson, M. H., Phys. Rev. 55, 898 (1939).

Harada, I. and Motizuki, K., J. Phys. Soc. Jap. 32, 927 (1972).

Harris, A. B., J. Phys. Chem. Solid 27, 1927 (1966).

Harris, A. B., Phys. Rev. Lett. 21, 602 (1968).

Harris, E. A., J. Phys. C 5, 338 (1972).

Heller, P. and Benedek, G. B., Phys. Rev. Lett. 8, 428 (1962).

Hennion, B. and Moussa, F., Ann. Phys. 233 (1972).

Holstein, F. and Primakoff, H., Phys. Rev. 58, 1908 (1940).

Hughes, A. E., Phys. Rev. B 3, 877 (1971).

Hutchings, M. T. and Samuelson, E. J., Sol. St. Comm. 9, 1011 (1971).

Iyengar, P. K., "Thermal Neutron Scattering", (edited by Egelstaff, P. A.), Acad. Press, 98 (1965).

Izyumov, Yu. A. and Ozerov, R. P., "Magnetic Neutron Diffraction", Plenum Press, 1970.

Jaccarino, V. and Walker, L. R., J. Phys. Radium 20, 341 (1959).

Kanamori, J. and Tachiki, M., J. Phys. Soc. Jap. 17, 1384 (1962).

Kaplan, J. I., J. Chem. Phys. 22, 1709 (1954).

Keffer, F. and O'Sullivan, W., Phys. Rev. 108, 637 (1957).

Keffer, F. and Loudon, R., J. Appl. Phys. Suppl. 32, 2S (1961).

Keffer, F., Handbuch Der Physik, XVIII/2, 1 (1966)

Kittel, C., "Thermal Physics", John Wiley & Sons, 1969.

Klein, M. J. and Smith, R. S., Phys. Rev. 80, 1111 (1951).

Kohgi, M., Ishikawa, Y. and Endoh, Y., Sol. St. Comm. 11, 391 (1972).

Kohgi, M., Ishikawa, Y., Harada, I. and Motizuki, K., to be published, 1973.

Kramers, H., Physica 1, 182 (1934).

Kramers, H. A. and Heller, G., Proc. Roy. Acad. Sci. 37, 378 (1934).

Kranendonk, J. V. and Van Vleck, J. H., Rev. Mod. Phys. 1 (1958).

Krupica, S. and Sternberk, J., "Elements of Theoretical Magnetism", CRC Press, 1968.

Kubo, R., Phys. Rev. 87, 568 (1952).

Li, Y. Y., Phys. Rev. 100, 627 (1955).

Lines, M. E., Phys. Rev. 135, A1336 (1964).

Lines, M. E., and Jones, E. D., Phys. Rev. 139, A1313 (1965).

Lines, M. E., Phys. Rev. B 3, 1749 (1971).

Liu, S. H., Phys. Rev. 142, 267 (1966).

Loly, P. D., Phys. Rev. 173, 603 (1968).

Loly, P. D., J. Phys. C 1, 1365 (1971).

Low, G. G., Proc. Phys. Soc. 82, 992 (1963).

Low, G. G., Neutron Inelastic Scatt. Symp., IAEA, 453 (1964).

Maleev, S. V., Sov. Phys.-JETP 6, 776 (1958).

Marshall, W. and Lovesey, S. W., "Theory of Thermal Neutron Scattering", Oxford Univ. Press, 209 (1971).

Mattis, D. C., "The Theory of Magnetism", Harper & Row, 1965.

Morosin, B., Phys. Rev. B 1, 236 (1970).

Nagai, O. and Yoshimori, A., Prog. Th. Phys. 25, 595 (1961).

Nagai, O. and Tanaka, T., Phys. Rev. 188, 821 (1969).

Nagai, O., Phys. Rev. 180, 557 (1969A).

Nagai, O., J. Appl. Phys. 10, 1116 (1969B).

Nagai, O. and Tanaka, T., Prog. Th. Phys. (Suppl.) 46, 113 (1970).

Nagamiya, T. and Motizuki, K., Rev. Mod. Phys. 30, 89 (1958).

Néel, L., Ann. de Phys. 17, 64 (1932).

Néel, L., Comptes Rendus 203, 304 (1948).

Oguchi, T., Phys. Rev. 117, 117 (1960).

Oguchi, T. and Honma, A., J. Phys. Soc. Jap. 16, 79 (1961).

Rado, G. T. and Suhl, H., "Magnetism", Acad. Press, 1963.

Richards, P. L., J. Appl. Phys. 34, 1237 (1963).

Rodbell, D. and Owen, J., J. Appl. Phys. 35, 1002 (1964).

Rodbell, D. S., Osika, L. M. and Lawrence, P. E., J. Appl. Phys. 36, 666 (1965).

Roth, W. L., Phys. Rev. 110, 1313 (1958).

Roth, W. L. and Slack, G. A., J. Appl. Phys. 31, 352S (1960).

Saunderson, D. H., Windsor, C. G., Briggs, G. A., Evans, M. T. and Hutchison, E. A., Neutron Inelastic Scatt. Symp., Grenoble, 1972.

Sell, D. D., J. Appl. Phys. 39, 1030 (1968).

Semura, J. S. and Huber, D. L., Phys. Rev. B 7, 2154 (1972).

Shull, C. G. and Smart, J. S., Phys. Rev. 76, 1256 (1949).

Shull, C. G., Strausser, W. A., Wollan, E. O., Phys. Rev. 83, 333 (1951).

Sievers, A. J. and Tinkham, M., Phys. Rev. 129, 1566 (1963).

Skalyo, J., Shirane, G., Birgeneau, R. J. and Guggenheim, H. J., Phys. Rev. Lett. 23, 1394 (1969).

Smart, J. S., Magnetism (Rado and Suhl, editors), Acad. Press, Vol. III, 63 (1963).

Tofield, B. C. and Fender, B. E. F., J. Phys. Chem. Solids 31, 2741 (1970).

Tombs, N. C. and Rooksby, H. P., Nature 165, 442 (1950).

Turberfield, K. C., Okazaki, A. and Stevenson, R. W. H., Proc. Phys. Soc. 85, 743 (1965).

Van Vleck, J. H., Phys. Rev. 52, 1195 (1937).

Windsor, C. G. and Stevenson, R. W. H., Proc. Phys. Soc. 87, 501 (1966).

Wortis, M., Phys. Rev. 138A, 1126 (1965).

Yelon, W. B. and Silberglitt, R., Phys. Rev. B 4, 2280 (1971).